School of Civil and Mechanical Engineering
Department of Civil Engineering

Effect of Iron Corrosion on the Fate of Dosed Copper to Inhibit Nitrification in Chloraminated Water Distribution System

Weixi ZHAN

This thesis is presented for the Degree of
Doctor of Philosophy
of
Curtin University

August 2011

ABSTRACT

Nitrification has been acknowledged as one of the major barriers towards efficient chloramination in water supply distribution systems. Many water utilities employing monochloramine as the final disinfectant have been encountering unwanted microbiologically assisted choramine decay and find it difficult to maintain desired chloramine residual at distribution system extremities. A novel method of using cupric sulphate (< 0.4 mg-Cu(II)/L) to inhibit ammonia oxidizing bacteria was recently granted a US patent (7465401). Efficient inhibition was achieved in bench scale work and a pilot reservoir in the field. However, unexpected dissolved Cu(II) loss occurred when copper salt was dosed into one pipe section of the Goldfield & Agricultural Water Supply System (G&AWSS) in Western Australia. It prevented dissolved copper from reaching extremities to protect chloramine from microbiologically assisted decay.

Our previous research and evaluation of the pipe environment suggested that severe dissolved copper loss could be related to iron pipe corrosion due to aging of the cement-lined steel pipe, extensive temperature fluctuation, chloramination and nitrification. A large amount of copper and iron found in sediments after the pipes' flushing provided further evidence. Although scale formation could be a complicated process that depends on a variety of physical and chemical conditions and the composition of corrosion scale can be distinct in each particular system, based on the literature review, ferric hydroxide flocs are acknowledged as one of the major corrosion products. Consistent severe copper loss over the three-year trial indicated that iron pipe corrosion is continuously occurring in the distribution system and thus supplying fresh iron salts. Ferrous ions could be released from new crevices during the initial stage of corrosion and oxidized to ferric ions. Ferric ions are further converted to ferric hydroxide flocs under drinking

water pH and oxidation conditions. Therefore, ferrous and ferric ions as well as ferric hydroxide were chosen as the major corrosion products in this research.

Bearing the goal of improving the inhibition strategy, this research investigated aqueous copper speciation in bulk waters, quantified dissolved Cu(II) removal by the iron corrosion products at trace concentrations (< 2 mg-Fe/L) and modelled dissolved Cu(II) loss subject to iron pipe corrosion. Mundaring raw water (MRW), which is the source water of G&AWSS, was employed as the main water source in this study. In addition, the nitrified water (NW) which was sourced from our laboratory reactors and the water containing humic substance (HAW) were used to investigate the effects of natural organic matter (NOM) of different characters on the fate of dissolved copper. Batch experiments were undertaken to measure Cu(II) solubility under various aqueous conditions. MINEQL+® (chemical equilibrium modelling system) was used to analyse Cu(II) speciation and cross-examine aqueous Cu(II) concentrations measured in the laboratory experiments. Aqueous ferrous ions, ferric ions and ferric hydroxide flocs, which are believed to be representatives of iron corrosion products, were added at low concentrations to remove dissolved Cu(II) in various bulk water samples. Their ability to remove dissolved Cu(II) was assessed individually, then the theory that a two-stage corrosion process removes Cu(II) was developed. The impact of NOM character on Cu(II)-NOM chelation in bulk water and their subsequent removal by ferric salts were elucidated by means of apparent molecular weight distribution and differential absorption spectra analysis. Finally, the dynamic process of dissolved Cu(II) removal by ferric salts was investigated. Combining both equilibrium and dynamic studies of dissolved Cu(II) removal by ferric salts, a model was established to predict dissolved Cu(II) loss in a corroded iron pipe distribution system. Aquasim® was used for

estimating parameters and simulating corrosion patterns and thus predicting Cu(II) loss in the field.

Cu(II)-NOM complexes were found to be the dominant forms in MRW, NW and HAW. Cu(II) solubility varied slightly in these bulk waters due to different NOM characters. Generally, intermolecular dicarboxylate chelation was considered to be the dominating chelation type between Cu(II) and organic compounds in MRW and NW, while salicylate chelation was prevalent in HAW due to more salicylate type binding sites available in humic substances. The removal of dissolved Cu(II) was assumed to occur via a two-stage process during corrosion: Stage I-coagulation and aggregation by released ferrous/ferric ions; Stage II-adsorption by iron hydroxide flocs formed afterwards. Both ferrous/ferric ions and ferric hydroxide flocs showed considerable capacity to remove dissolved Cu(II). Addition of 2 mg-Fe/L ferric ions was sufficient to remove the majority of dissolved Cu(II) in MRW and NW. The dissolved Cu(II) removal by $Fe(OH)_3$ flocs in MRW and NW could be explained as multilayer adsorption obeying a Freundlich isotherm. In addition, the adsorption process could be interfered with by the presence of heterogeneous Cu(II)-containing particles (CuO and $Cu(OH)_2$), which rendered less dissolved Cu(II) removal. Cu(II)-NOM in HAW demonstrated a relatively high resistance to removal by ferric salts. From these observations, Cu(II) was thought to preferentially complex with small organic molecules until saturation is reached. Slightly higher Cu(II) solubility and less dissolved Cu(II) removal observed in NW indicated that a proportion of small soluble organic substances was probably produced and chelated with Cu(II) during nitrification. In humic acid water (HAW), Cu(II) bound with small MW organic matter could be shielded by a relatively high proportion of large MW organic matter. The dynamic process of dissolved Cu(II) removal by $Fe(OH)_3$ flocs can be described by Pseudo

second order decay. From the comparison of dissolved Cu(II) loss between the modelling results and field data, the loss of dissolved Cu(II) could be due to removal by iron corrosion products and modelled by a reasonable assumption of the iron corrosion situation in the distribution system. At the end, Cu(II)-based inhibition and chloramination strategies are recommended.

ACKNOWLEDGEMENTS

It has been a long journey to come to the end of this research project. In retrospect, it is always easier to reflect on a few exciting moments when encouraging findings were discovered than the countless days when one was toiling away in hundreds of failures. In a long expedition, those people who light up the torch when one is exploring in the dark, and those who lend their helping hands when one is struggling in difficulties, will never be forgotten and always be appreciated.

The author holds his most sincere gratitude for his supervisor, A/Prof. Arumugam Sathasivan. Words alone cannot express the author's appreciation. It is the author's honour and privilege to have Sathasivan as a mentor and to share his valuable experience. Without his guidance, this research would be a mission impossible. It was also a happy experience to work together with A/Prof. Sathasivan. His optimistic character and encouragement made this journey much shorter. The author would also like to extend his thanks to A/Prof Anna Heitz and Cynthia Joll, who are from the Curtin Water Quality Research Centre (CWQRC), for their help with sample testing and related technical advice.

The author is grateful to the Australian Research Council (ARC) and Curtin University for the scholarships awarded during his PhD study ("Novel Technology for Improving Disinfection Outcomes in Regional and Remote Drinking Water Distribution Systems", project No.LP0776766). Particularly, the author would like to extend his gratitude to Prof. Hamid Nikraz, the head of the Department of Civil Engineering in Curtin University, for his generous support both financially and mentally. Special

thanks are given to the author's enthusiastic colleagues. It is a precious experience to work with them in the same group. Also, many staff in the Department of Engineering deserve the author's thanks for their kindness and support.

The author's gratitude goes to Water Corporation for funding this research. Many staff in Water Corporation deserve compliments for their help collecting water samples and efficient management during the field trips. A special thank goes to Chris Taylor for the English editing.

The last but not the least, I give my sincere and affectionate gratitude to my lovely wife. You are my rock, my inspiration and the reason of my life. Special thanks are given to my parents. You give me all the strength to conquer any barrier in my career and move forward forever.

Weixi Zhan

TABLE OF CONTENTS

LIST OF TABLES

LIST OF FIGURES

CHAPTER 1

INTRODUCTION

1.1 Chloramination in the Drinking Water Distribution Systems (DS)

1.1.1 Characteristics of Chloramine and its Application in the Drinking Water DS

Chloramines are the products of the reaction between free chlorine and ammonia. Chloramine species generally include monochloramine (NH_2Cl), dichloramine ($NHCl_2$) and trichloramine (NCl_3). From a disinfection point of view, monochloramine is the preferred final disinfectant in many drinking water DS. Compared with chlorine, chloramine's advantages are considered to be chemical stability (lower decay rates), sustained disinfection capability, low DBPs such as THMs, control of biofilm regrowth and minimal taste and odour (Kirmeyer et al., 2004). An increasing number of water utilities are replacing chlorine with monochloramine in long-distance water supply systems. However, chloramination is not as simple as an add-on process. Its application is subjected to operations and designs of water utilities as well as conditions in DS (Kirmeyer et al., 2004). It is inherently unstable in natural pH environments. Auto-decomposition, caused by chemical reactions which result in hydrolysis, disproportionation and redox reactions, is inevitable. The reactions are controlled by temperatures, Cl_2/N ratio, pH and some redox chemicals existing in natural water (Vikesland et al., 2001).

1.1.2 Nitrification and Microbiological Decay of Chloramine

Subject to the qualities of the water and pipeline conditions, nitrification has been widely acknowledged as one of the major causes accelerating the microbiological decay of chloramine. Nitrifiers present in water consume free and combined ammonia from chloramine and convert it to nitrite (NO_2^-) and nitrate (NO_3^-) through microbiological reactions (Krimeyer, et al., 2004). Compared with auto-decomposition, nitrification is thought to accelerate chloramine decay dramatically. Once the disinfectant residuals decrease to a certain level, the quality of service water deteriorates and the health of users is undoubtedly threatened.

Sathasivan et al. (2005) introduced the microbial decay factor (F_m) to quantify the microbiologically assisted chloramine decay in bulk water. Silver nitrate was used to inhibit nitrifying activity in bulk water. The difference between two decay coefficients (the decay coefficient of the unprocessed sample and of the inhibitor added sample) indicated the relative contribution of microbiologically assisted chloramine decay to total chloramine decay in bulk water. The ratio of microbial decay rate (k_m) to chemical decay rate (k_c) is defined as the microbial decay factor (F_m). Typical results from G&AWSS are shown in Appendix A. The relatively high F_m indicated the severeness of microbiological decay.

1.2 Cupric Sulphate: an Inhibitor Against Nitrification in Chloraminated Water and the Health Concern Regarding its Application

Cupric sulphate has been successfully used as a biocide to control micro-organisms and bacteria (fungi, algae) in water dams or reservoirs (Van Hullebusch et al., 2003). In laboratory experiments, copper was found to be toxic (affecting the metabolism and/or assimilation) to nitrifying bacteria including other micro-organisms. Recent investigations revealed the effectiveness of Cu(II) to inhibit ammonia oxidizing bacterial (AOB) growth (Koska, 2008). With encouraging results achieved at laboratory scale, Cu(II) was expected to be applied in water distribution systems to inhibit nitrifying activity and hence increase chloramine penetration to extremities.

The allowable concentration of copper in water is 2 mg/L (WHO, 2008). However, for the aesthetic reason, the World Health Organization (WHO) guideline imposed a limit of not more than 1 mg/L dissolved Cu(II) in drinking water (WHO, 2008). The Department of Public Health (WA) has approved the use of cupric sulphate up to 0.40 mg-Cu(II)/L in field trials.

1.3 Challenges to Application of Cu(II) Salt in the Goldfields & Agricultural Water Supply System (G&AWSS) in Western Australia

1.3.1 The Pilot Experiments in G&AWSS

The WA Goldfields and Agricultural Water Supply System (G&AWSS, Figure1.1) is perhaps the world's most extensive water distribution system. The pipeline was commissioned in 1896 and was completed in 1903. This was primarily constructed to deliver water to the communities that had rapidly grown due to a gold rush in Western Australia's "Eastern Goldfields", such as Coolgardie and Kalgoorlie. The pipeline

connects Mundaring Weir, near Perth, Western Australia, with Mount Charlotte Reservoir at Kalgoorlie, 530 km (330 miles) away. It also serves towns further inland via extensions to the north and the south. Mundaring Weir is fed with water from Helena River in the Darling Scarp and has also been augmented with treated groundwater in recent years. It continues to operate, supplying water to over 100,000 people and more than six million sheep in 33,000 households, mines, farms and other enterprises.

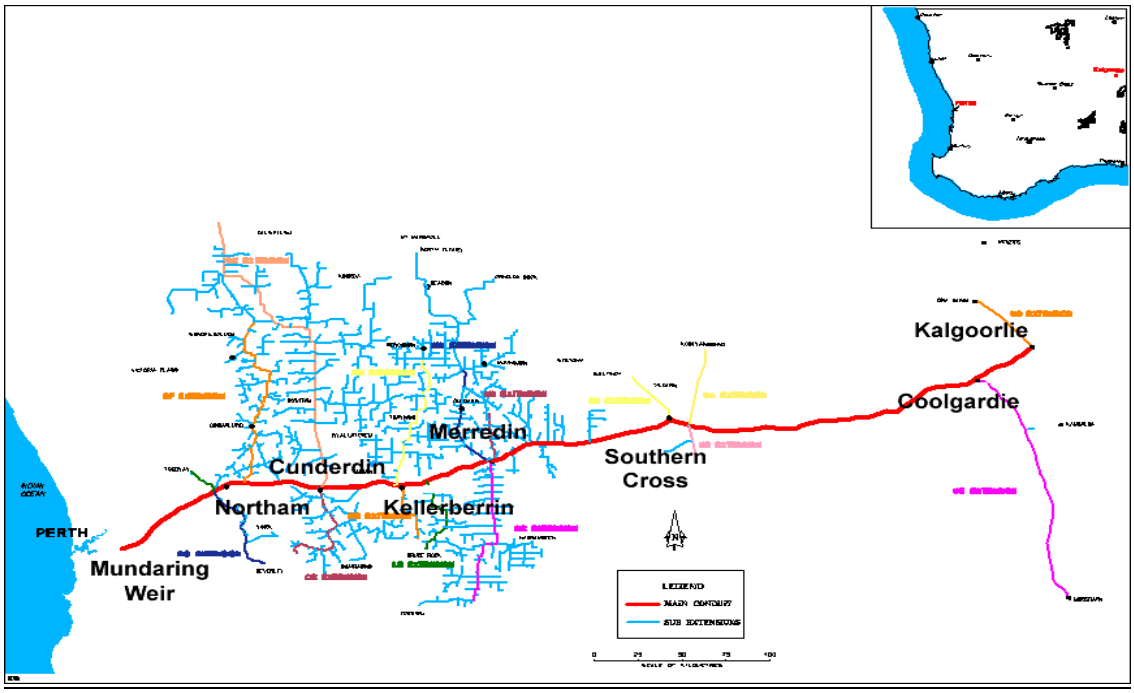

Figure 1.1: Goldfields & Agricultural Water Supply System (Water Corporation, WA)

Water Corporation is the owner and operator of the G&AWSS. It conducted Cu(II) dosing in the field to test the feasibility and efficacy of copper inhibition. Copper was dosed in two locations: Merredin reservoir (in 2005) and reticulating pipes at the C-K extension (from Cunderdin north toward Minnivale tank). Trials at Merredin suggested that it is possible to keep the copper concentration in bulk water to the required level after about two weeks of saturation. Copper sulphate ($CuSO_4$) had been dosed

continuously in the C-K extension since April 2006. This was achieved by dosing copper sulphate solution directly into the main at the outlet of Cunderdin reservoir. Initially the copper sulphate was dosed at 0.25 mg-Cu/L in the bulk water. Later the concentration was adjusted to a higher level. It was expected that there would be some delay in achieving the required copper concentration at further points of the distribution system. At Merredin reservoir it took about two weeks to stabilize the copper concentration to the required level. In the C-K main, it was found that soluble copper concentration gradually decreased along the distribution system to an unexpectedly lower level. Consequently, the desired copper concentration could not be maintained to inhibit the growth of nitrifying bacteria at furthest points of the distribution pipe lines. This led to the accelerated decay of the disinfectant residuals at farthest points and accumulation of copper in the main in the form of sediments or in the form of adsorbed metals on the pipe walls closer to the dosing.

1.3.2 A Summary of the Fate of Dosed Copper Salt from Previous Research

Preliminary laboratory scale experiments and field data analysis was carried out as a master thesis (Zhan, 2007) to investigate the loss of dissolved Cu(II) after copper salt dosing. The achievements are summarized as follows:

- The concentration of cupric ions (Cu^{2+}) was negligible in Mundaring raw water at pH >7.0. Instead, the majority of dissolved copper were thought to be a mixture of organic Cu(II) complexes and inorganic Cu(II) compounds. However, comprehensive distribution and abundance of copper species were not identified and their relative proportions were not quantified.

- Possible factors which may control the fate of copper in bulk water samples and distribution systems were investigated: hydraulic conditions during copper salt dosing, pH, the effects from ammonia and chlorine, surface adsorption simulation using glass fibre filters as media and ferric chloride addition in bulk water samples. Adsorption onto pipe walls was considered one potential mechanism taking copper away from bulk waters. However, the copper removal via adsorption by glass fibre papers could not be used to accurately quantify copper loss in the field due to the complexity of pipe walls. On the other hand, ferric chloride in low concentrations did show considerable capacity to remove dissolved Cu(II) in various water samples. This formed a major portion of the thesis.
- A large amount of Fe and Cu were found in sediments in the distribution system (Appendix F). When considered with laboratory results from ferric chloride treatment, iron salts released from pipe corrosion were thought to be one of the major causes sweeping Cu(II) away. This finding suggested that further investigation of the impact of iron pipe corrosion on copper loss was needed. However, more delicate and systematic experiments are required for both qualitative and quantitative study.

1.3.3 Corrosion Potential in G&AWSS and Its Probable Impacts on Dissolved Cu(II)

Concluded from the previous study (Zhan, 2007), ferric salts were indicated as a major cause of copper loss in pipelines. The G&AWSS is mostly made of cement-lined steel pipes. Considering the long history of the distribution system (some parts are one hundred years old), damage to the inner cement layer could occur in some places simply due to material aging. In addition, with a large proportion of the pipeline built above ground, pipes are susceptible to temperature fluctuations ranging from 4 to 50^{o}C. It can

exacerbate the damage to pipes and accelerate the development of cracks due to excessive shrinkage/expansion caused by temperature fluctuation. When the iron surface is not protected by cement material and exposed to bulk water, it corrodes more easily depending on aqueous conditions. For instance, nitrification detected in some areas might assist the corrosion process by causing a negative Langelier Index. Chloramine can act as an oxidizer to accelerate iron corrosion as well. When corrosion happens, not only is the corroded iron surface in direct contact with dissolved copper contained in water, but also the released corrosion products can interact with dissolved Cu(II). According to the previous findings that revealed dissolved Cu(II) was removed by ferric salts present at low concentration, iron pipe corrosion could make a major contribution to removal of dissolved Cu(II) from the distribution system.

Two basic aspects of the impact of iron pipe corrosion on dissolved Cu(II) loss must be discussed and clarified in this study. One is the potential redox reactions between free cupric ions (Cu^{2+}) and an exposed iron surface. The other is the interaction between dissolved Cu(II) compounds or complexes and the released iron-containing products during and after iron corrosion.

1.4 The Objectives and the Scope of the Research

To achieve the ultimate goal of modelling dissolved Cu(II) loss in an iron pipeline, optimizing copper salt dosing strategy accordingly, the fate of dissolved Cu(II) when encountering iron pipe corrosion must be thoroughly understood. Our previous study only found dissolved Cu(II) as a mixture comprised of organic and inorganic copper compounds. Further investigation needed to be done to identify particular dissolved Cu

species and quantify their relative proportions in order to find the dominant dissolved Cu(II) species under various aqueous conditions. In addition, the major products from iron corrosion had to be confirmed and the dynamic process of their interaction with dissolved copper during corrosion had to be investigated. Furthermore, regarded as a crucial factor controlling Cu(II) solubility, the complexation between NOM and Cu(II) and their impacts on dissolved copper removal were yet to be understood.

According to the outstanding problems above, this research focused on the following aspects:

- To identify different Cu(II) species and quantify their proportions in bulk waters (including Mundaring source water) under various aqueous conditions, and confirm dominant copper species in bulk water of interest.
- To quantify dissolved Cu(II) removal in a series of water samples by individual iron corrosion product separately and Cu(II) loss through corrosion process when a series of corrosion products are released into bulk water.
- To elucidate the impact of NOM characteristics on Cu-NOM complexation and dissolved Cu(II) removal by the iron corrosion products in a series of water samples.
- To develop a simple model to predict dissolved Cu(II) loss in a corroded iron-pipe distribution system.

1.5 Research Significance

With the increasingly stringent requirements for drinking water quality demanded by the World Health Organization (WHO) and US environmental protection agency, allowable DBP levels continuously decrease and thus force more water utilities to switch to chloramination. Surveys report that 60% of US water treatment facilities are

using chloramine as a final disinfectant (Kirmeyer et al., 2004). As mentioned previously, chloramine as a secondary disinfectant has many advantages compared with chlorine, such as lower level DBP and more stable residual.

However, recognizing chloramine's potential vulnerability to the microbiological process known as nitrification, many utilities in Europe have given up using chloramine as a disinfectant. The attempt to apply copper to control or inhibit the growth of nitrifiers in drinking water distribution system could change the way chloramine will be considered. Unfortunately, dissolved copper concentration in distribution systems was found to decrease with distance, especially in the pipe line. After acknowledging iron pipe corrosion as one of the major causes of copper loss, this research focused on the impact of iron pipe corrosion on the fate of dissolved copper. At the end, suggestions on how to establish an effective inhibition system and maintain chloramine stability are given for water utilities.

1.6 Composition of the Thesis

This research was triggered by challenges encountered in the chloraminated drinking water distribution system where copper sulphate is dosed as an inhibitor against the growth of nitrifying bacteria. Based on the findings of a previous study that acknowledged iron pipe corrosion as one of the major causes to the loss of dosed copper, further qualitative and quantitative study have been carried out in this research in order to fully understand corrosion related copper removal and model copper loss in the distribution system.

Chapter 1 begins with advantages and disadvantages of choosing chloramine as a final disinfectant. The strategy of inhibiting nitrifying bacteria using cupric sulphate is introduced and copper loss encountered in G&AWSS is discussed. The achievements from previous research is summarized and given as a ground on which further study is based. Then, the main purpose and significance of this research are highlighted in the first chapter.

Chapter 2 recounts valuable information reviewed from previous research related to the theme of the thesis. Critical points from historical research have been reinforced. The important aspects of the research are emphasized.

Chapter 3 details water sample collection, preparation of bulk water samples, general methods about water analysis and reagent preparation involved in every experiment. A general experimental procedure is schemed and illustrated.

Chapter 4 discusses Cu(II) solubility and Cu(II) speciation. It summarizes dominating Cu(II) species under various aqueous conditions.

Chapters 5 to 9 comprise the main part of the thesis. Chapter 5 and Chapter 6 provide details of experiments on dissolved copper removal by iron corrosion products present at low concentrations. Chapter 5 investigates Cu(II) removal by ferrous and ferric ions which can be released from iron surface when corrosion occurs. Chapter 6 investigates Cu(II) removal by ferric hydroxide flocs which can be formed from released ions afterwards. Results and conclusions are given in each experiment. Chapter 7 processes experimental data from Chapter 5 and Chapter 6 and quantifies dissolved copper removal at each stage of iron pipe corrosion. Chapter 8 elucidates the mechanisms

governing Cu-NOM complexation and the impact of NOM on the fate of dissolved copper encountering corrosion products by analysing UV absorbance, DOC and the apparent molecular weight profile of experimental bulk waters. Chapter 9 establishes a simple model to predict copper loss in a corroded iron pipeline using Aquasim®.

Chapter 10 summarizes the achievements from this research. Meanwhile, suggestions for further work and inhibition strategies for water utilities are given.

CHAPTER 2

LITERATURE REVIEW

2.1 Introduction

Two basic aspects were studied in earlier research (Zhan, 2007). One was copper solubility in bulk water. The other aspect was possible factors affecting the fate of dissolved copper. It found little dosed copper could be lost as sediments or filterable particles in Mundaring water at the pH (7.8~8.2) usually maintained in the distribution system. Although it recognized that the majority of dosed copper existed in dissolved forms, it only divided them into two fundamental groups: inorganic and organic copper compounds. To further understand the fate of dosed copper, more studies were required to understand copper speciation and quantify the composition of dissolved copper under various aqueous conditions. Iron pipe corrosion was elucidated in our early study as the main possible reason leading to copper loss. However, it was yet to be known how corrosion could affect dissolved copper in distribution systems. The reason behind the connection between corrosion and copper loss was yet to be elucidated. In addition, natural organic matter (NOM), which ubiquitously exist in a diversity of natural water sources, were believed to play an important role in aqueous copper speciation and consequently could impact interactions between dissolved copper and corrosion. In terms of the context, detailed literature review was undertaken and provided below:

2.2 Copper(II) Toxicity and Inhibition

The use of cupric sulphate ($CuSO_4$) in lakes, reservoirs and other managed bodies remains the most effective algicidal treatment (Elder and Horne, 1978; Whitaker et al., 1978; 1983; Haughey et al., 2000). However, copper speciation can affect its toxicity and bioavailability. Speciation is important because only certain forms of a given metal are biologically available. Speciation of many biologically active trace metals is controlled by complexation with strong organic ligands (Bruland et al. 1991; Sunda, 1994). Complexation generally lowers the biological availability of a given metal because the free metal ions are the most biologically available forms (Sunda, 1994). Copper toxicity is attenuated by association with organic matter, the complexed form of metal being generally less toxic than the free form (Tessier and Turner, 1995; Moffett and Brand, 1996). Nevertheless, encouraging bench scale results were achieved when copper sulphate was dosed in bulk water containing NOM to inhibit nitrifying activity, 250 µg-Cu(II)/L dissolved copper was found effective to inhibit ammonia oxidizing bacteria growth (Koska, 2008). Copper speciation in natural water bodies has been extensively studied and this information rendered insights into likely forms of copper under specific aqueous conditions in distribution systems.

2.3 Copper solubility and speciation

2.3.1 Complexation between Cu(II) and Ammonia

In a chloraminated distribution system like G&AWSS, chlorine and ammonia are added to form chloramine. In order to maintain the chemical stability of chloramine and

maintain the water slightly encrustive (scale forming), pH is controlled at 8.0. Sillen and Martell (1971) gave a series of equilibrium constants for Cu-Ammonia complex formation. The higher the pH the more ammonia is present. At pH 8.5, the fraction of ammonia present is 5% of total ammonia-N. Current total-ammonia (NH_3+NH_2Cl) levels are in the range of 0.8 mg/L or 47 μM. Five percent of 0.8 mg/L is only 0.04 mg/L or 2.35 μM. At this concentration, the predominant species will be Cu^{2+} (about 95% of copper). This calculation was made assuming only Cu^{2+} and ammonia are present in the water. With possible combinations of other metals and ligands present in the water, it is expected that the Cu-NH_3 complex will be much lower in concentration. Our previous research (Zhan, 2007) confirmed that the Cu-NH_3 complex is negligible using Milli-Q water dosed with chlorine and ammonia at the concentrations required in G&AWSS.

2.3.2 Cu(II) Solubility in Carbonate Buffered Water and Separation of Cu(II)-containing Particles

Snoeyink and Jenkins (1980) summarized the status of various inorganic copper compounds (e.g. $CuCO_3^o$, $CuOH^-$) when they were in equilibrium with tenorite (CuO) in carbonate buffered water. Carbonate alkalinity is governed by the partial pressure of CO_2 in the atmosphere, so the extent of exposure to air of a bulk water system impacts on the solubility of inorganic copper. Both open and closed systems and a situation in between can be expected to be present in G&AWSS. Depending on different ambient conditions, for instance, open or closed system or the content of NOM, the solubility of copper in bulk water is controlled by equilibrium between the soluble copper complex and the metastable solid phase such as cupric hydroxide ($Cu(OH)_2$), tenorite (CuO) etc (Broo et al., 1999). The size of $Cu(OH)_2$ particles varies with pH. At pH 8, which was

the normal pH of the water source studied in this research (Mundaring), the size of $Cu(OH)_2$ particulates was reported to be about 400 nm (Sun and Skold, 2001), increasing with ascending pH. Our laboratory experiments proved that both $Cu(OH)_2$ and CuO particles could be removed by 0.2μm membrane filters (Zhan, 2007), which therefore were chosen to filter particulate copper formed in bulk waters.

2.3.3 Impacts of Natural Organic Matter on Copper Solubility and Organo-copper Complexation

Metal fate and transport is strongly influenced by metal speciation. In particular, naturally occurring organic ligands can bind metals in aqueous solution. Natural organic matter (NOM) is a heterogeneous mixture of potential metal binding sites. Within NOM the macromolecular portions are termed humic and fulvic acids (Smith and Kramer, 2000). Wagemann and Barica (1978) claimed that only 0.5% of total Cu(II) could be found as cupric ions in natural water systems. Breault et al. (1996) found that in copper contaminated stream water, 84–99% of dissolved copper was organically bound. The majority of dissolved copper, existing in natural water bodies, is believed to be in the form of Cu-NOM complexes, because NOM contains various ligands which can bind with soluble copper, forming soluble or colloidal compounds (Lehman and Mills, 1994). Edwards and Nicolle (2001) reported the effects of NOM on copper corrosion by-product release and found that NOM can even interfere with the formation of a solid scale layer of $Cu(OH)_2$ and dramatically increase soluble copper concentration in water. Dodrill et al (1996) reported that even trace (0.1 mg/L) levels of NOM produce marked increases (>0.8 Cu mg/L) in copper release to water, while further increase in NOM concentration produces only slight additional increases to copper concentration. Hullebusch et al. (2003) suggested a proportional relation between organic copper

compounds and dissolved organic carbon (DOC), although the bioavailability of copper bound to specific organic matter is not fully understood. Sarathy and Allen (2005) found that conditional stability constants for copper–ligand complexes for dissolved organic matter (DOM) steadily increased with pH, indicating that the copper–ligand complexes become more stable at higher pHs. Louis et al (2009) concluded the effect of salinity on copper-NOM complexation by showing the increasing trend of distribution of apparent copper-dissolved-natural-organic-matter (DNOM) stability constants towards higher salinities. Despite the presence of various types of organic matter, the structure of fulvic acid (FA) and humic acid (HA) and their interactions with Cu(II) have been thoroughly studied. Binding properties of organic matter for Cu suggested evenly distributed proportions of strong and weak binding mechanisms, of which formation of organometallic compounds and chelating complexes with functional groups of humic substances seemed to be the major strongly and moderately binding mechanisms, in parallel with cation exchange as weak bounds (Twardowska and Kyziol, 2003). Gamble et al. (1980) demonstrated useful and convenient calculation procedures for the fulvic acid-Cu(II) complexing and chelation equilibrium, indicating the heterogeneity of naturally occurring ligands. By controlling pH values, copper complexometric titration gives an end point able to distinguish between intra-molecular bi-dentate chelation and inter-molecular pseudo-chelation during the complexation between Cu(II) and fulvic acid (Gamble et al., 1985). Gamble et al. (1985) also pointed out the aggregation employed by Cu(II) when binding poly molecules. Perdue and Lytle (1983) developed a Gaussian distribution model for modelling complex ligand mixtures in homogeneous solutions. However, due to the complexity of a mixture of binding ligands involved in aquatic humus, no single chemical model is suitable to describe the complexation between Cu(II) and humic substances. Smith and Kramer (2000) modelled Cu(II) binding to Suwannee River fulvic acid (SRFA) using multiresponse

fluorescence. The resultant multi-response data were fit to a five-site speciation model for Cu-SRFA interactions. However, due to the heterogeneity of NOM, the results can only be interpreted as qualitative-possible average sites. The dynamic process of organo-copper complexation was also studied. Calculated association rate constants indicate that copper complexation by DNOM takes place relatively slowly. The time needed to achieve a new pseudo-equilibrium induced by an increase of copper concentration is estimated to be from 2 to 4 hours (Louis et al., 2009).

Dryer et al. (2008) compared the NOM contained in Mundaring water with that in Suwannee River fulvic acid (SRFA) via differential absorbance spectral analysis. Their research concluded that Mundaring NOM lacks phenolic chromophores, which are the major constituents of the hydrophobic fraction of NOM. The general postulate was adopted that phenolic chromophores contribute to salicylic type of bidentate chelating sites, which is believed to preferentially chelate with Cu^{2+} and form relatively stable chelates (Gamble et al., 1980). Controversially, one striking finding revealed that the removal of the hydrophobic acid fraction had little effect on Cu binding. In other words, Cu binding affinity to phenolic sites are weaker than carboxylic sites (Olsson et al., 2007). Stability of the Cu-NOM complex is reported to be quite strong at higher pH (8 or above) and weaker at lower pH although more binding sites are available on NOM to form complexes at lower pH (Takacs et al., 1999). Our previous study also showed high solubility of copper in natural water (Zhan et al., 2009). Therefore, NOM was believed to considerably enhance copper solubility in the experimental bulk waters.

In G&AWSS, nitrification has been acknowledged as one of the major causes accelerating chloramine decay. It also is reported that nitrifiers can excrete organic

compounds that lead to proliferation of heterotrophic micro-organisms (Lipponen et al., 2002). Krishna and Sathasivan (2010) found that organic matter in natural waters could be broken down to smaller molecules when they react with chlorine or chloramine. These soluble microbial products can also increase the copper concentration by forming organic copper complexes.

2.4 Iron Pipe Corrosion Potentials and Corrosion Products

2.4.1 Iron Pipe Corrosion Potentials and Impact Factors

Our earlier study (Zhan, 2007) showed that iron-compounds present in natural water or released from distribution systems, mainly because of pipe damage or corrosion, can be responsible for a proportion of dissolved copper loss. Vulnerability of distribution systems to corrosion depends on chemical properties of water delivered (e.g. pH, alkalinity, dissolved oxygen, total dissolved solids) and its physical characteristics (temperature, velocity) as well as the nature of pipe materials (AWWARF, 1996). Aquatic conditions with low chloramine (less than 0.3 mg/L) and low dissolved oxygen (DO) can enhance severe iron release from aged cast iron pipes due to the breakdown of "passivated-outer-layer of scale" in reductive environment (Wang et al., 2009). Generally, the corrosion rate increases with increased DO concentration (Gedge, 1992). When DO is present in water, higher amounts of iron release is observed during stagnation in comparison to flowing water conditions (Sarin et al., 2004). Due to economic restriction, iron pipes are still in use in a considerable proportion of old water supply systems in Australia. Some parts are more than a hundred years old. Pipelines in

G&AWSS can also be subjected to an extensive temperature fluctuation causing cracks in cement-iron pipes.

In addition, microorganisms are present in many distribution systems and they can influence corrosion in a number of ways (Holden et al., 1995; Emde et al., 1992). The role of biological activity in a water pipe can be mixed but is generally considered detrimental to most aspects of iron corrosion (McNeill and Edwards, 2001). Various bacteria can affect iron speciation by reducing ferric ions or oxidizing ferrous ions (Nemati and Webb, 1997; Chapelle and Lovley, 1992). Biofilm could promote corrosion by converting Fe to Fe(II) and Fe(III) via iron bacteria (Teng et al., 2008).

Previous research has also reported possible links between certain corrosion problems and nitrification (Edwards and Triantafyllidou, 2007; Douglas, et al., 2004; Powell, 2004). It has been suspected that the reduction of pH from nitrification increased corrosion of lead pipe (Douglas, et al., 2004). Elevated copper concentrations at the tap were also linked to the action of nitrifying bacteria (Murphy, et al., 1997a). The lower pH resulting from nitrification could be a contributing factor (Zhang, 2009). Nitrification can also influence corrosion through factors other than pH. It can increase the growth of bacteria that might stimulate microbiologically influenced corrosion (MIC) (Cantor et al., 2006). Zhang and Edwards (2007) reported that cast iron could also reduce nitrite/nitrate to ammonia, indicating that nitrified water might cause iron pipe corrosion. Disinfectant residuals, in general, increase corrosion rate (Benjamin et al., 1996). Both chloramination and nitrification are taking place along G&AWSS and hence these can be expected to exacerbate the corrosion problem.

When copper sulphate is dosed into G&AWSS to inhibit nitrification, potential redox reactions involved are listed as follows (Snoeyink and Jenkins, 1980):

Reaction	Standard Electrode Potentials at 25°C (Volt)
$O_2(ag) + 4H^+ + 4e^- = 2H_2O$	+1.27
$NO_3^- + 2H^+ + 2e^- = NO_2^- + H_2O$	+0.84
$Cu^{2+} + 2e^- = Cu_{(s)}$	+0.34
$Fe^{2+} + 2e^- = Fe_{(s)}$	-0.44

Arranging them in an order of oxidizing capacity, one would obtain the following: $O_2 > NO_3^- > Cu^{2+} > Fe^{2+}$. In bulk water with aerating conditions or nitrification, which are considered possible aquatic conditions in the distribution system, direct reaction between Cu^{2+} and exposed iron can be overruled by the presence of stronger oxidizers (O_2 and NO_3^-). Besides, monochloramine, which has electrochemical potential of +1.25 at pH 8 (Snoeyink and Jenkins, 1980), is also a stronger oxidizer than Cu^{2+} that can corrode element iron. Our earlier study (Zhan, 2007) found little dissolved copper existing in natural water in the form of cupric ions. This finding further excluded the possible reaction between free cupric ions and iron. Therefore, the effect of iron pipe corrosion on dissolved Cu(II) can literally be referred to as dissolved Cu(II) compounds or complexes removal by released corrosion products.

2.4.2 Iron Corrosion Products

Iron corrosion scales include goethite (a-FeOOH), lepidocrocite (g-FeOOH), magnetite (Fe_3O_4), siderite ($FeCO_3$), ferrous hydroxide ($Fe(OH)_2$), ferric hydroxide ($Fe(OH)_3$), ferrihydrite ($5Fe_2O_3 \bullet 9H_2O$), green rusts (e.g. $Fe_4^{II}Fe_2^{III}(OH)_{12}CO_3$) and calcium carbonate ($CaCO_3$) (Benjamin et al., 1996 ; Tang et al., 2006). The scale layer may provide passivation by limiting the diffusion of oxygen to the metal surface. On the

other hand, the scale can also contribute iron to the water. This includes both soluble species from scale dissolution as well as scale particles that detach from the surface (McNeill and Edwards, 2001). High concentration of readily soluble Fe(II) content is present inside scales (Benjamin et al., 1996; Tang, et al., 2006). Therefore, ferrous ions can be released into bulk water during corrosion and oxidized to ferric particles. McNeill and Edwards (2001) did a comprehensive review on iron pipe corrosion in distribution systems. According to their research, dissolved oxygen (DO) plays an important role in iron corrosion.

$Fe + 0.5O_2 + H_2O \leftrightarrow Fe^{2+} + 2OH^-$

DO also play a role in the oxidation of ferrous ions.

$Fe^{2+} + 0.25O_2 + 0.5H_2O + 2OH^- \leftrightarrow Fe(OH)_{3(s)}$

Scale formation is a complicated process that depends on a variety of physical and chemical conditions in each particular system. It is difficult to model scale behaviour (McNeill and Edwards, 2001). However, McNeill and Edwards (2001) listed a few typical iron corrosion compounds in which ferrous hydroxide and ferric hydroxide are ranked top two. Therefore, among a diversity of possible corrosion products, pre-formed ferric hydroxide flocs were chosen in this research as one of the representatives of corrosion products which could react with dissolved Cu(II) in distribution systems. Sarin et al. (2004) also reported that iron is released to bulk water primarily in the ferrous form. However, soluble ferrous compounds are converted into ferrous solids (e.g. $Fe(OH)_2$), which may then be converted to ferric solids (e.g. $Fe(OH)_3$) after reaction with oxygen (AWWARF, 1996). When a new surface of iron is exposed to bulk water during the initial stage of corrosion, ferrous ions and ferric ions may exist for a short time when they are released from iron-corroded crevices. The interactions between ferrous or ferric ions and dissolved copper also need to be investigated.

2.5 Aqueous Cu(II) Removal

Heavy metals removal by ferric salts is extensively documented. Streat et al (2008) reported the effective arsenic removal from wastewater by granular ferric hydroxide through the BET (Stephen Brunauer, Paul Hugh Emmett, and Edward Teller) surface adsorption process. Ridge and Sedlak (2004) reported that Cu^{2+} and Cu-EDTA compounds up to 13 mg-Cu/L were noticeably removed by addition of $FeCl_3$ and adsorption onto hydrous ferric oxide (HFO) in wastewater treatment. Iron oxides are found as good absorbents to remove high concentrations of cupric ions and ammonia-complexed copper in wastewater (Benjamin et al., 1996). It was suggested that the absorbent surface was composed of different binding sites: the strength of different binding sites varied considerably. Adsorption was also a function of metal ion concentrations, absorbent concentration and pH. At small adsorption densities, the adsorption can be described by the Langmuir Isotherm (Benjamin et al., 1996).

In addition, presence of organic matter (e.g. humic substance) is reported to have effect on removal of metal ions. Humic substances (HS) are found in all soils and waters that contain organic matter. They bind metals, molecules, ions and other biopolymers (Davies et al., 1998). Hankins et al. (2005) reported that removal of heavy metals, such as Pb^{2+} and Zn^{2+}, can be enhanced by binding the metal ions to humic acid (HA) and hence facilitate coagulation and flocculation through a complexation-flocculation process. Lai and Chen (2001) studied the capacity of iron-coated sand to remove cupric ions at relatively high concentrations (3~6 mg-Cu(II)/L) and found high removal efficiency at low pHs (< 7). As humic substances ubiquitously exist in natural waters, aqueous Cu(II) complexation with HS at very low copper concentrations (< 1 mg/L) and

removal of Cu-HS complexes by trace ferric salts (< 2 mg/L) are investigated in this research.

2.6 Summary of Literature Review

The literature review above can be summarized as follows:

1. The effect of chloramination on the solubility of Cu(II) can be neglected.
2. Cu(II) solubility can be affected by a carbon buffered system. The increased partial pressure of CO_2 above the water surface can increase Cu(II) concentration through increased carbonate forming inorganic copper compounds.
3. The solubility of Cu(II) in bulk water is controlled by the equilibrium between the soluble copper complexes and metastable solid phase such as cupric hydroxide ($Cu(OH)_2$) or tenorite (CuO), depending on open or closed system.
4. Natural organic matter (NOM) plays an important role in governing copper solubility in natural water bodies. Copper solubility in Mundaring water is believed to be primarily controlled/enhanced by NOM. Therefore, Cu-NOM complexes are believed to be the dominant forms of dissolved Cu(II) in G&AWSS.
5. Both hydrophobic and hydrophilic fractions of NOM have been reported to be able to chelate with dissolved copper, although the preferentiality of Cu(II) binding to them is not clear.
6. Organic compounds excreted via nitrification might enhance dissolved copper concentration.
7. Iron pipe corrosion is subjected to both physical and chemical aspects, e.g. extensive temperature fluctuation, pipe aging, chloramine, DO, nitrification etc. Low chloramine residual and DO can cause and accelerate aged iron corrosion and release Fe salts.

8. The direct interaction between cupric ions and exposed iron surface through redox reaction in G&AWSS can be excluded. The effects of iron pipe corrosion on dissolved Cu(II) loss therefore literally refer to the interaction between released iron corrosion products and dissolved Cu(II) compounds or complexes.
9. Ferrous ions can be released into bulk water during corrosion and converted to ferric ions or ferric solids after reacting with oxygen.

Based on these previous studies, Cu(II)-NOM complexes are unanimously acknowledged as the major soluble copper form in natural water, though the structure and preference of copper chelation with certain fractions of specific organic matter remains unresolved. High concentrations of cupric ions and complexed copper (up to 500 mg/L) in wastewater can be removed by adsorption to iron oxide media and filtration. However, from the perspective of protecting low concentrations of dissolved Cu(II) in distribution systems (e.g. as a nitrification inhibitor), little research has been done on dissolved Cu(II) removal by iron pipe corrosion products released from corroded or damaged pipes in distribution systems like G&AWSS, with the Cu(II) present at low concentrations(< 2 mg/L). According to the 8th and 9th items summarized above, ferrous ions, ferric ions and ferric hydroxide flocs were chosen as the representatives of iron corrosion products in this research to study dissolved Cu(II) removal in the distribution system. Dissolved Cu(II) loss during iron pipe corrosion can be divided into two stages: Stage I: Cu(II) removal by fresh ferrous and ferric ions in a short period when they are released from corroded cavities; Stage II: Cu(II) removal by ferric hydroxide flocs formed afterwards. The laboratory experiments were generally designed based on the concept of the two-stage corrosion process. Furthermore, impacts of NOM on Cu-NOM chelation and their removal by corrosion products under various aqueous conditions are yet to be investigated.

CHAPTER 3

SAMPLE MANAGEMENT AND METHODOLOGY

3.1 Sample Sources, Collection, Preservation and Preparation

3.1.1 Sample Sources, Collection and Preservation

Mundaring raw water (MRW): The majority of the water samples used in the laboratory experiments were sourced from the outlet of Mundaring weir (the feed water for G&AWSS) upstream of the chloramination point. At the chloramination point, both ammonia and chlorine were dosed simultaneously. Containers were pre-cleaned with sodium hypochlorite (2~3%) to remove indigenous dissolved organic carbon (DOC). Milli-Q Water (18 MΩ/cm, <100 ppb-C/L) was used to wash all the containers afterwards. All containers were then rinsed with Mundaring raw water (MRW) three times prior to sample collection. MRW was stored in the refrigerator at 4^{o}C and water quality analysis was undertaken immediately after every sample collection. Our group had conducted regular sample collection from Mundaring Weir every month from 2008 to present. The quality of Mundaring water varied slightly in terms of pH (7.6~8.1), DOC (2.4~3.1 mg-C/L) and UV_{254} absorbance (0.031~0.038 cm^{-1}).

Prior to any bulk water experiment, Mundaring water was filtered through 0.45 µm pre-washed cellulous acetate membrane to remove suspended solids or particles before

copper salt dose. Samples for ongoing experiments were normally stored in plastic jars at room temperature. All the stand-by samples were preserved in the refrigerator at 4^{o}C and intact except for sampling and analysis.

Nitrified water (NW): Two identical reactor systems, each assembled in series with five 20 L reactors (R1 to R5), were set up in the laboratory. Automatic flow rate and temperature control were installed for the reactors. Chloraminated Mundaring water was fed into the reactor, with mass ratio of (Cl:NH_3-N) 4.5 to 1 maintained in the 25-litre feeding tank. In the start-up period, chlorine was maintained at about 1mg/L. To expedite nitrification and to obtain the DS inoculums, chloraminated water collected from G&AWSS was added into the reactors except R1. The chloramine concentration was gradually increased up to 2.5 mg/L in the feeding tank. Water (20 L) was fed into the system continuously every day to gain retention time of 20±2 hrs. Water temperature was maintained at 20±2^{o}C in the reactors R1~R3 whereas 23±2^{o}C was maintained in R4 and R5 in order to achieve accelerated microbial activities. By varying hydraulic conditions, temperature and chloramine residuals, nitrification occurring in the distribution system can be simulated in the laboratory. In this research, NW was collected from R4. NW contained 0.10 mg/L NH_3-N, 0.2 mg/L NO_2-N and 0.1 mg/L NO_3-N. The levels of these inorganic nitrogen products indicated that severe nitrification occurred in NW (Sathasivan et al., 2008).

The characteristics of the source waters are shown in Table 4.1, Chapter 4.

3.1.2 Preparation of the Bulk Water Samples

In addition to the main source waters (MRW and NW), some other bulk waters were made in the laboratory offering variables needed for investigation on copper solubility and dissolved copper removal under different aqueous conditions. The preparation and characteristics of these samples are described as follows:

Milli-Q Water (MQW): Milli-Q water (ultra-pure water) was produced by Purelab UHQ-II in order to confirm Cu(II) solubility in an open system (bulk water surface open to the atmosphere) at various pH. Milli-Q water was made by sending tap water through a series of cartridges sequentially containing or filled with reverse osmosis (RO), activated granular carbon, ion exchange and micro-filtration. The product had a resistivity of 18 MΩ/cm. DOC concentration was less than 100 ppb. In the experiment undertaken in the closed system, nitrogen gas was used to purge CO_2 out of the sealed sample bottle.

$CaCO_3$ buffered water (CaBW): In order to confirm Cu(II) solubility enhanced by inorganic carbon through formation of inorganic copper compounds in carbon buffered bulk water, $CaCO_3$ was used to make buffered solution. Calcium carbonate was dosed into Milli-Q water to make a $CaCO_3$ concentration of 50 mg/L. Ion strength was maintained at 1.5 mmol-eq/L by adding NaCl. Considering aqueous carbon content is controlled by the partial pressure of CO_2 in the air, both open and closed systems were experimented. In the open system, the bulk water was simply left in an uncapped plastic container. In the closed system experiment, the water sample was sealed airtight using plastic wraps after adding $CaCO_3$.

Mundaring water after coagulation (MCW): Ferric chloride was employed as the coagulant to remove coagulable NOM in MRW. Coagulation experiments showed that

maximum DOC removal was achieved by adding a coagulant dose of 40 mg-$FeCl_3$/L at pH 5~5.5, which is in agreement with Kastl et al (2004). A jar tester was used to control the coagulation process. The stirring speed was set at 200rpm for the initial 2 minutes, after which ferric chloride was dosed. Stirring of 20 rpm was then applied for another 20 minutes afterwards. During and after stirring and coagulation, the pH of the bulk water was adjusted and maintained at 5~5.5 using a HACH40d pH meter. HCl (1 N) and NaOH (1 N) were used to modify pH values. After the coagulation was completed, bulk water was kept intact for sedimentation and then filtered through 0.45 µm and 0.2 µm polycarbonate membranes consecutively to remove flocs. NaOH (1 N) was titrated into the filtrate to increase the pH to 7.8±0.2. The concentration of dissolved Fe(II) or Fe(III) in the filtrate was determined using atomic absorption spectroscopy in SGS.Pty.Ltd (WA) and found to be <0.02 mg/L.

Humic acid water (HAW): Humic acid water was prepared by diluting stock HA solution (3 g-C/L) with MilliQ water (18 MΩ/cm, DOC<100 ppb). Humic acid was acquired from Sigma Aldrich®, containing 20% ash. HA solid was dissolved in MilliQ water first then centrifuged at 4000 rpm for 5 minutes to separate ash and other insoluble particles from the solution. The supernatant was withdrawn and filtered through 0.45 µm membrane to further remove insoluble impurities. The final filtrate was treated as the stock HA standard solution (3 g-C/L). This solution was diluted to give HAW, which contained 2.5±0.1 mg-C/L DOC and had UV Abs=0.248/cm (254 nm, 10 cm quartz cell). This concentration of DOC was chosen to be as equal as possible to the DOC concentration in MRW.

The water quality characteristics of the bulk waters are shown in Table 4.1, Chapter 4.

3.2 Preparation of Standard Solutions, Dissolved Cu(II) measurement and Analytical Methods

Copper sulphate stock solution: Standard $CuSO_4$ stock solution (1 g/L as Cu) was prepared by dissolving $CuSO_4 \bullet 5H_2O$ in Milli-Q water. The pH of the standard solution was maintained at 4.0 so that aqueous Cu(II) could be maintained as cupric ions. The volume of bulk water samples was 1.5 L, and consequently 0.375 mL~1.5 mL standard solution was dosed using volumetric pipettes to achieve a target concentration of 0.25~1.0 mg-Cu/L. The relative change of sample volume was therefore within 0.1%.

Ferrous and Ferric stock solutions: $FeCl_3 \bullet 6H_2O$ (crystal) and Milli-Q water were used to make ferric stock solution of 1 g-Fe^{3+}/L. The $FeCl_3$ solution was maintained at pH 3±0.2 and ready for addition into experimental samples. $FeSO_4 \bullet 7H_2O$ was used to make ferrous stock solution of 1 g-Fe^{2+}/L. To avoid gradual oxidation of Fe^{2+} to Fe^{3+}, ferrous standard solution was made instantly before the addition without delay.

$Fe(OH)_3$ flocs suspension were made by titrating $FeCl_3$ standard solution (1 g-Fe/L) with NaOH (5 N). The $FeCl_3$ solution was maintained at pH 3±0.2 to keep all Fe(III) in the form of free ferric ions. $FeCl_3$ solution was titrated by NaOH (5 N) at increments to make the target pH 5.0~5.1. A magnetic stirrer was used at 150 rpm during the titration to keep $Fe(OH)_3$ flocs uniformly distributed in the suspension. With the fixed pH value and stirring speed, the variation of the size of $Fe(OH)_3$ flocs was maintained within a narrow range. The particle size distribution of $Fe(OH)_3$ was analysed by Mastersizer2000 Particle Size Analyzer (See Appendix B).

Copper measurement: The total Cu(II) concentration was analysed using the bicinchoninate spectrophotometric method (Hach method 8506; HACH DR2800). This method has a measuring range of 0.04~5 mg/L with ±20 µg/L accuracy. Samples were digested using nitric acid (1:1) at pH 4~6 for total copper measurement. A potable pH meter (HACH40d) with temperature compensation was used to measure pH values. Measurement of pH had an accuracy of ±0.2. As for measuring the dissolved copper concentration, samples were filtered through a 0.2 µm PC (polycarbonate) membrane and total Cu concentration in the filtrate was measured. In order to minimise interaction between the sample and membrane and to prevent speciation changes, the volume of the filtrate was chosen to represent approximately 50% of the volume of the raw sample (Hoffmann et al., 1981). For instance, to obtain 50 mL filtrate, 100 mL sample water was added and 50mL was filtered through the filter paper.

Organic carbon measurement: Water samples were filtered through a 0.45 µm membrane before the analysis of UV absorbance and DOC. As for the spectroscopy analysis, water samples used as differential absorbance references were filtered through a 0.2 µm polycarbonate membrane in order to keep consistency with the filtrates of samples containing dissolved copper. Both spectroscopy analysis and UV abs was measured in a 10 cm quartz cell by Helios UV/Vis Spectrophotometer. UV absorbance was measured at 254 nm. DOC was analysed by GE 5310C TOC analyser with ±100 ppb accuracy.

Molecular weight distribution analysis: The apparent molecular weight distribution of the UV254-absorbing DOC in the samples was analysed by high performance size exclusion chromatography (HPSEC) according to the method of Allpike et al., (2005) and Warton et al. (2007), except that a Agilent 1100 Series HPLC system was used and

that polystyrene sulfonate standards (840 Da, 1290 Da, 3610 Da, 6520 Da, 15200 Da, 81800 Da) were used for molecular weight calibration. SEC was performed using a TSK G3000SWxl (TOSOH Biosep, 5 µm resin) column and a Agilent 1100 HPLC instrument with diode array detection at 254 nm. The column had an internal diameter of 7.8 mm and a length of 30 cm, with a void volume of 5.5 mL, as determined with dextran blue. The eluent used was the 20 mM phosphate buffer (1.36 g/L KH_2PO_4 and 3.58 g/L Na_2HPO_4.12H2O) at a pH of 6.85. Sample volume was 100 µL and the flow rate was 1 mL/minute. Samples were first filtered through a 0.45 µm nylon filter. The system was calibrated using a combination polystyrene sulfonate (PSS) standards of varying molecular weights. The calibration curve was linear (R^2 = 0.991) over the apparent MW range tested.

Soluble Cu(II), Fe(II) and Fe(III) concentrations in the source waters and bulk water samples prepared in the laboratory were measured by atomic adsorption spectroscopy (AAS) in SGS before any relevant experiment started. Total Cu(II) concentration was found to be less than 20 µg/L before the copper salt dose and the dissolved Fe(II) and Fe(III) was below 0.05 mg/L before ferrous or ferric salt addition.

3.3 The Systematic Approach of the Research and the Scheme of the Laboratory Experiments

As mentioned in the objectives of the research, the laboratory scale experiments focused on two basic aspects: one is to identify and quantify particular and dominant Cu(II) species under various aqueous conditions; the other is to investigate removal of dissolved Cu(II) by the corrosion products (ferrous ions, ferric ions and ferric hydroxide flocs) present at low concentrations (< 2 mg-Fe/L). Dissolved Cu(II) removal occurring

in each stage of the two-stage corrosion process was derived from the experimental data. Finally, a simple model predicting Cu(II) loss in the distribution system was established.

The laboratory experimental procedures are detailed in each relevant chapter. Copper speciation and solubility are studied in Chapter 4. Figure 3.1 is a flowchart of the scheme investigating dissolved Cu(II) removal by the corrosion products.

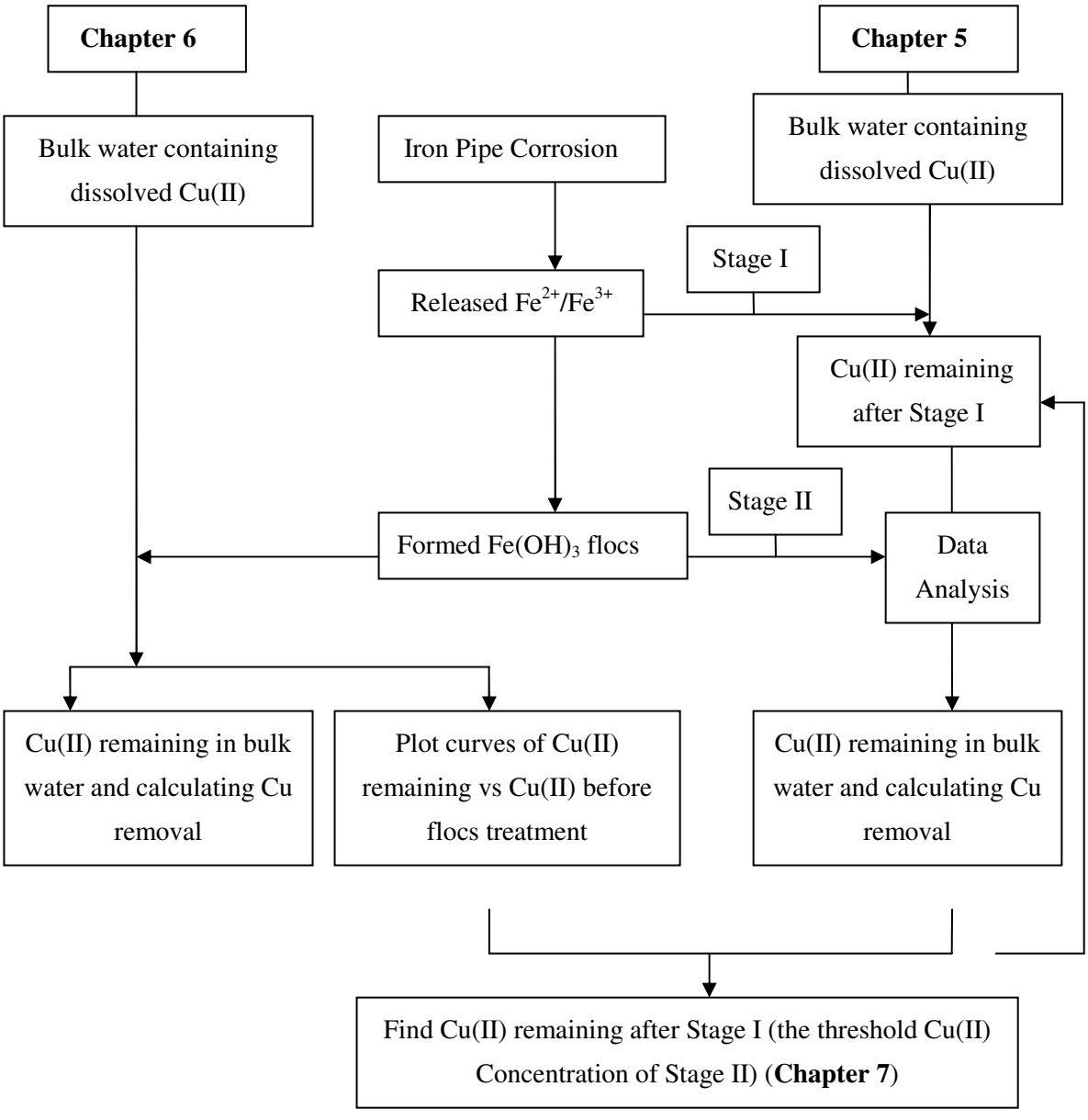

Figure 3.1: Conceptual experimental method to investigate dissolved Cu(II) removal by the two-stage corrosion process

CHAPTER 4

CHARACTERISTICS OF BULK WATERS & Cu(II) SOLUBILITY AND SPECIATION UNDER VARIOUS AQUEOUS CONDITIONS

4.1 Water Quality Characteristics of Bulk Water Samples

Water quality analysis has been undertaken in all bulk water samples described in Chapter 3. The selected water quality characteristics of the bulk water samples are presented in Table 4.1.

Table 4.1: Water quality characteristics of the bulk water samples

Water Samples	pH	UV_{254}	DOC	SUVA	Total dissolved Fe(II)+Fe(III)	Ca
	-	cm^{-1}	mg-C/L	$L \cdot mg^{-1} \cdot m^{-1}$	mg/L	mg/L
MQW	pH=6.3±0.1 or 7.9±0.2	0.003	< 0.1	_	_	_
CaBW	7.9±0.2 Open	0.0035	< 0.1	_	_	50
	Closed					50

MRW	7.9±0.2	0.035±0.002	2.6±0.1	1.35	<0.02	18
MCW	7.9±0.2	0.010±0.002	0.90±0.1	1.11	<0.05	_
HAW	7.9±0.2	0.248±0.002	2.4±0.1	10.33	<0.02	_
NW	7.9±0.2	0.026±0.002	2.5±0.1	1.04	<0.02	_

Note: MQW-Milli-Q water; CaBW-$CaCO_3$ buffered water; MRW-Mundaring raw water; MCW-Coagulated Mundaring water; HAW-Humic acid water; NW-water containing nitrifying bacteria. Refer to Chapter 3 for details of samples' preparation.

Total copper concentration was measured in Mundaring raw water and found to be less than the instrument detection level of 20 µg/L.

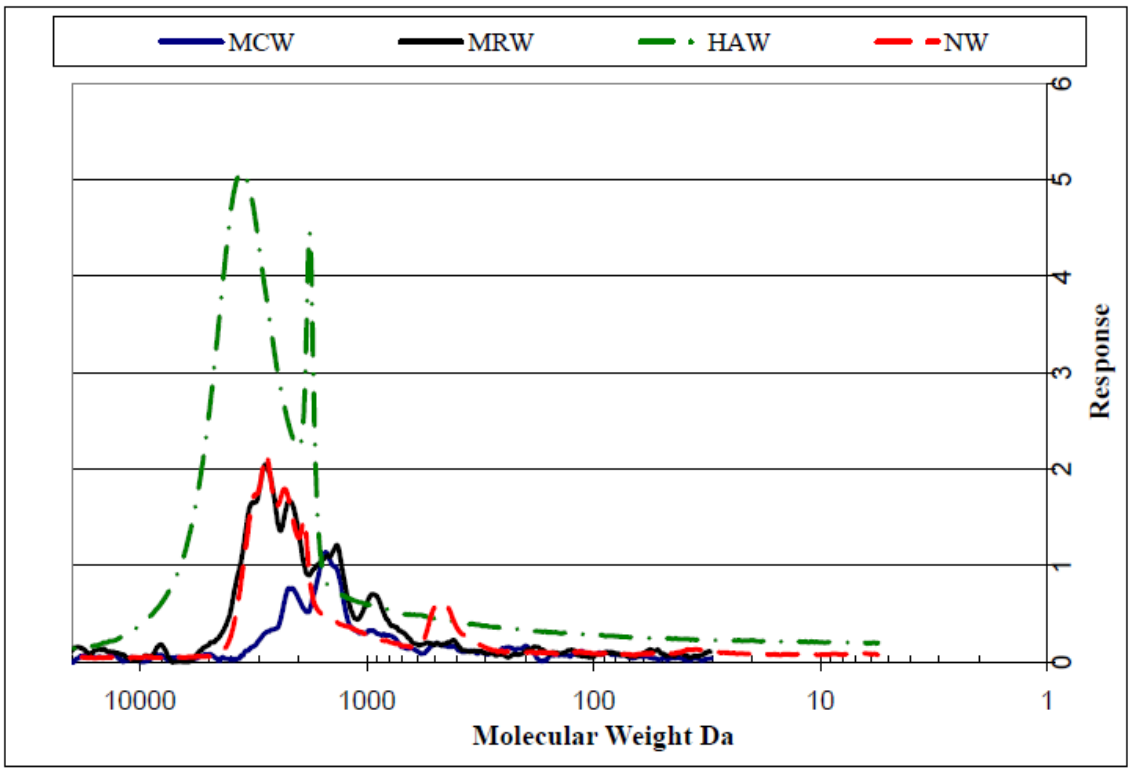

Figure 4.1: Apparent molecular weight distribution of UV_{254}-Absorbing DOC in MRW, MCW, HAW and NW

Apparent molecular weight (AMW) analysis was undertaken on four NOM-containing samples (Figure 4.1). The DOC concentration of MRW, HAW and NW were similar, while MCW had a lower DOC concentration after removal of part of the DOC via coagulation. Despite having a slightly lower DOC concentration than MRW, HAW had a much higher $SUVA_{254}$ than MRW (1.35 vs 10.33 L mg^{-1} m^{-1}, respectively (Table

4.1)), indicating a substantially higher aromatic character of HAW NOM (Weishaar et al., 2003). The majority of UV_{254}-absorbing DOC in MRW had an AMW distribution between 2000 and 3000 Da (Figure 4.1). For ease of discussion, NOM in Mundaring water was classified into two fractions: coagulable (removed by coagulation, i.e. the NOM present in MRW but not in MCW) and uncoagulable (NOM_{uc}; NOM remaining post-coagulation in MCW). The majority of the 2000-3000 Da material in MRW was removed by coagulation, leaving part of the DOC with AMW 1000-2000 Da as the predominant fraction in MCW. This is consistent with the conclusion that coagulation removes predominantly higher MW NOM (Warton et al., 2007; Chadik and Amy, 1987; Allpike et al., 2005). In the NW sample, representing MRW subjected to nitrification, there was a noticeable increase in one lower AMW UV_{254}-absorbing fraction, centred around 500 Da. Two peaks between 900~1500 Da in MRW disappeared in NW, possibly indicating production of more lower AMW material due to microbiological activity. The much higher UV_{254} response for DOC in HAW AMW compared to MRW is consistent with the much higher $SUVA_{254}$ measured in the former sample. The AMW profiles suggest that HAW NOM is comprised of much higher MW components (2-10 kDa) (Rajec et al, 1999) than MRW NOM (1-3 kDa) and clearly show that there is a substantial difference in the character of these two NOM types.

4.2 Investigation of Cu(II) Solubility and Speciation in the Bulk Waters under Various Aqueous Conditions (Laboratory Data + MINEQL+® Calculation)

4.2.1 Introduction

The possible factors which were thought to affect Cu(II) solubility in Mundaring water had been investigated in our previous research (Zhan, 2007). These factors included stirring speed during copper salt dosing, pH, $CaCO_3$ addition, chlorine and ammonia addition, NOM and bacteria. It concluded that pH, carbon buffering and NOM are the major factors governing Cu(II) solubility in natural waters. However, Zhan (2007) only elucidated that the major Cu(II) species in Mundaring raw water are comprised of particles, inorganic copper compounds and organic copper complexes and estimated their proportions. In order to further verify particular and dominant Cu(II) species in the distribution system, to quantify each particular copper species, more delicately designed experiments were required.

4.2.2 Methodology

Similar methodology used in our previous research was adopted to investigate copper solubility subject to various conditions: MilliQ water (DOC<100 ppb, 18 MΩ/cm), $CaCO_3$ buffered Milli-Q water (50 mg-$CaCO_3$/L), MRW, MCW, HAW and NW (Table 4.1).

A 1 mL aliquot was withdrawn from $CuSO_4$ stock solution (1 g-Cu(II)/L) and added into 1 L of the bulk water of interest, aiming to make a total Cu(II) concentration of 1 mg-Cu(II)/L. Bulk water samples had then been left intact at the ambient temperature (15~25^oC) for 48 hours to allow Cu-NOM complexation and the formation of CuO or $Cu(OH)_{2(s)}$ to reach equilibrium (Appendix C). Dissolved Cu(II) was measured 2, 4, 24 or 48 hours after copper dosing.

As mentioned earlier, copper solubility can be affected by the partial pressure of CO_2 in contact with the water surface (Snoeyink and Jenkins, 1980) and therefore both open and closed systems were investigated in $CaCO_3$ buffered water (CaBW). In the open system, the bulk water surface was open to the atmosphere (LgP_{CO2}=-3.50) without capping the containers during the course of the entire experiment. Nitrogen gas was used to purge CO_2 out of the sealed jar to create a closed system during the experiment and storage.

To investigate the effect of pH on copper solubility, two different pHs (6.3 and 7.8) were trialled in Milli-Q water (MQW).

The copper solubility measured in MQW and CaBW was cross-examined with the data calculated using MINEQL+® (chemical equilibrium modelling system). Due to the complexity of binding ligands in NOM, it was difficult to decide the equilibrium coefficients for Cu-NOM chelation in MRW, MCW, NW and HAW and program them into MINEQL+®. However, the quantification of Cu-NOM in these samples can be deduced from the results achieved in the other bulk water samples investigated.

4.2.3 Results and Discussion

The comparison of the results between laboratory experiments and software prediction are shown in Table 4.2.

Table 4.2: Major copper (II) species in the bulk water samples ($CuSO_4$ was dosed at 1000 µg-Cu/L in each testing bulk water)

Bulk Water Conditions	**Intermediate[1] / Equilibrated[2] Copper Species**	**MINEQL+® Calculation**	**Laboratory Data**
MQW pH=6.3±0.1, Open system	Cu^{2+}	Cu^{2+}=1 mg/L	Dissolved copper was measured at 0.98 mg/L 1 day after Cu dose
MQW pH=7.5±0.2, Open system	$Cu(OH)_2$ / CuO	Cu^{2+}=3 µg/L + $CuO_{(s)}$	Dissolved copper (< 20 µg/L) was measured both 2hrs and 2 days after Cu dose
CaBW solution, pH=7.5±0.2, Open system	$CuCO_3^o$, $CuOH^+$ and $Cu(OH)_2$ / only CuO	Total soluble Cu=9 µg/L + $CuO_{(s)}$	100 µg/L and 10 µg/L dissolved Cu were found 2 hrs and 1 day after Cu dose respectively, the latter occurs when the system is in equilibrium with CuO
CaBW solution, pH=7.5±0.2, Closed system	Cu^{2+}, $CuCO_3^o$, $CuOH^+$ and $Cu(OH)_2$	Cu^{2+}=30 µg/L, $CuOH^+$=30 µg/L, $CuCO_3^o$= 48 µg/L + $Cu(OH)_{2(s)}$	150 µg/L dissolved Cu was measured 1 day after Cu dose. The system may be in equilibrium with $Cu(OH)_{2(s)}$
MRW pH=7.9±0.2, DOC=2.6±0.1 mg-C/L, Open system	$CuCO_3^o$, $CuOH^+$, $Cu(OH)_2$ and Cu-NOM / CuO and Cu-NOM	*Dependent on availability of binding ligands of MRW NOM	950 µg/L and 840 µg/L dissolved Cu was found 2 hrs and 1 day after Cu dose respectively. The latter occurs when the system reaches equilibrium with both CuO and Cu-NOM complexes
MCW pH=7.9±0.2, DOC=0.9±0.1 mg-C/L, Open system	$CuCO_3^o$, $CuOH^+$, $Cu(OH)_2$ and Cu-NOM / CuO and Cu-NOM	*Dependent on availability of binding ligands of MRW NOM	340 µg/L dissolved Cu was found 1 day after Cu dose when the system reached equilibrium with both CuO and Cu-NOM complexes
NW pH=7.9±0.2, DOC=2.5±0.1 mg-C/L, Open system	$CuCO_3^o$, $CuOH^+$, $Cu(OH)_2$ and Cu-NOM / CuO and Cu-NOM	*Dependent on availability of binding ligands of MRW NOM	900 µg/L dissolved Cu was found 1 day after Cu dose when the system reached equilibrium with both CuO and Cu-NOM complexes
HAW pH=7.9±0.2, DOC=2.4±0.1 mg-C/L, Open system	$CuCO_3^o$, $CuOH^+$, $Cu(OH)_2$ and Cu-NOM / CuO and Cu-NOM	*Dependent on availability of binding ligands of MRW NOM	940 µg/L dissolved Cu was found 1 day after Cu dose when the system reached equilibrium with both CuO and Cu-NOM complexes

Note: Intermediate[1] Copper Forms: possible Cu species existing in bulk water only 2 hours after dosing $CuSO_4$.
Equilibrated[2] Copper Forms: possible Cu species existing in bulk water 1 day after copper dose (Appendix C).
*Cu-NOM chelation coefficient is dependent on a series of binding ligands varying in different NOM-containing water samples. They were not programmed into MINEQL in this study. Alternatively, the proportion of Cu-NOM was deducted from the difference between the total dissolved Cu(II) and the sum of inorganic copper compounds plus free cupric ions.

According to Table 4.2, the concentration of Cu^{2+} is negligible in all the bulk waters at pH >7.5±0.2, which covered the optimum pH range (pH 8.0) for chloramine in the distribution system. At equilibrium with CuO(s) in the open system, Cu-inorganic compounds can be neglected, though increased inorganic carbonate in CaBW did increase Cu(II) solubility via formation of inorganic copper compounds (e.g. $CuOH^+$, $CuCO_3^o$) in the closed system. However, compared with 1 mg/L copper dose, 150 µg/L inorganic dissolved Cu(II) found in 50 mg-$CaCO_3$/L buffered water in the closed system was still a small proportion. Much less inorganic copper compounds can be expected in MRW with only 9.3 mg-$CaCO_3$/L of alkalinity. Therefore, the dominant dissolved copper species in NOM-containing bulk waters (MRW, MCW, NW and HAW) must be Cu-NOM complexes. Strikingly enhanced Cu(II) solubility in MRW, NW and HAW was attributed to dissolved natural organic matters (NOM). For instance, in Mundaring raw water (MRW), with an initial copper salt dose of 1000 µg/L, 840 µg/L dissolved Cu(II) was found to be in the form of Cu-NOM complexes. The remaining 160 µg-Cu/L filtered out as copper particles possibly comprised of $Cu(OH)_2$ and CuO. In the distribution system starting from Mundaring weir, the dosed copper would exist mainly in the form of Cu-NOM complexes. NW and HAW also had high Cu(II) solubility, with 900 and 940 µg/L remaining as dissolved copper respectively.

Compared with Mundaring raw water (MRW) in which 840 µg/L dissolved Cu(II) was measured after a 1000 µg-Cu(II)/L dose, Mundaring water after coagulation (MCW) saw much less dissolved copper remaining (340 µg/L). To complete the comparison between these two samples, copper was dosed to achieve 250 and 400 µg-Cu(II)/L in the duplicate samples of MRW and MCW in an open system. Figure 4.2 shows dissolved Cu(II) concentrations in MRW and MCW when different copper salt dose was varied.

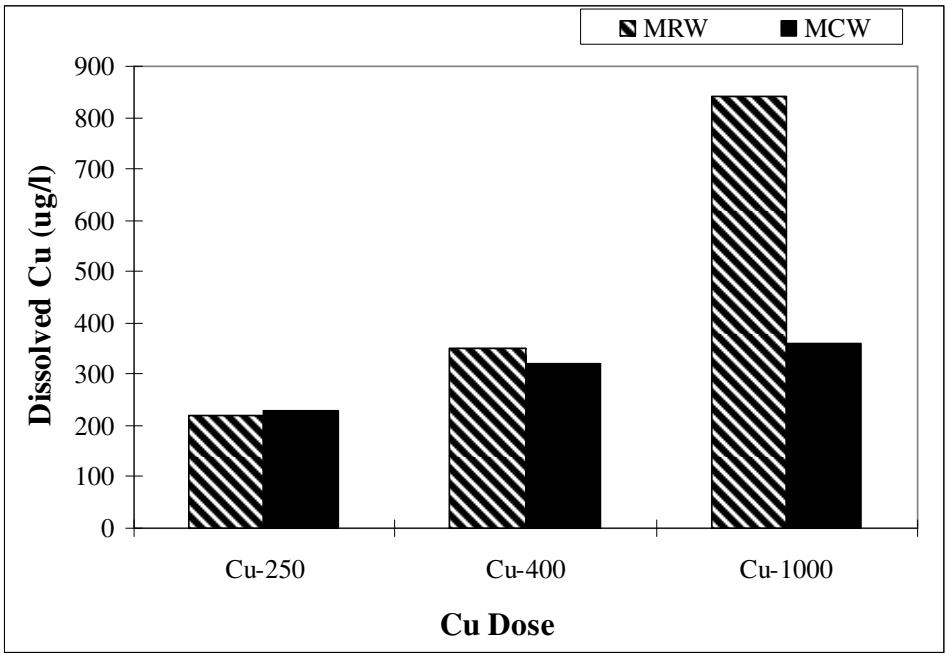

Figure 4.2: Copper solubility in MRW and MCW at various copper salt doses (e.g. "Cu-250": Copper dose is 250 µg-Cu(II)/L).

According to Figure 4.2, dissolved Cu(II) (mostly Cu-NOM) was almost equal in MRW and MCW when the copper dose was 250 µg-Cu(II)/L and 400 µg/L, with only 20~30 µg/L and 50~80 µg/L, respectively, found to be in the particulate forms. However, copper solubility became strikingly different between MRW and MCW when the copper dose was increased to 1000 µg-Cu(II)/L. In MRW, the majority of dosed copper (840 µg/L) was converted to dissolved Cu-NOM, but in MCW only 340 µg/L existed

mainly as dissolved Cu-NOM. Figure 4.2, therefore, indicated that coagulable NOM in MRW contributed significantly to increasing Cu(II) solubility in the bulk water by forming Cu-NOM_c (Cu-coagulable-NOM complex) when the copper dose was relatively high. However, at low copper doses (250 µg-Cu(II)/L and 400 µg-Cu(II)/L), uncoagulable NOM remaining in Mundaring water (MCW) was still capable of maintaining Cu-NOM_{uc} (Cu-uncoagulable-NOM complexes) at similar concentrations as found in MRW. When the copper dose was further increased to 1 mg/L, the uncoagulable NOM was saturated.

4.2.4 Conclusion

In summary, at pH 7.6~8.0, the usual range of pH maintained in G&AWSS, cupric ions are negligible. As the source water of G&AWSS, little inorganic Cu(II) compounds existed in Mundaring raw water after copper dosing. Cu(II) solubility was strikingly enhanced by NOM contained in the water samples like MRW, MCW, NW and HAW, though less Cu-NOM was found in MCW in which only uncoagulated NOM was available to complex with copper. The dominant Cu(II) species in the distribution system were concluded to be in the form of Cu-NOM complexes. The following chapters hence describe the details of investigation of the fate of Cu-NOM in the waters containing trace iron corrosion products.

CHAPTER 5

REMOVAL OF DISSOLVED Cu(II) BY LOW-LEVEL FERROUS/FERRIC IONS IN BULK WATERS

5.1 Introduction

Based on the concept of the two-stage corrosion process, dissolved Cu(II) removal by ferrous, ferric ions and ferric hydroxide flocs was investigated. As previously discussed, ferrous ions can be released into water when freshly corroded surface is exposed or passivated-out-layers is broken down and converted to ferric ions in a short time. This chapter, therefore, studied the removal of dissolved Cu(II) by either ferrous or ferric ions present at low concentrations (< 2 mg/L). When ferrous or ferric ions are released into bulk water, they may interact with dissolved Cu(II) for a short time (< 5 mins). Ferric hydroxide flocs will be formed afterwards due to the prevalent pH (> 7.6) in the distribution system. The interaction between dosed copper and the flocs will last for a relatively long time until equilibrium is achieved. Consequently, dissolved Cu(II) measured at the end would be the equilibrium dissolved Cu(II) concentration. In other words, it was the result from the completed two-stage corrosion process.

5.2 Experimental Procedure and Method

In this experiment, MRW, HAW and NW were chosen for the following reasons: MRW is the source water for G&AWSS and hence the main interest of investigation. NW is the nitrified product water of MRW from the laboratory reactor, which has similar DOC concentration but slightly different characteristics in terms of NOM content. In addition, nitrification was observed in G&AWSS. It can affect the fate of dosed copper. HAW was made to have a similar DOC concentration as MRW, but it had strikingly different characteristics of NOM, which is mainly composed of hydrophobic chromophores. Investigation of these three types of waters can help to understand the impact of NOM on dissolved copper. In each type of bulk water, two different doses of copper salt were applied by adding aliquots of an aqueous copper sulphate solution (1 g-Cu(II)/L) into 1.5 L bulk water, with the aim to make initial Cu(II) concentrations of 400 and 1000 µg-Cu(II)/L. The samples dosed with copper salt had been kept intact at room temperature (20~30^{o}C) for 24 hours. Then, the dissolved Cu(II) concentration in each sample was measured before addition of the ferrous or ferric ions in order to know the initial dissolved Cu(II) concentration (i.e. Cu(II) containing particles $Cu(OH)_2$ and CuO can form after copper salt dose).

To investigate dissolved Cu(II) removal by adding Fe^{2+} ions at different concentrations, trace $FeSO_4$ was released into each bulk water sample containing a known dissolved copper concentration. The appropriate Fe(II) concentration was achieved by adding aliquots of $FeSO_4$ stock solution (1 g-Fe(II)/L) (The preparation of $FeSO_4$ solution is detailed in Chapter 3). Tested Fe(II) concentrations were 0.1, 0.3 0.5, 1.0 and 2 mg-Fe(II)/L. A jar tester was used to stir (60 rpm for 30 mins) bulk water during and after ferrous ion addition. After the jar test, the samples were left for sedimentation for 4 hours (4 hours was found to provide sufficient time to reach equilibrium between dissolved Cu(II) species and $Fe(OH)_3$ flocs; See Figure 9.1 in Chapter 9). During this

time, the pH of each sample was monitored and adjusted to around pH 7.8-8.2 by adding HCl solution (1 N) or NaOH solution (1 N), as necessary. Subsamples were then filtered through 0.2 μm polycarbonate membranes and the Cu(II) concentration remaining in the filtrate was measured. The copper removal was calculated as the difference between the dissolved Cu(II) in the bulk water before and after Fe(II) salt treatment.

The same procedure was followed for adding Fe^{3+} ions to remove dissolved Cu(II) in the bulk waters. Instead of adding $FeSO_4$ solution, $FeCl_3$ (1 g-Fe(III)/L) was used.

5.3 Results and Discussion

Figure 5.1, 5.2 and 5.3 show the removal of dissolved Cu(II) by either ferrous or ferric ions in MRW, NW and HAW respectively. The results are plotted as final remaining dissolved Cu(II) concentration, after the iron treatment in the form of ferrous or ferric ions at different concentrations.

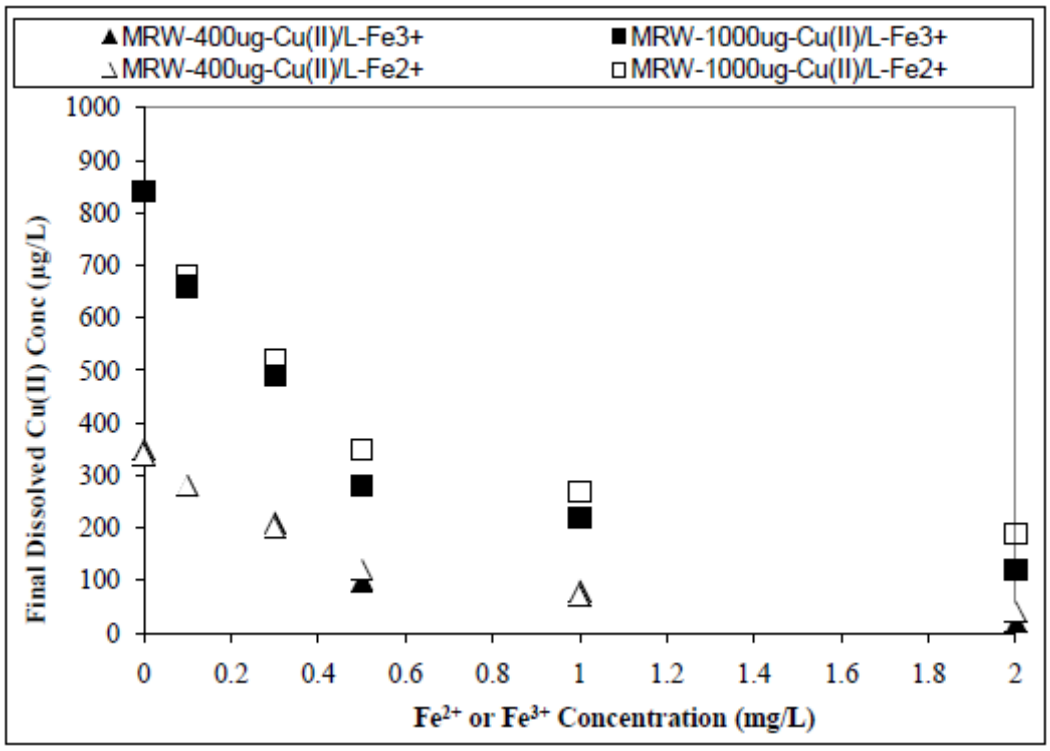

Figure 5.1: Dissolved Cu(II) removal by ferrous & ferric ions in MRW ("MRW-400 µg-Cu(II)/L-Fe^{3+}": In MRW, 400 µg-Cu(II)/L copper salt was dosed and Fe^{3+} ions were added to remove dissolved Cu(II). The other legends can be interpreted analogously.)

In Mundaring raw water (MRW) (Figure 5.1), initial dissolved Cu(II) concentrations of 840 and 340 µg-Cu(II)/L were measured at 0 mg-Fe/L addition for copper doses of 1000 and 400 µg-Cu(II)/L respectively. The minimum addition of Fe^{2+} (0.1 mg-Fe(II)/L) removed 160 µg/L dissolved Cu(II) from the bulk water from an initially dosed copper of 1000 µg-Cu/L (empty square dots). In the bulk water dosed with 400 µg-Cu(II)/L copper salt, little dissolved Cu(II) was left after 2 mg/L Fe^{2+} treatment (empty triangle dots). Compared with Fe^{2+}, Fe^{3+} addition (solid dots) led to the same trend of copper removal and showed only a slightly stronger capacity. However, considering the dissolved Cu(II) measurement has ±20 µg/L error, the capacity between these two types of ions cannot be explicitly differentiated. In the bulk water with 400 µg/L initial copper dose, two data series (triangle dots) overlapped, indicating the comparable capacity of Fe^{2+} and Fe^{3+} ions to remove dissolved copper in MRW.

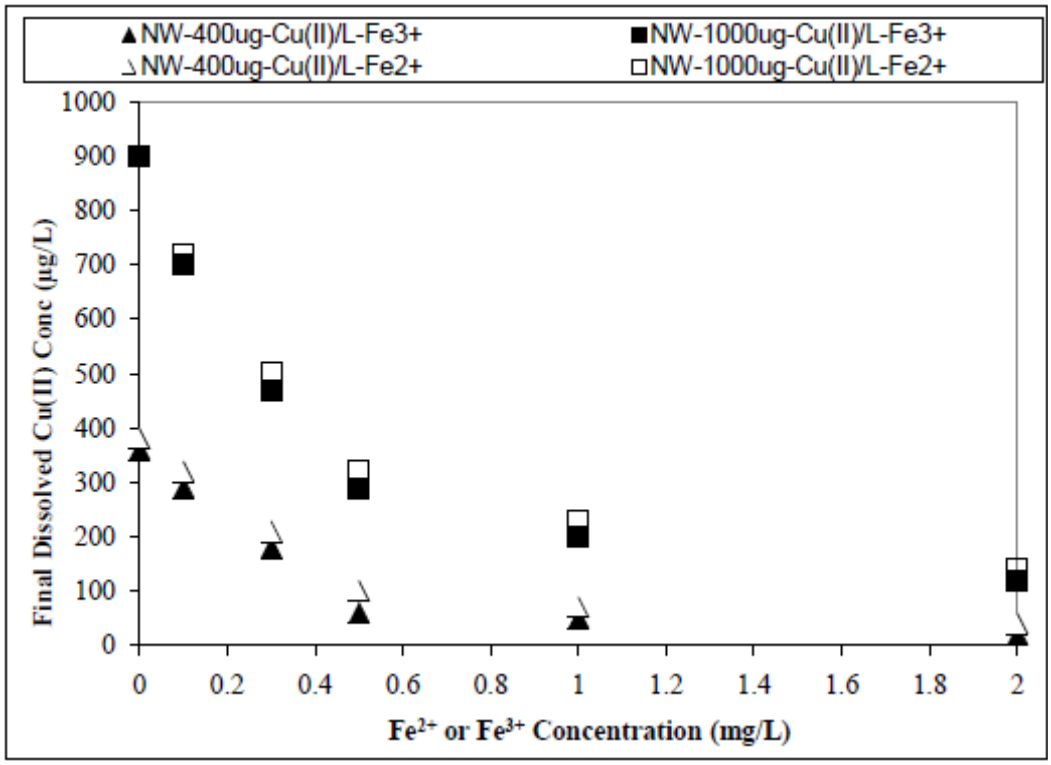

Figure 5.2: Dissolved Cu(II) removal by ferrous & ferric ions in NW ("NW-400 µg-Cu(II)/L-Fe^{3+}": In NW, 400 µg-Cu(II)/L copper salt was dosed and Fe^{3+} ions were added to remove dissolved Cu(II). The other legends can be interpreted similarly.)

In the nitrified water (NW) (Figure 5.2), dissolved Cu(II) concentrations of 900 and 360~380 µg-Cu(II)/L at 0 mg-Fe/L addition were measured after 1000 and 400 µg-Cu(II)/L copper salt were dosed respectively. Despite the slightly higher initial dissolved copper concentrations found in NW than in MRW, a similar trend of dissolved Cu(II) loss was observed in NW for Fe^{2+} or Fe^{3+} ion treatment. However, compared with MRW, slightly more dissolved Cu(II) was removed in NW after the corresponding Fe^{2+} or Fe^{3+} ion treatment. This difference may be contributed to by the change of NOM composition during the nitrification. The detailed explanation is given in Chapter 8.

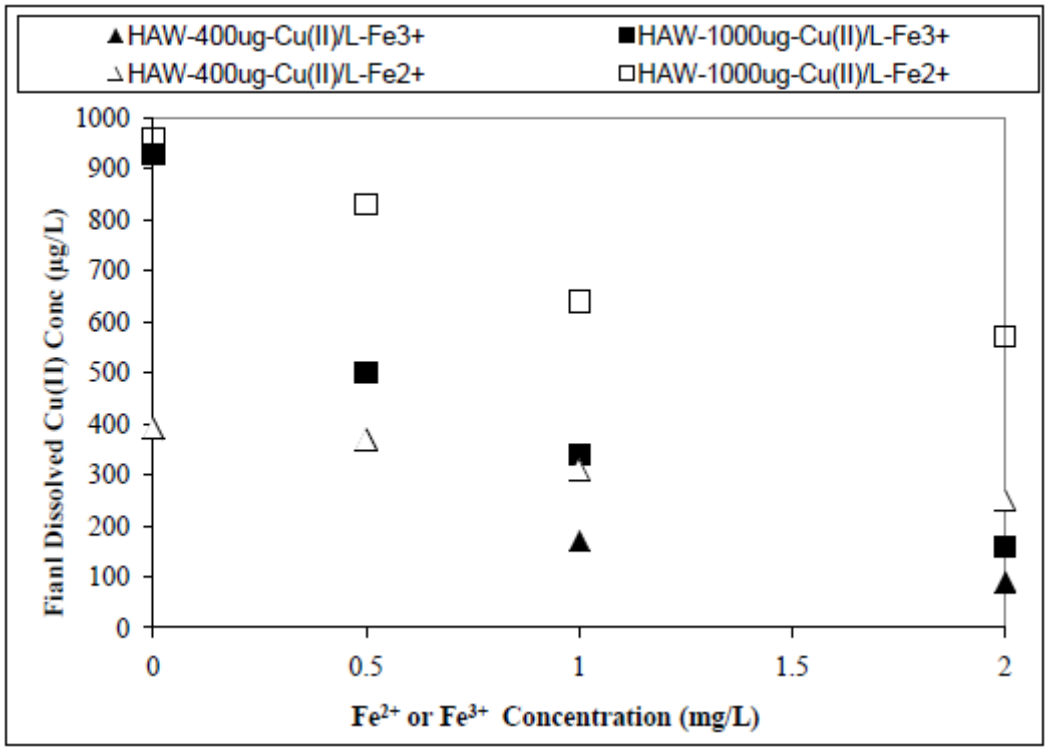

Figure 5.3: Dissolved Cu(II) removal by ferrous & ferric ions in HAW ("HAW-400 µg-Cu(II)/L-Fe^{3+}": In HAW, 400 µg-Cu(II)/L copper salt was dosed and Fe^{3+} ions were added to remove dissolved Cu(II). The other legends can be interpreted analogously.)

In the humic acid water (HAW) (Figure 5.3), 920~940 and 400 µg-Cu(II)/L existed as dissolved copper for 0 mg-Fe/L addition after 1000 and 400 µg-Cu(II)/L copper salt were dosed respectively. Generally, less dissolved Cu(II) removal by either Fe^{2+} or Fe^{3+} ions was observed in HAW than in MRW or NW. Neither ferrous nor ferric ions at 0.5 mg/L (overlapped triangle dots) removed dissolved Cu(II) in the waters dosed with 400 µg-Cu(II)/L copper salt. After the maximum addition of Fe^{2+} or Fe^{3+} (2 mg-Fe/L), 240 and 100 µg/L dissolved Cu(II) still remained respectively. Ferric ions showed much larger capacity than ferrous ions to remove copper in HAW. The difference in behaviour of copper removal observed in HAW may have been caused by the distinct characteristics of HAW NOM. The details related to Cu-NOM chelation and its impact on dissolved Cu(II) removal are discussed in Chapter 8.

5.4 Conclusion

Although NOM contained in bulk waters enhanced Cu(II) solubility through forming Cu-NOM complexes, dissolved Cu(II) is still vulnerable to the iron corrosion products even when they were present at low concentrations (< 2 mg/L). Both ferrous and ferric ions showed considerable and similar capacity to remove dissolved Cu(II) in the Mundaring water and the nitrified water (NW). Cu-NOM in humic acid water (HAW) demonstrated relatively high resistance to Cu(II) ion removal. However, 2 mg/L ferric ions were still able to remove the majority of dissolved Cu(II) in HAW.

CHAPTER 6

REMOVAL OF DISSOLVED Cu(II) BY LOW-LEVEL FERRIC HYDROXIDE FLOCS IN BULK WATERS

6.1 Introduction

Chapter 5 discussed dissolved Cu(II) removal by ferrous and ferric ions which could be released into bulk water at the early stage of iron corrosion. The final dissolved Cu(II) concentration was measured after iron salt treatment at various additions. However, ferrous or ferric ions are believed to be only existing in bulk water for a short time at pH 7.6~8.0. Soluble ferrous ions are converted into ferrous solids (e.g. $Fe(OH)_2$), which may then be converted to ferric solids (e.g. $Fe(OH)_3$) after reaction with oxygen (AWWARF, 1996). The conversion to $Fe(OH)_3$ flocs in bulk water were also observed in our laboratory experiments. The growing $Fe(OH)_3$ flocs started to be visible to naked eyes within 5 minutes after ions addition. It indicated that longer lasting interaction occurred, indeed between dissolved copper and $Fe(OH)_3$ flocs. The dissolved Cu(II) finally remaining in bulk water is hence governed by the equilibrium reached between dissolved Cu(II) and $Fe(OH)_3$ flocs. This chapter investigated removal of dissolved Cu(II) by $Fe(OH)_3$ flocs.

6.2 The Experimental Procedure and the Method

MRW, MCW, HAW and NW were chosen for the experiments. In each type of bulk water, different copper doses (250, 400 and 1000 µg-Cu(II)/L) were applied in its duplicates. The same procedure of aqueous copper dosing and dissolved Cu(II) measurement before $Fe(OH)_3$ addition was followed, as illustrated in 5.2 (Chapter 5).

In order to evaluate the effect of the pre-formed Cu(II) particles (e.g. $Cu(OH)_2$, $CuO_{(s)}$) on dissolved Cu(II) removal by $Fe(OH)_3$, the post-Cu(II)-dose samples were divided into two groups. In one group (MRW and MCW), pre-formed particles were allowed to remain in bulk waters during $Fe(OH)_3$ treatment. In the other (MWF, NW and HAW), the pre-formed Cu(II) particles were filtered out by a 0.2 µm polycarbonate membrane before $Fe(OH)_3$ treatment (MWF: MRW with pre-formed Cu(II) particles removed by filtration).

$Fe(OH)_3$ flocs were added into each water sample and its duplicates at different concentrations (0.5, 1.0 and 2 mg-Fe(III)/L). The same procedure of jar test and dissolved copper measurement after $Fe(OH)_3$ treatment was followed, as illustrated in 5.2 (Chapter 5).

6.3 Results and Discussion

6.3.1 The Adsorption of Dissolved Cu(II) by $Fe(OH)_3$ Flocs in Tested Bulk Waters

Figure 6.1~ 6.5 show the removal of dissolved Cu(II) by $Fe(OH)_3$ flocs in MRW, MFW, NW, MCW and HAW sequentially. As mentioned earlier, in MWF, NW and HAW, after copper dosing, any particulate copper formed before $Fe(OH)_3$ treatment was removed through 0.2 µm filtration. For MRW and MCW, the filtration step was not exercised.

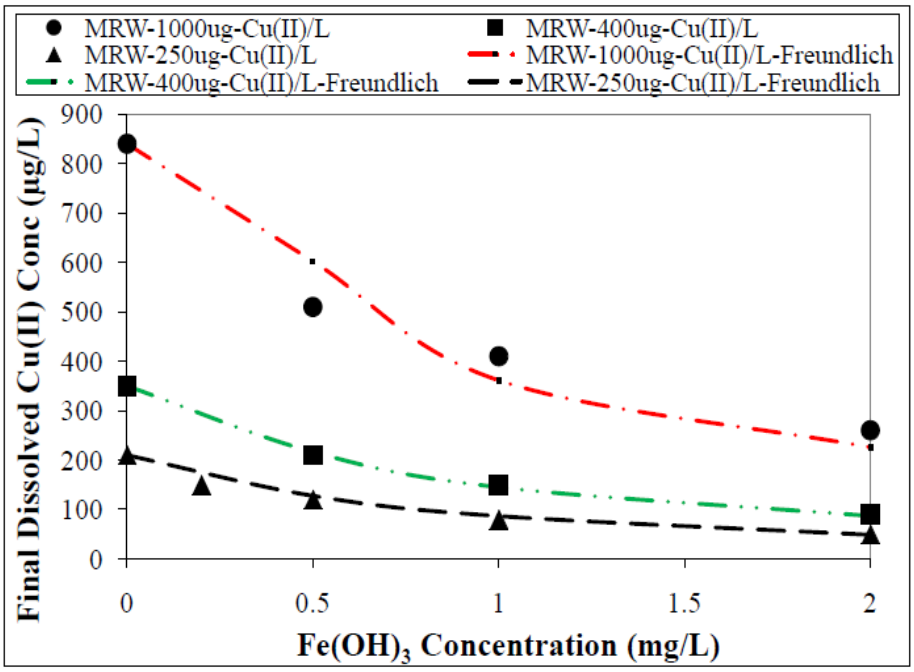

Figure 6.1: Dissolved Cu(II) removal by $Fe(OH)_3$ flocs in MRW

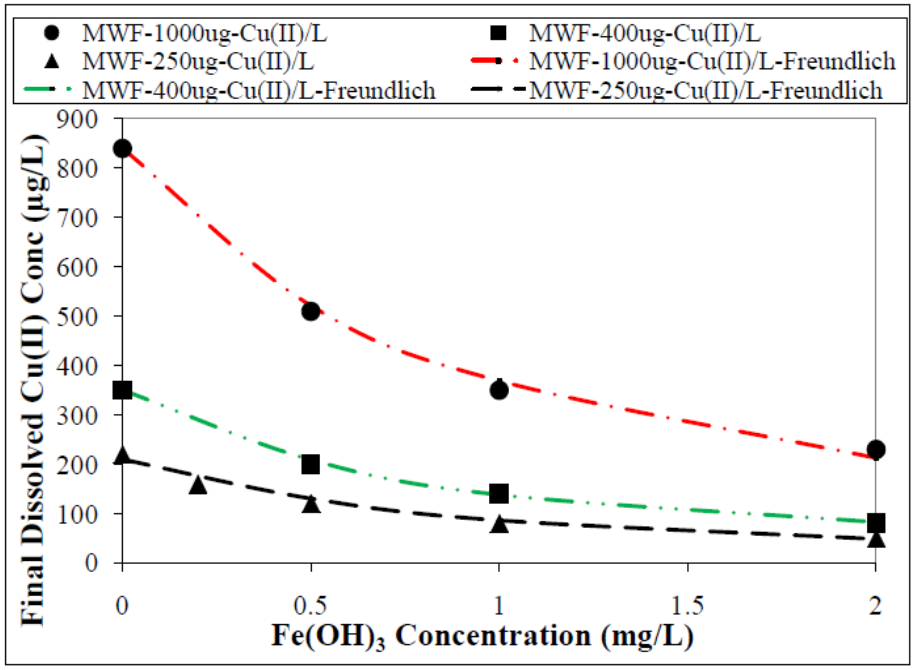

Figure 6.2: Dissolved Cu(II) removal by $Fe(OH)_3$ flocs in MWF

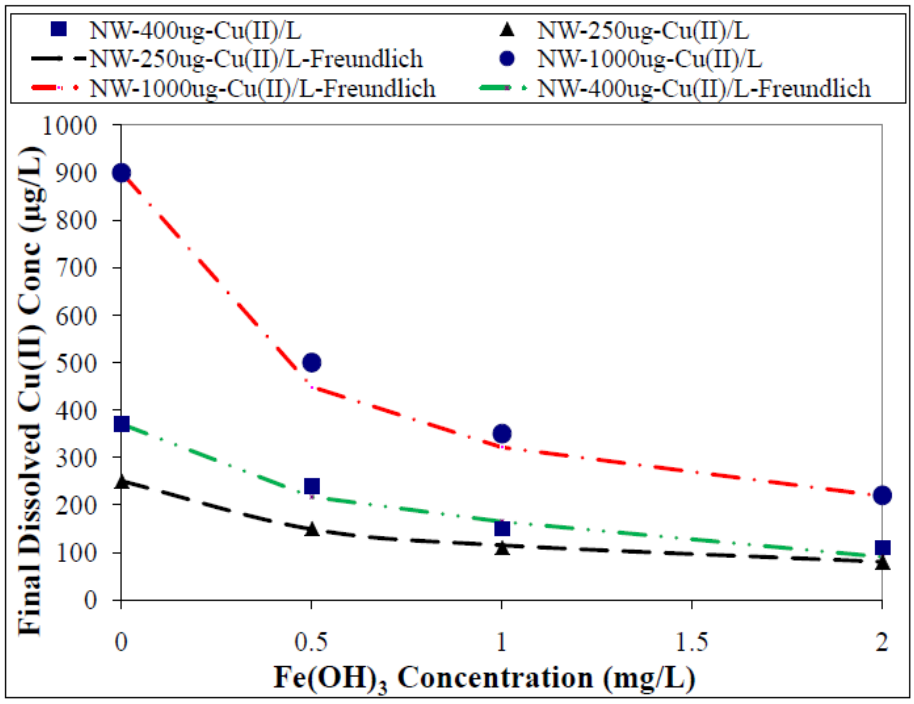

Figure 6.3: Dissolved Cu(II) removal by $Fe(OH)_3$ flocs in NW

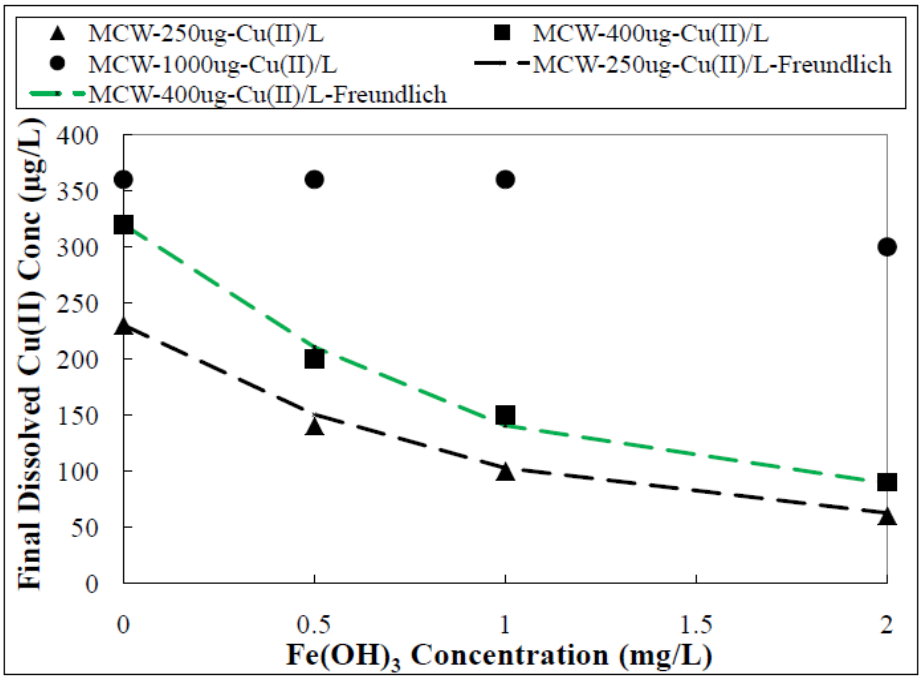

Figure 6.4: Dissolved Cu(II) removal by $Fe(OH)_3$ flocs in MCW

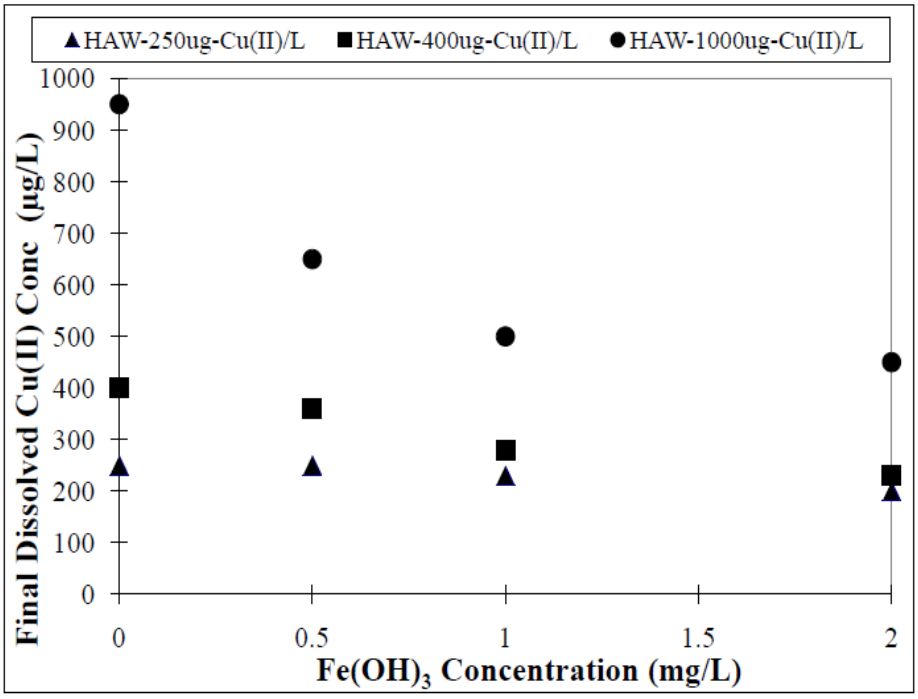

Figure 6.5: Dissolved Cu(II) removal by $Fe(OH)_3$ flocs in HAW

In MRW and MWF (Figure 6.1 and 6.2), before ferric flocs addition, initial dissolved Cu(II) concentrations of 220, 350 and 840 µg/L were measured when Cu(II) was dosed at 250, 400 and 1000 µg/L respectively. NW had a slightly higher Cu(II) solubility than MRW and MWF (Figure 6.3, 6.1 and 6.2), as 900 µg/L dissolved Cu(II) was found at 0 mg-Fe(III)/L addition after 1000 µg-Cu(II)/L copper salt dosing. Similar Cu(II) solubility as that in MRW or MWF was found in MCW (Figure 6.4) when Cu(II) was dosed at 250 and 400 µg/L. However, much less dissolved Cu(II) (360 µg/L) was measured when Cu(II) was dosed at 1000 µg/L in MCW, as discussed in Figure 4.2.

In the samples dosed with 1000 µg-Cu(II)/L copper salt (round dots), the maximum Fe(III) addition (2 mg-Fe(III)/L) left only 300, 230 and 230 µg/L dissolved Cu(II) in MRW, MWF and NW respectively (Figure 6.1~6.3). Addition of the flocs at a concentration of 2 mg-Fe(III)/L removed most of the dissolved Cu(II) in MRW, MCW, MWF and NW (Figure 6.1~6.4) when the 250 or 400 µg-Cu(II)/L copper salt was

dosed, indicating the considerable impact of trace ferric hydroxide flocs on the concentration of dissolved copper.

The relative capacity of NOM to stabilize soluble Cu(II) was found to be stronger in HAW than in NW or MRW with higher concentrations of dissolved Cu(II) measured in HAW at all floc concentrations (Figure 6.5). Removal of dissolved Cu(II) by ferric hydroxide flocs was lower in HAW than in MRW or NW. For instance, only 20µg/L dissolved Cu(II) was removed by 2 mg-Fe(III)/L flocs when copper was dosed at 250µg/L. These observations can be attributed to the distinct character of HAW NOM which gave higher SUVA (Table 4.1) and contained more large MW components as evidenced in the AMW profile (Figure 4.1). Adsorption of Cu(II) in HAW did not obey Freundlich isotherm.

This phenomenon is related to the distinct characteristics of HAW NOM in terms of its ability to adsorb onto the ferric flocs or complex with Cu(II). When ferric hydroxide flocs were added at low concentrations (< 2 mg/l), it was believed that the majority of available adsorption sites on the coagulants were preferentially and readily occupied by large organic molecules (Volk et al., 2000). On the other hand, the complexation between Cu(II) and organic molecules starts preferentially from small molecular weight compounds (evidence is provided in Chapter 8). Consequently, the relatively small Cu(II)-NOM complexes were shielded from ferric adsorption by those large organic molecules in HAW which were not bound with copper. Therefore, the Freundlich adsorption relationship attempted only between Cu(II)-NOM complexes and $Fe(OH)_3$ flocs could not be established since in HAW a significant proportion of available adsorption sites on $Fe(OH)_3$ flocs were occupied by the large organic matter which were not complexed with copper. The degree to which Cu(II)-NOM involved in adsorption is

dependent on the proportion of large organic molecules and the concentration of ferric flocs. When small molecules of NOM are saturated through complexation with Cu(II), the increased copper dose can result in Cu(II) complexation with large molecules which can be more easily removed by the ferric flocs. Meanwhile, increasing ferric addition can also remove more Cu(II)-NOM if most of the Cu(II) binding free molecules have been occupied by Cu(II) through complexation. It explains in Figure 6.5 why little Cu(II)-NOM was removed in 250 µg/L copper dose case while 1000 µg/L copper dose saw more copper removal. The elucidation of above theory was further supported by the discussion of apparent molecular weight analysis and UV_{254} absorbance analysis in Chapter 8.

The laboratory results were tested against known adsorption isotherms, Freundlich, Langmuir and BET. Freundlich isotherm was found to be capable of explaining the observed dissolved copper removal. In Figure 6.1~6.4, the dashed lines derived from the Freundlich adsorption isotherms are compared against the measured results (discrete points) following the formula:

$$\frac{Dissolved\_Cu\_removal}{Fe(III)\_Conc} = K_F \times (Equilibrium\_dissolved\_Cu)^{1/n}$$

Each dashed line represents the model predicted dissolved Cu(II) removal through adsorption at different Fe(III) concentrations when copper salt was dosed at a specific concentration. For example, the red dashed line in Figure 6.2 (labelled as "MWF-1000µg-Cu(II)/L-Freundlich") demonstrates the trend of dissolved Cu(II) adsorption by $Fe(OH)_3$ flocs in increments when 1000 µg-Cu(II)/L was dosed.

The experimental results from other bulk water samples were also tested against the known adsorption isotherms. Freundlich adsorption isotherm was found to be capable of modelling dissolved Cu(II)-Ferric flocs interaction in MRW, MWF, NW and MCW (except for 1000 µg-Cu(II) copper salt dose in MCW, the discussion is given in 6.3.2). The best fit parameters for Freundlich isotherms are shown in Table 6.1.

Table 6.1: The parameters adapted in Freundlich Adsorption Isotherm

Variables &Constants	**Cu removal/µg $Fe(OH)_3$**	**K_F**	**Final Dissolved Cu(II)**	**n**	**R^2**
Unit	µg/µg		µg/L		
MRW	$Y=(Cu_o-[Cu])/$ Fe(III) Conc	0.0031	C	1.19	0.98
MWF	$Y=(Cu_o-[Cu])/$ Fe(III) Conc	0.0030	C	1.16	0.99
MCW	$Y=(Cu_o-[Cu])/$ Fe(III) Conc	0.0028	C	1.17	0.99
NW	$Y=(Cu_o-[Cu])/$ Fe(III) Conc	0.0002	C	0.73	0.98

Note: Cu_o: dissolved bulk copper concentration at 0-mg-Fe(III)/L addition

C: dissolved copper concentration after $Fe(OH)_3$ treatment

Freundlich isotherm: $y = K_F C^{1/n}$

R^2: coefficient of determination

Adsorption phenomenon generally occurred between dissolved copper and $Fe(OH)_3$ flocs, as shown by the well-matched (R^2=0.98 in MRW, R^2=0.99 in MWF, R^2=0.99 in MCW and R^2=0.98 in NW) Freundlich isotherm curves calculated from the adapted parameters in Table 6.1. Considering "K_F" and "n" reflect the characteristics of adsorbent ($Fe(OH)_3$ flocs) and adsorbate (Cu-NOM), it is reasonable to see similar K_F

and n values (K_F=0.003, n=1.16~1.19) for MRW and MWF due to their common composition in NOM spectrum.

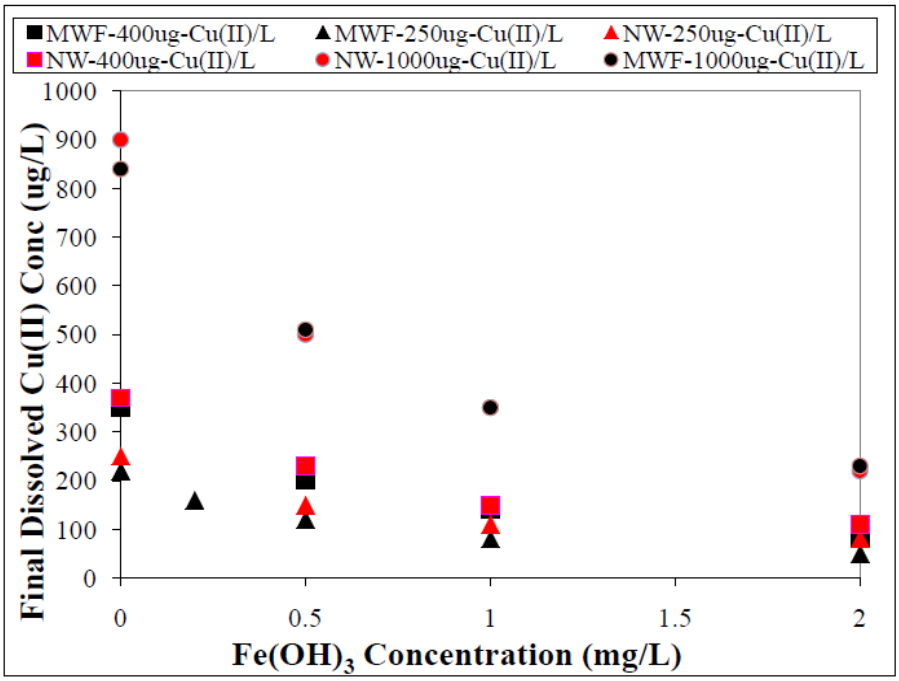

Figure 6.6: The comparison of dissolved Cu(II) removal by $Fe(OH)_3$ flocs from MWF and NW

Since higher dissolved Cu(II) concentrations were observed at 0 mg-Fe/L in NW than in MRW or MWF as, more Cu(II) may have been complexed with NOM in NW than in MRW or MWF. A direct comparison of Cu(II) removal between MWF and NW is given in Figure 6.6. Slightly less dissolved Cu(II) was removed in NW than in MWF for 250 and 400 µg-Cu(II)/L copper doses while Cu(II) removal was similar in both waters for 1000 µg-Cu(II)/L copper dose. Considering the measuring error of ±20 µg/L, the difference shown in Figure 6.6 is not significant. However, the same Freundlich isotherm parameters adopted for MRW or MWF could not be fit to NW. Instead, different "K_F" and "n" values were calculated for NW (K_F=0.0002, n=0.73). "K_F" and "n" values are interpreted in Freundlich Adsorption Isotherm in terms of fundamental

kinetics and diffusion based properties (Skopp, 2009). Skopp (2009) suggested that "K_F" is related to the diffusion coefficient of an adsorption-desorption dynamics and "n" reflects the probability distribution for a molecule to access adsorption sites. The different K_F and n values are believed to be related to soluble microbial products from nitrification (Krishna and Sathasivan, 2010), which were chelated with dissolved copper and had a different character from Cu-NOM complexes formed in MRW or MWF. The detailed discussion is given in Chapter 8.

Figure 6.4 shows the removal of dissolved Cu(II) in MCW containing only uncoagulable NOM (NOM_{uc}). Therefore, Figure 6.4 can be regarded as the removal of Cu(II)-NOM_{uc}. Despite the difference in DOC concentration between MRW (2.6 mg-C/L) and MCW (0.9 mg-C/L), for 250 and 400 µg-Cu/L copper doses, similar trends (MCW "n=1.17" and "K_F=0.0028") of Cu(II) removal were observed for these waters, indicating that the same type and number of Cu(II)-NOM complexes (i.e. mostly Cu(II)-NOM_{uc}) may have formed.

6.3.2 The impact of pre-formed Cu(II)-containing particles on dissolved copper removal

Some deviation of the experimental data from the Freundlich isotherm was observed in MRW at 1000 µg-Cu(II)/L copper dose (red dashed line in Figure 6.1). It shows the impact of pre-formed Cu-containing particles (CuO and $Cu(OH)_2$) on dissolved Cu(II) removal. When copper is added to bulk water it potentially forms either particulate or stay as dissolved. Dissolved copper can be measured easily by filtering through 0.2 µm filter paper. However the amount not appearing in the dissolved form can be considered

particulate copper (e.g. $CuO_{(s)}$ and $Cu(OH)_2$). If the particulates are removed prior to ferric hydroxide floc addition, one can easily find the impact of particulates which existed in the water before ferric salts were added. This is similar to the case of MWF. When 1000 µg-Cu(II)/L copper was dosed (Figure 6.2), 160 µg-Cu/L as particulates had been removed from the reaction system before ferric hydroxide was added. In this experiment, 350 µg-Cu(II)/L remained in MWF after 1 mg-Fe(III)/L $Fe(OH)_3$ treatment, while 410 µg-Cu/L was measured in MRW in which these pre-formed copper particulates remained. This indicates that the presence of these copper particulates prevents removal of some of the dissolved Cu(II)-NOM from the flocs. However, one could note that the pre-filtration step had little effect on dissolved Cu(II) removal at the two lower Cu(II) dose cases (250 and 400 µg-Cu(II)/L) due to negligible Cu(II) particles formed in MRW.

This impact from the particles became obvious when 1000 µg-Cu(II)/L copper salt dose was practiced in MCW (Figure 6.4). Only around 350 µg-Cu/L remained in MCW at 0 mg-Fe(III)/L addition, slightly higher than that remained in solution (340µg-Cu(II)/L) in the 400 µg-Cu/L copper dose experiment. Sufficient Cu(II) complexing sites on the lower concentration of NOM_{uc} must only have been available to complex with around 350 µg-Cu/L, with the remaining copper presumably forming precipitates such as $Cu(OH)_2$ and $CuO_{(s)}$. When $Fe(OH)_3$ floc was added, the presence of this large proportion of Cu-containing particles severely interfered with dissolved copper removal. With 2 mg-Fe/L, only 60 µg/L Cu-NOM_{uc} was removed. This dramatic change in the dissolved Cu(II) removal could be due to preferential adsorption of the large copper-based precipitates on the $Fe(OH)_3$ flocs, consistent with similar effect observed in MRW for 1000 µg-Cu(II)/L copper salt dose experiment.

6.4 Conclusion

$Fe(OH)_3$ flocs showed considerable capacity to remove dissolved Cu(II) from the water sourced from Mundaring weir and NW. The interaction between dissolved Cu(II) and $Fe(OH)_3$ flocs can be explained by multilayer adsorption, obeying the Freundlich isotherm. The characteristics of NOM contained in bulk waters have effects on both Cu-NOM complexation and dissolved Cu(II) removal. Both coagulable and uncoagulable NOM are capable of binding with Cu(II). Highest resistance of dissolved Cu(II) removal and strongest adsorption of NOM to ferric flocs were observed in humic acid containing water (HAW) while smaller molecules, with which dissolved Cu(II) is believed to be preferentially bound, are shielded by a relatively large amount of large organic molecules from ferric flocs adsorption. However, this postulate needed further investigation in order to reveal the mechanisms governing Cu-NOM chelation and the fate of Cu-NOM in bulk waters with various NOM compositions when either NOM or Cu-NOM complex are removed by iron corrosion products. Heterogeneous copper species (e.g $CuO_{(s)}$ and $Cu(OH)_2$ particles) can reduce adsorption of dissolved Cu(II) on $Fe(OH)_3$ flocs, the degree of which is dependent on the proportion of the particles. It was thought that the particulate copper interfered Cu-NOM adsorption.

The details of Cu-NOM chelation and the interpretation of different Cu-NOM behaviour during the Fe treatment are discussed in Chapter 8. However, before exploring the mechanisms behind Cu-NOM chelation, it is necessary to summarize dissolved Cu(II) removal by released iron corrosion products ($Fe^{2+}/Fe^{3+} \rightarrow Fe(OH)_3$ flocs) through two-stage corrosion process. This process is illustrated and summarized in Chapter 7 by combining the results achieved in Chapter 5 and Chapter 6.

CHAPTER 7

DISSOLVED Cu(II) REMOVAL BY LOW-LEVEL IRON CORROSION PRODUCTS VIA TWO-STAGE PROCESS: A NOVEL MODELLING APPROACH

7.1 Introduction

According to the concept demonstrated in Figure 3.1, removal of the dissolved Cu(II) takes place in two stages in sequence after corrosion occurs (Figure 7.1): Stage I- removal by Fe^{2+} or Fe^{3+} ions; Stage II- removal by $Fe(OH)_3$ flocs formed from the released ions. Removal by Fe^{2+} or Fe^{3+} need not be differentiated, because the release of Fe^{2+} from pipe walls and its transformation to Fe^{3+} can happen quickly and the impact of both types of ion on copper removal was found to be similar in Chapter 5.

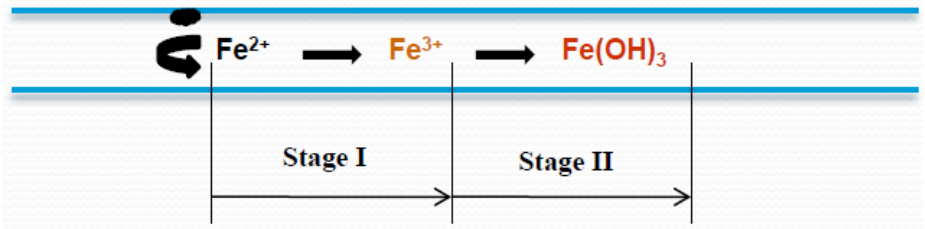

Figure 7.1: Iron salts being released via the two-stage iron corrosion process

Chapter 5 revealed the sum of dissolved Cu(II) removal of Stage I and Stage II by adding the ions while Chapter 6 focused on the removal occurring only in Stage II by adding pre-formed ferric hydroxide flocs. However, the removal of dissolved Cu(II)

occurring only in Stage I was yet to be quantified. This was accomplished by reprocessing the laboratory results from the previous two chapters.

7.2 Method of Data Processing from Chapter 5 and Chapter 6

In Stage I, dissolved Cu(II) removal is achieved by the freshly released ions (Fe^{2+} and Fe^{3+}) through coagulation and neutralization. It is followed by Stage II, the removal through adsorption by the $Fe(OH)_3$ flocs which formed afterwards.

The figures in Chapter 6 show that the equilibrium concentration of dissolved Cu(II) that finally remains is not only governed by ferric floc addition but also the initial Cu(II) concentration before the adsorption process starts (i.e., before adding ferric hydroxide flocs). By re-arranging the figures shown in Chapter 6, Figure 7.2 to 7.4 show the relationship between the Cu(II) concentrations before and after adding ferric hydroxide flocs at various concentrations. Therefore, the intermediate dissolved Cu(II) concentration, i.e. after Stage I but before Stage II, can be found when equilibrium Cu(II) concentration and ferric flocs addition are known. For instance, in MRW (Figure 7.2), the equilibrium Cu(II) concentration of 80 µg/L corresponds to an intermediate Cu(II) concentration of 220 µg/L, according to the Freundlich isotherm curve of MRW-Fe 1 mg (when 1 mg/L ferric flocs is added). When a batch experiment as described in Chapter 6 is carried out, the intermediate Cu(II) concentration is exactly the result of the copper dose. In the above example, 220 µg/L dissolved Cu(II) can be found after 250 µg/L Cu(II) is dosed.

The dissolved Cu(II) concentration remaining in the bulk waters after addition of Fe^{2+} or Fe^{3+}, as shown in Figure 5.1 to 5.3, was the final equilibrium Cu(II) concentration after both Stage I and Stage II were completed in sequence. For example, when 400 µg/L copper was dosed, 350 µg/L initial dissolved Cu(II) was found. After adding 1 mg/L ferric ions, the final dissolved Cu(II) concentration of 80 µg/L was measured. So, the process of copper removal can be calculated as follows:

350 µg/L - Cu(II) removed in Stage I = intermediate dissolved Cu(II)

Intermediate dissolved Cu(II) - Cu(II) removed in Stage I = 80 µg/L

According to the previous discussion, the intermediate dissolved Cu(II) can be located in Figure 7.2. In this example, it was 220 µg/L. Therefore, Cu(II) removal in Stage I is calculated as 350 µg/L - 220 µg/L = 130 µg/L.

Following the same procedure, the intermediate dissolved Cu(II) in NW and HAW can be located in Figures 7.3 and 7.4 respectively. The Stage I dissolved Cu(II) removal can be calculated accordingly.

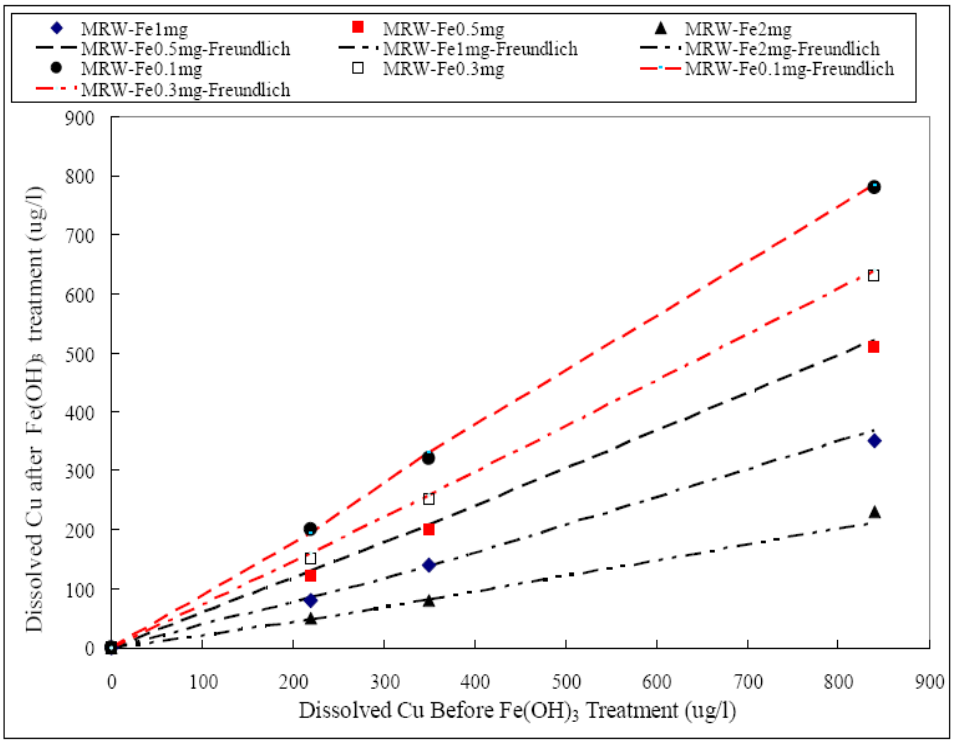

Figure 7.2: Dissolved Cu(II) after $Fe(OH)_3$ treatment vs before the treatment in MRW

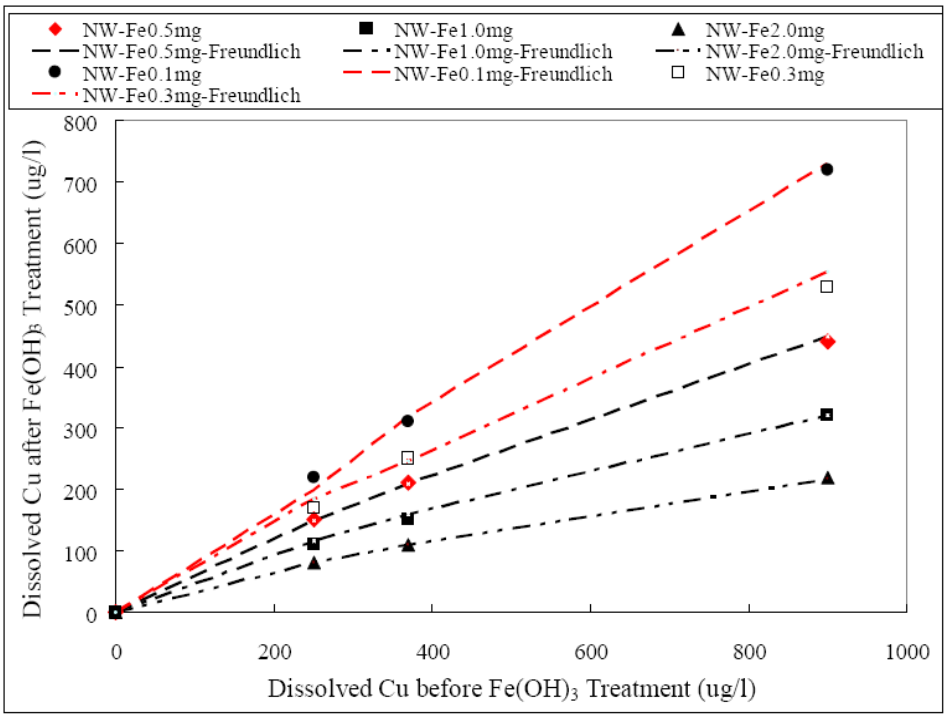

Figure 7.3: Dissolved Cu(II) after $Fe(OH)_3$ treatment vs before the treatment in NW

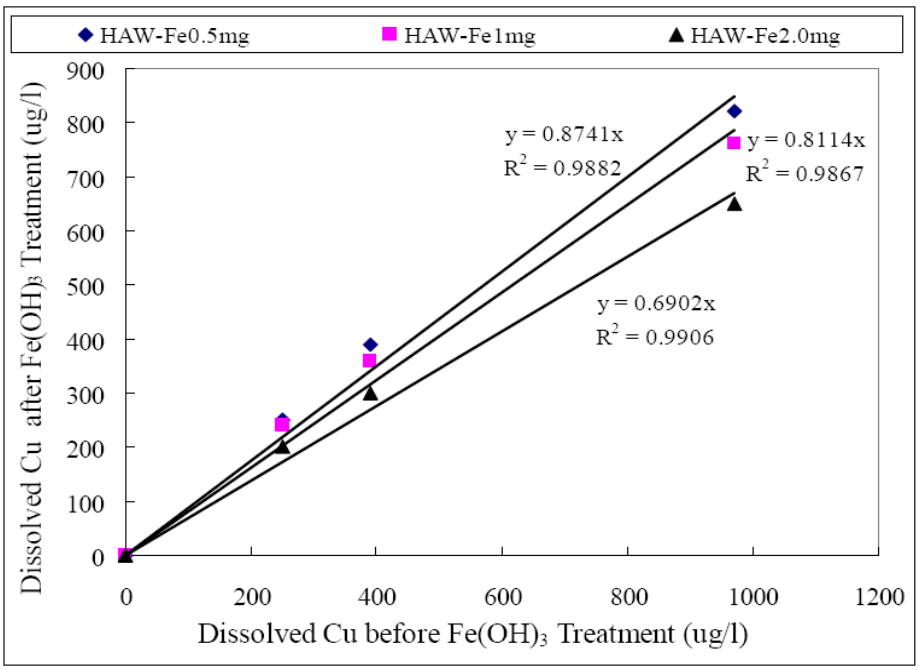

Figure 7.4: Dissolved Cu(II) after $Fe(OH)_3$ treatment vs before the treatment in HAW

7.3 Results and Discussion

Figures 7.5 to 7.10 demonstrate the two-stage process and show the removal of dissolved Cu(II) at each stage. The pink dots represent the total removal occurred during both first and second stages. By extracting the information from Chapter 5 and following the procedure described above in Section 7.2, the calculated removal in Stage I is plotted in blue dots. The vertical distance between the blue line and the pink line in each figure consequently represents the removal only in Stage II (the adsorption process).

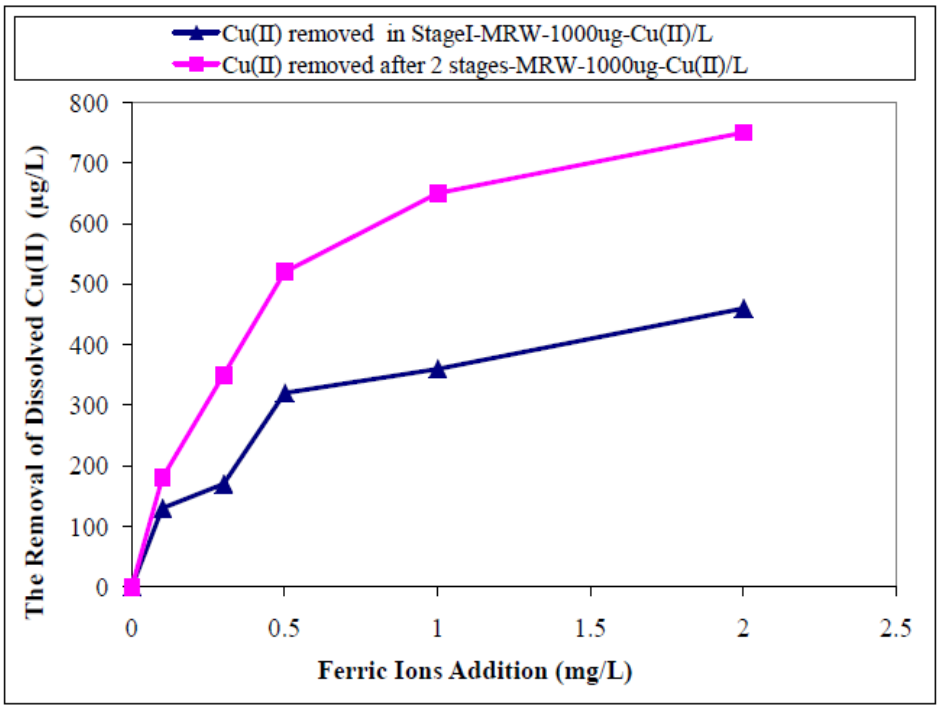

Figure 7.5: Removal of dissolved Cu(II) through the two-stage corrosion process in MRW: 1000 µg/L copper dose case

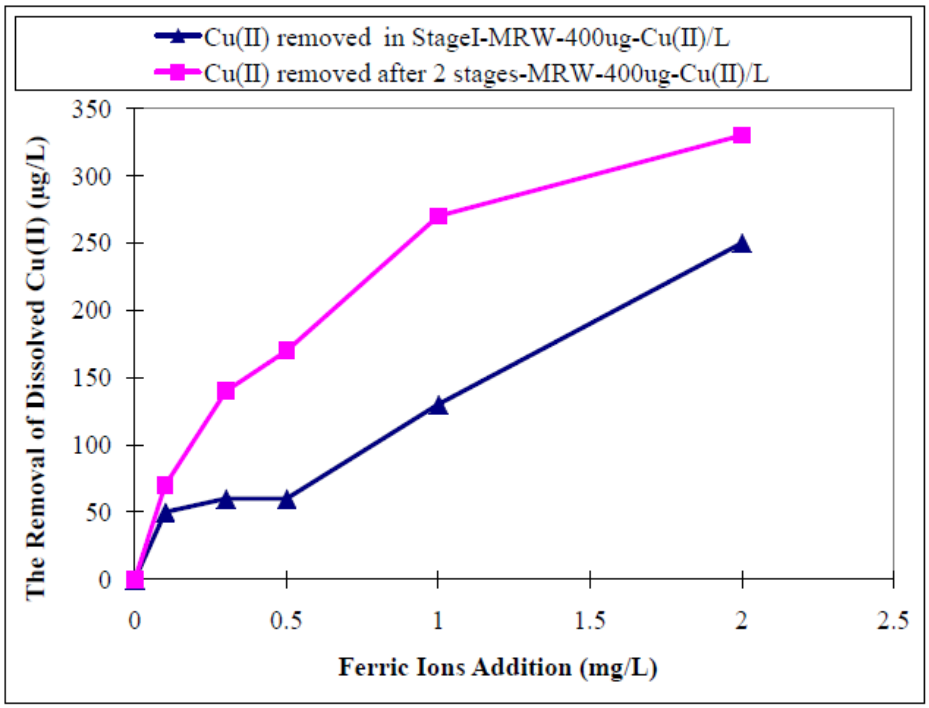

Figure 7.6: Removal of dissolved Cu(II) through the two-stage corrosion process in MRW: 400 µg/L copper dose case

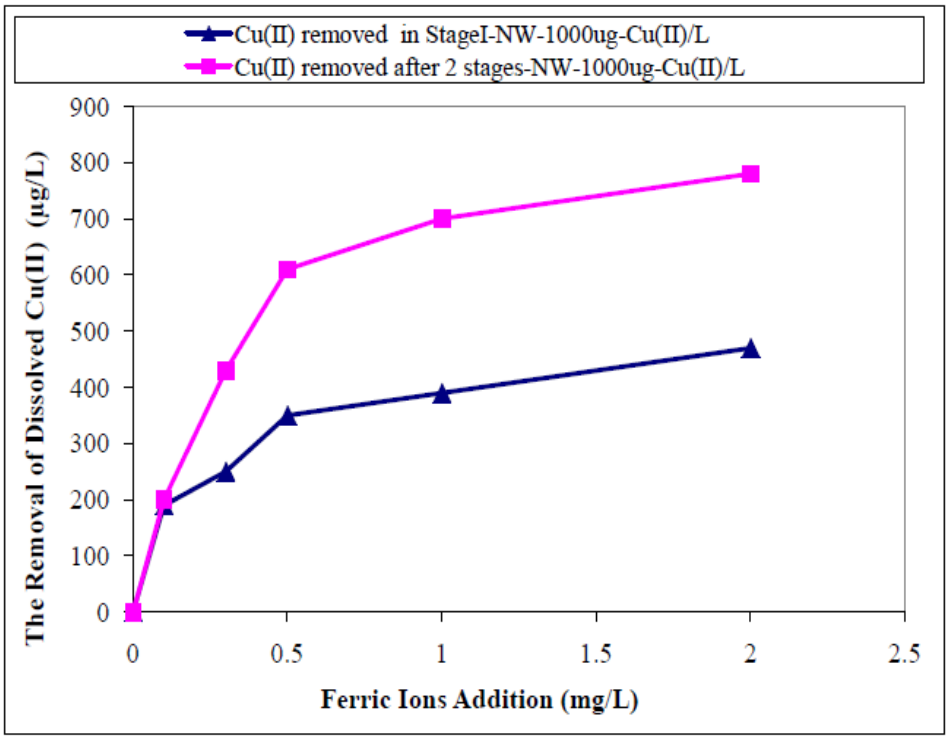

Figure 7.7: Removal of dissolved Cu(II) through the two-stage corrosion process in NW: 1000 µg/L copper dose case

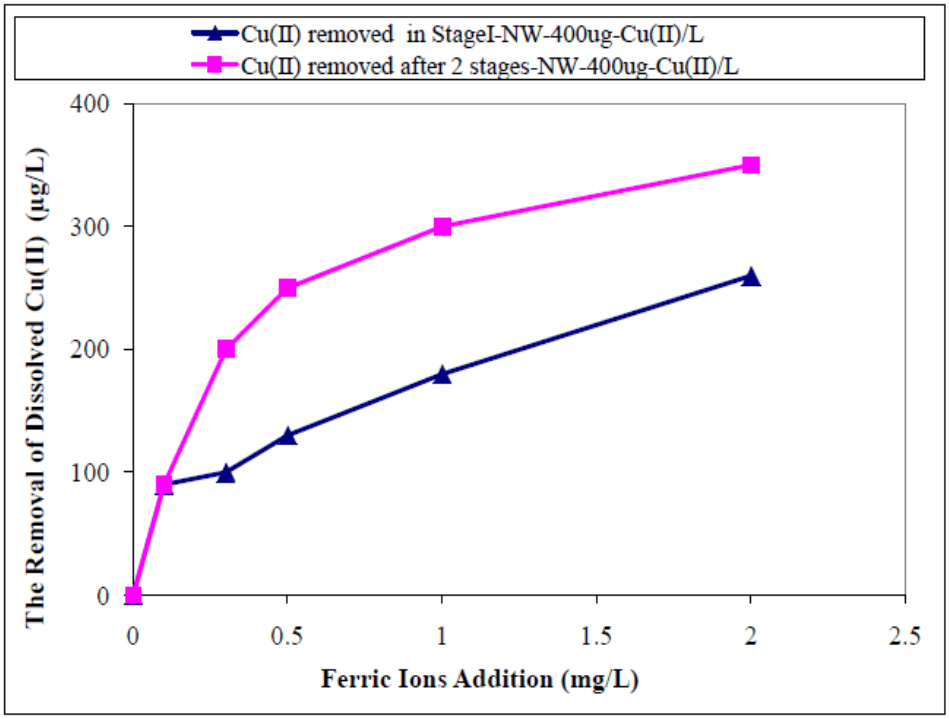

Figure 7.8: Removal of dissolved Cu(II) through the two-stage corrosion process in NW: 400 µg/L copper dose case

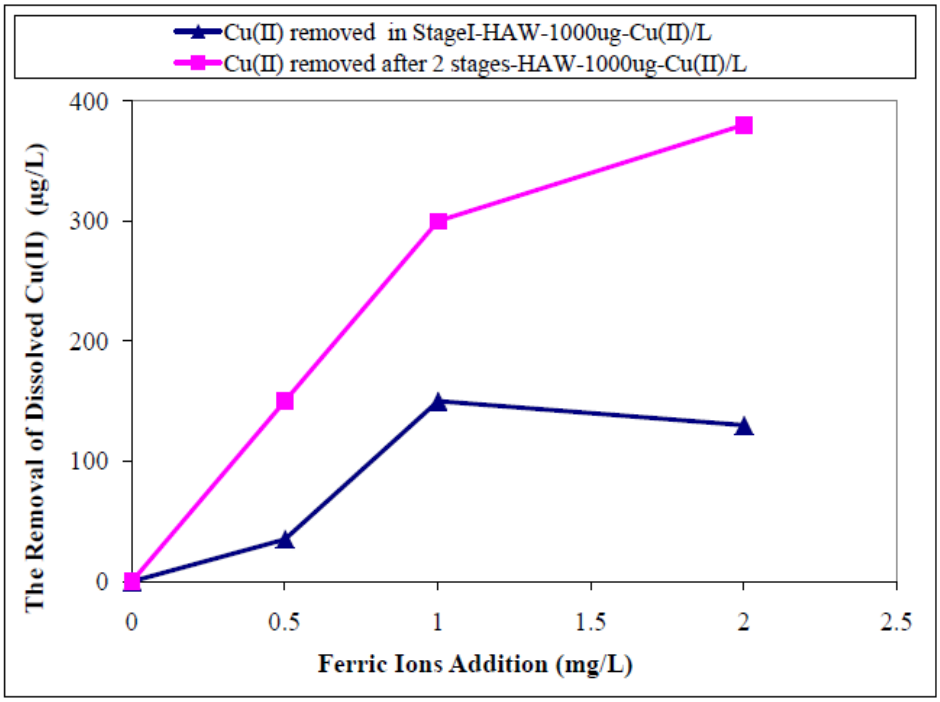

Figure 7.9: Removal of dissolved Cu(II) through the two-stage corrosion process in HAW: 1000 µg/L copper dose case

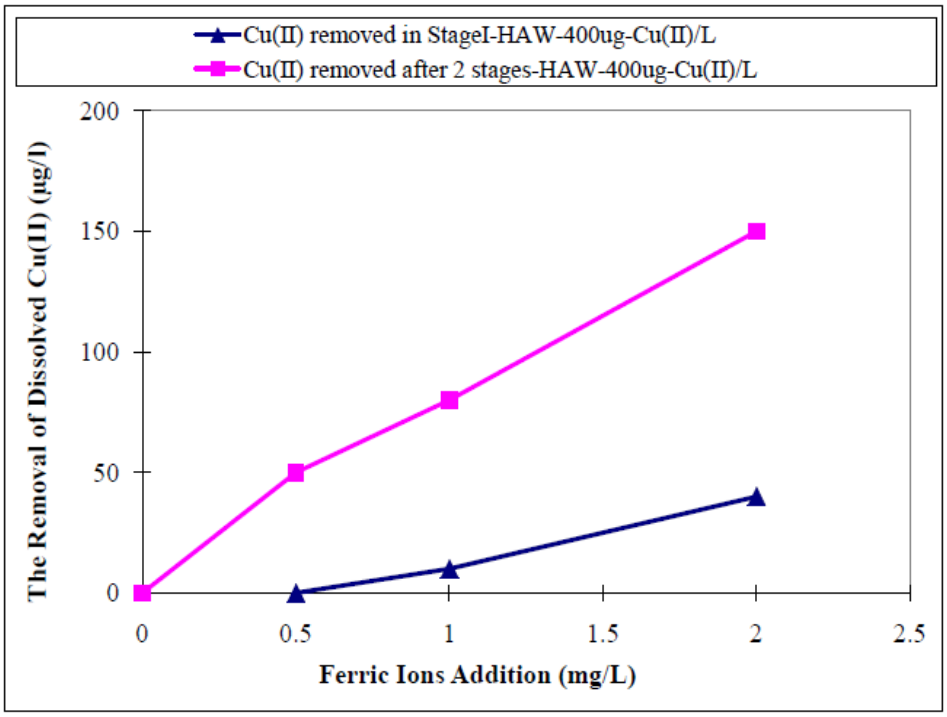

Figure 7.10: Removal of dissolved Cu(II) through the two-stage corrosion process in HAW: 400 µg/L copper dose case

Figures 7.5 and 7.6 show the two-stage removal of dissolved Cu(II) in MRW when copper was dosed at 1000 and 400 µg-Cu(II)/L respectively. The minimum gap between

the blue and the pink lines was observed when trace ions (0.1 mg /L) were added, indicating that Stage I was responsible for the majority (70%) of total copper removal. However, with increasing addition of the ions from 0.3 to 2.0 mg/L, the Cu(II) loss contributed by the adsorption in Stage II was augmented and accounted for 40~50% and 25~65% of the total removal when copper was dosed at 1000 and 400 µg-Cu(II)/L respectively. Generally, total removal of dissolved Cu(II) showed a power increase with increased ion addition. The removal occurring in Stage I increased linearly with ion addition of more than 0.5 mg/L.

The striking feature observed in Figure 7.5 and 7.6 is that the two curves are close to parallel for the ion addition of 0.5 mg/L and above. In other words, the removal occurring in Stage II did not increase proportionally even though the ion addition was increased. This can be attributed to the decreasing intermediate Cu(II) concentration when the ion addition was increased to remove more Cu(II) in Stage I. According to the Freundlich adsorption relationship, the removal in Stage II is not only augmented by increasing the $Fe(OH)_3$ floc concentration but also diminished with the intermediate Cu(II) concentration at the beginning of Stage II. Table 7.1 gives the calculation step by step and demonstrates how the removal in Stage II is governed by both increased ion addition and diminished intermediate Cu(II) which are counteracting each other.

Table 7.1 Calculation Table of Cu(II) Removal via Two Stage Corrosion Process (MRW)

Ion Addition (mg/L)	Cu(II) Dose (µg/L)	Initial Cu(II) (µg/L)	Removal in Stage I (µg/L)	Intermediate Cu(II) (µg/L)	Equilibrium Cu(II) (µg/L)	Removal in Stage II (µg/L)
0.5	1000	840	320	520	320	200
1	1000	840	360	480	190	290
2	1000	840	460	380	90	290
0.5	400	350	60	290	180	110
1	400	350	130	220	80	140
2	400	350	250	100	20	80

The same trend of removal was observed in NW (Figure 7.7 and 7.8). Copper removal occurring in Stage I dominated when only 0.1 mg-Fe/L ferric ions were added. At the higher ion addition, 30~50% copper loss was attributed to the adsorption process in Stage II.

A strikingly different result was observed in HAW (Figure 7.9 and 7.10). Only 16% of total dissolved Cu(II) loss occurred in Stage I when 0.5 mg-Fe/L ions were added into the sample with a copper salt dose of 1 mg-Cu(II)/L (Figure 7.9). In Figure 7.9, the maximum proportion of Cu(II) loss in Stage I accounted for 50% when 1 mg-Fe/L ions were added. Figure 7.10 shows that even generally, a smaller proportion of total Cu(II) loss happened in Stage I, with no copper removal during Stage I at 0.5 mg-Fe/L ion addition and maximum 16% of total Cu(II) loss occurring in Stage I at 2 mg-Fe/L ion addition. As discussed earlier, less dissolved Cu(II) was removed in HAW due to its distinct NOM character. In addition, the proportion of total dissolved Cu(II) removal contributed by Stage I was generally smaller in HAW. In other words, Cu(II) loss in HAW mainly happened during the adsorption process. This finding again indicated the impact of large organic molecules in HAW on the coagulation process occurring in Stage I, i.e. coagulation, employing ferric ions, mainly removed large molecules while the majority of Cu(II) chelated with relatively small molecules.

7.4 Conclusion

The removal of dissolved copper was achieved via the two-stage process sequentially occurring during corrosion: Stage I-coagulation and aggregation by ferrous/ferric ions; Stage II-adsorption controlled by iron hydroxide flocs, which formed from dosed

ferrous/ferric ions. Both ferrous/ferric ions and iron hydroxide flocs demonstrated considerable capacity to remove dissolved copper in bulk waters. MRW and NW showed nearly equal impacts of each stage on dissolved Cu(II) loss, except for the case of 0.1 mg-Fe/L ferric ion addition in which the total dissolved Cu(II) removal had nearly finished in Stage I. The degree of dissolved Cu(II) removal can be affected by the NOM composition in bulk waters. The effect of coagulation on Cu(II) removal in Stage I was attenuated in HAW due to the presence of large organic molecules. Therefore, less dissolved Cu(II) removal was observed in HAW. This observation is consistent with what was discussed in Chapter 5 and Chapter 6: both $Fe(OH)_3$ flocs and ferrous/ferric ions show weaker capacity to remove dissolved Cu(II) in HAW than in MRW.

CHAPTER 8

MECHANISMS GOVERNING Cu-NOM CHELATION AND THE EFFECT OF NOM CHARACTERISTIC ON DISSOLVED COPPER REMOVAL BY Fe(II)/Fe(III) SALTS

8.1 Introduction

In terms of the results shown in Chapter 5 and Chapter 6, differences in Cu(II) solubility and the behaviour of dissolved copper removal were observed between three major experimental water samples: Mundaring weir water, the water containing nitrifying bacteria and humic acid water. According to the AMW profiles in Figure 4.1, both Cu(II) binding preferentiality and distinct NOM character are thought to play an important role in Cu-NOM chelation and dissolved Cu(II) removal. However, further investigation is required to understand the mechanisms behind this. The comparison with respect to Cu-NOM chelation and dissolved Cu(II) removal was made between MRW, NW and HAW in the following discussion.

8.2 Mundaring raw water (MRW) vs Nitrified water (NW)

As discussed in previous chapters, Cu(II) solubility was slightly higher in NW than MRW and dissolved Cu(II) in NW also manifested a slightly stronger resistance to $Fe(OH)_3$ adsorption than that in MRW when the copper salt dose was either 250 or 400

µg-Cu(II)/L (Figure 6.6, Chapter 6). Chapter 6 provides the explanation based on the AWM profile (Figure 4.1), showing additional peaks of UV_{254}-absorbing DOC emerging in NW AWM in a low molecular weight range. However, the difference in AWM profile between MRW and NW is not explicit enough to distinguish their NOM composition.

Dryer et al. (2008) proposed a novel method called differential absorbance spectra to differentiate various compositions of NOM and characterized their complexation with copper. Therefore, NOM was believed to be chiefly responsible for the high solubility of copper found in the experimental bulk waters. Cu-NOM complexation was analysed by employing the differential absorbance spectroscopy principle:

$$\Delta A_{Cu}(\lambda) = \frac{1}{l_{cell} \times DOC}(A_{Cu}(\lambda) - A_{Cu\_reference}(\lambda))$$

$A_{Cu\_reference}$ is the absorbance of the experimental sample containing no copper. Based on the spectra of samples obtained for the complexation of copper experiment with similar dissolved organic carbon (DOC) but different NOM composition, it could render an explanation of distinct dissolved copper removal among various samples.

Figure 8.1 shows the variation of the spectra of MRW NOM when copper salt was dosed in increments (250, 400 and 1000 µg-Cu(II)/L) into MRW, using the spectrum of MRW NOM with 0 µg-Cu(II)/L copper salt dose as a reference line. Three curves are dominated by a peak at around 275 nm, with growing absorbance by increasing Cu(II) concentration. It indicates the prevalent fraction which tended to bind copper and form Cu-NOM complexes.

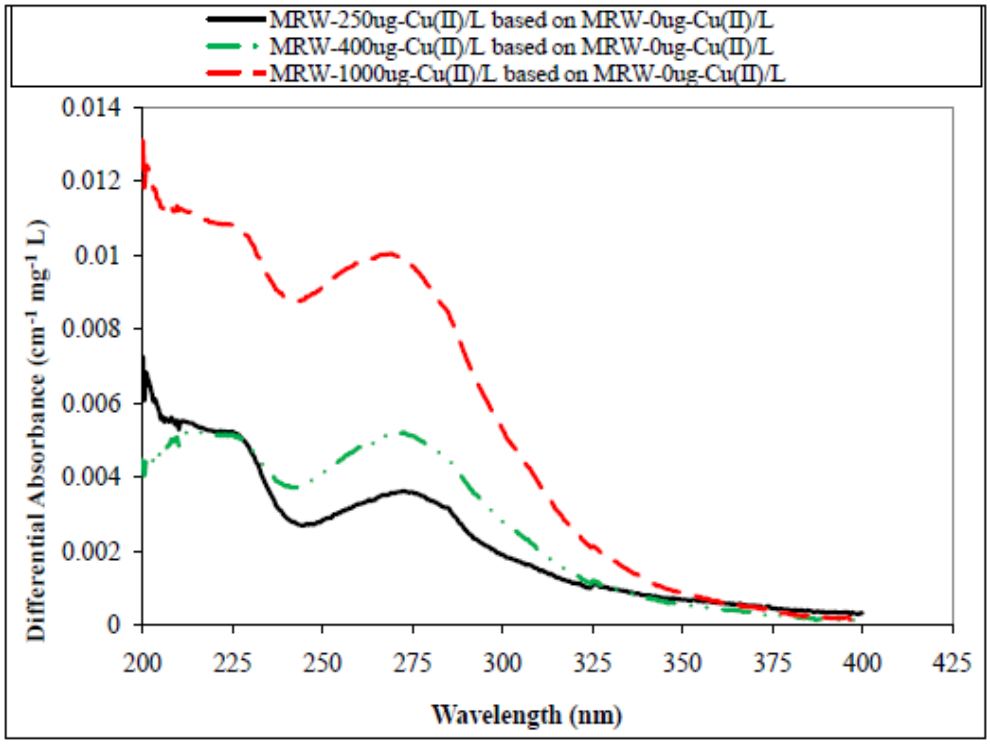

Figure 8.1: Differential absorbance spectra of MRW NOM bound with Cu(II)

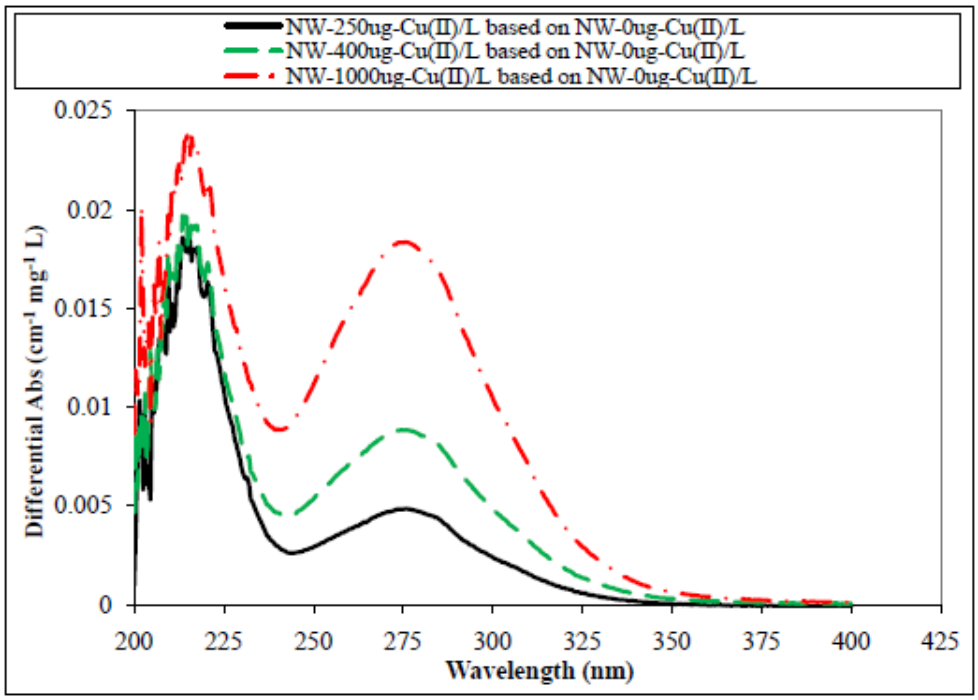

Figure 8.2: Differential absorbance spectra of NW NOM bound with Cu(II)

The peaks in the same wavelength range (~275 nm) can be found in the spectra of NW NOM (Figure 8.2), indicating a common fraction contained in both NW NOM and

MRW NOM which is able to chelate with Cu(II). This explains some resemblance observed in copper removal (Figure 6.6) between MRW and in NW, which is probably attributed to the common fraction of DOC which was chelated with Cu(II) in both waters. Nevertheless, NW showed one additional narrow peak at 215 nm, indicating a proportion of smaller soluble organic substances produced to chelate with Cu(II) during nitrification.

NW can be expected to have more organic compounds of small molecular weight. When MRW was fed into the system, chlorine and chloramine were dosed consecutively. When organic matters react with chlorine and chloramines, they can be broken down to ones of smaller molecular weight (Sathasivan et al., 1999). During nitrification, higher microbiological activities are possible. Such microbial processes may break down organic matters present in the water or may produce soluble microbial products (SMP) (Krishna and Sathasivan, 2010), possibly resulting in low molecular weight organic compounds. The production of SMP from nitrifying bacteria may increase metal solubility (e.g. Cu) via complexation (AWWARF&DVGW-TZW, 1996). Slightly higher absorbance and the additional peak indicated the possibility that there can be smaller molecular weight organic compounds, like SMP, produced and chelated with Cu(II). This might explain why slightly higher dissolved copper was found in NW than MRW before Fe addition.

8.3 Mundaring raw water (MRW) vs Humic acid water (HAW)

During the course of the experiments on dissolved Cu(II) removal by $Fe(OH)_3$ flocs from MRW and HAW, the analysis of AMW distributions of UV_{254}-absorbing DOC was conducted. It compared the AMW distribution of DOC with and without dosed

copper as well as before and after the treatment by $Fe(OH)_3$ flocs. The results of change of AMW distribution in MRW and HAW are presented in Figure 8.3 and 8.4, respectively. The samples with a copper dose of 400 µg/L (MRW-400µg-Cu(II)/L; HAW-400µg-Cu(II)/L) and $Fe(OH)_3$ addition of 0.5mg/L (MRW-400µg-Cu(II)/L-0.5mg-Fe/L, HAW-400µg-Cu(II)/L-0.5mg-Fe/L) were used for the AMW distribution analysis.

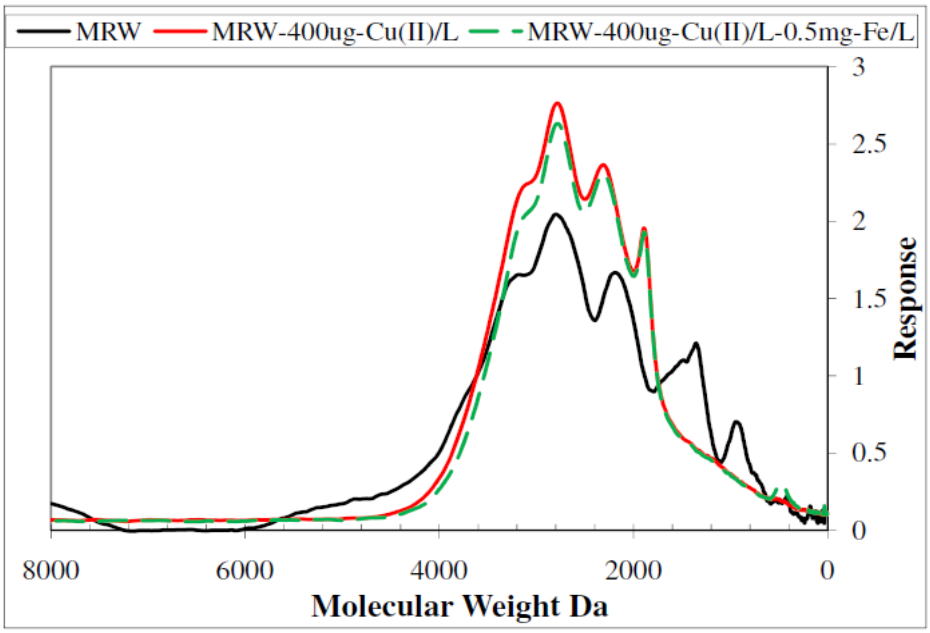

Figure 8.3: AMW distributions of UV_{254}-absorbing DOC in MRW after Cu(II) salt dose (400 µg/L) and Fe(III) treatment (0.5 mg/L)

In the MRW samples, addition of copper considerably increased the UV_{254} Abs at the MW range between 2000~4000 Da. This increase reflects a restructuring of DOC after the organic matter complexes or chelates with copper, perhaps through intermolecular bidentate chelation between smaller organic molecules. The removal of Cu-NOM by 0.5 mg-Fe/L $Fe(OH)_3$ is also concentrated on a narrow spectrum between 2500 Da and 3500 Da. According to Dryer et al. (2008), the hydrophobic fraction of NOM, which is generally rich in phenolic chromophores, is depleted in Mundaring water, because the

water comprises partly of groundwater treated by alum coagulation. Therefore, the increased UV_{254} Abs can be attributed to the conversion of the hydrophilic fraction in the MRW DOC to a hydrophobic fraction through complexation with copper, which was acting as a bridging ion able to aggregate two or more small molecules to form big molecules.

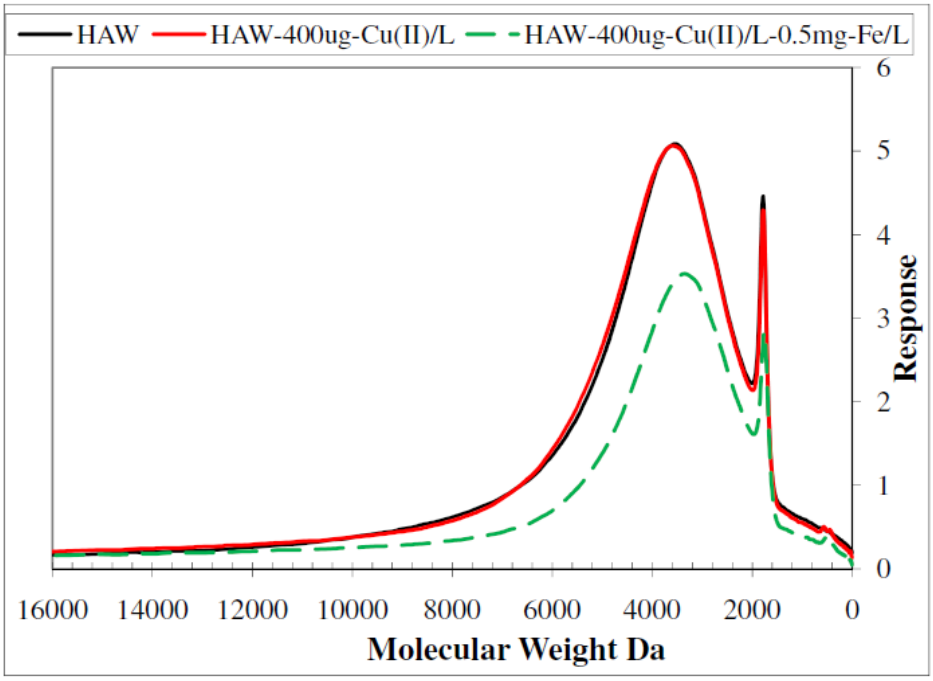

Figure 8.4: AMW distributions of UV_{254}-absorbing DOC in HAW after Cu(II) salt dose (400 µg/L) and Fe treatment (0.5 mg/L)

By contrast to the corresponding situation of MRW, dosed copper did not change the AMW profile of DOC in HAW (Figure 8.4). However, the addition of $Fe(OH)_3$ flocs had considerably reduced UV_{254}-absorbing DOC on a more extensive AMW range (2000-6000 Da), indicating that $Fe(OH)_3$ flocs removed the large MW components. This is in line with previous observations that coagulation readily and preferentially remove hydrophobic fractions mainly contained in aquatic humic material with high MW (Volk et al., 2000). In addition, little dissolved Cu(II) removal by 0.5 mg/L

$Fe(OH)_3$ as discussed previously (Figure 6.5) indicates that dosed Cu(II) may preferentially chelate with small MW components or a hydrophilic fraction in HAW and consequently be shielded from $Fe(OH)_3$ adsorption by large MW components or hydrophobic fractions that are not bound with copper, especially when the copper dose is less than 400 µg/L (binding sites on small molecules in HAW are still not saturated) .

Gamble et al. (1980) reported two general types of bidentate chelating sites for dissolved Cu(II): salicylate and dicarboxylate type (Figure 8.5). The dicarboxylate type could be both intra-molecular and inter-molecular, depending on the functional groups available. According to the shift of UV_{254}-absorbing DOC in MRW to higher AMW upon addition of copper (II), intermolecular dicarboxylate chelation is mainly responsible for copper binding in MRW resulting in the aggregation of small molecules, while salicylate chelation may be more prevalent in HAW in which the NOM may contain more salicylate type binding sites.

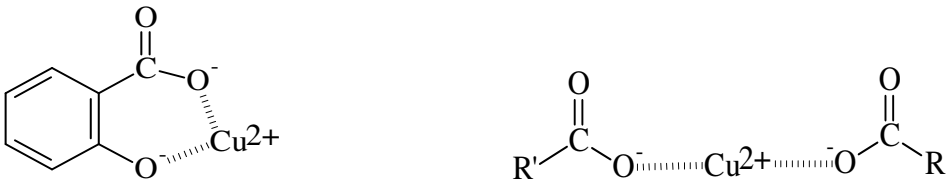

Salicylate chelation Dicarboxylate chelation

Figure 8.5: Cu(II) chelation with two types of bidentate chelating sites

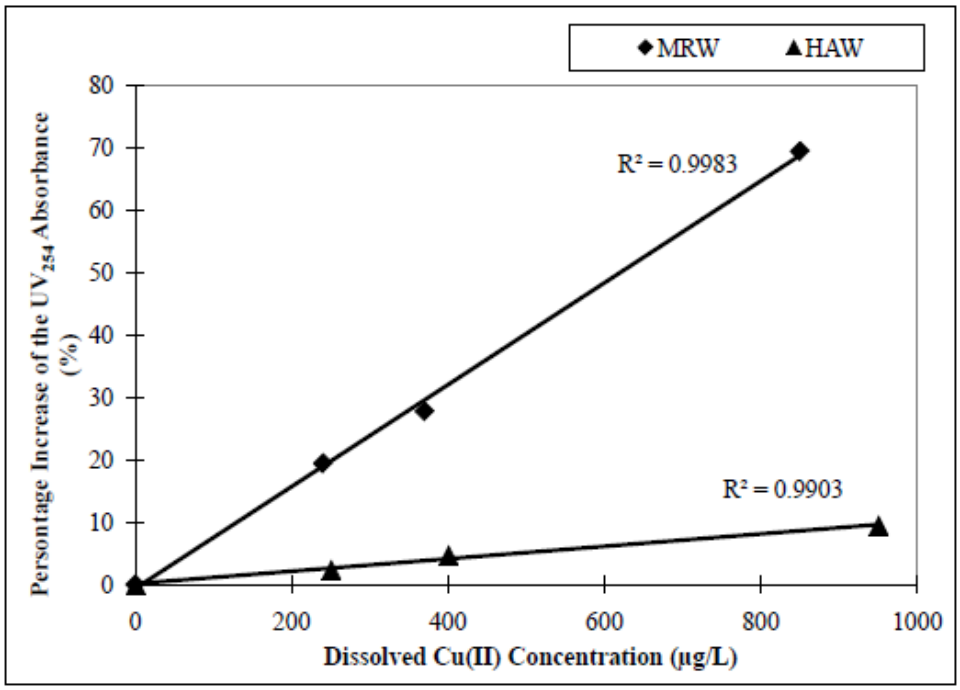

Figure 8.6: Percentage increase of UV_{254} absorbance vs Dissolved Cu(II) concentration in MRW and HAW

(Percentage increase of UV_{254} absorbance= $\frac{UVabswithCu(II) - UVabswithoutCu(II)}{UVabswithoutCu(II)}$)

Figure 8.6 shows the impact of Cu-NOM complexation on UV_{254} absorbance of MRW DOC and HAW DOC by plotting the percentage increase of UV_{254} absorbance of MWR and HAW DOC against dissolved Cu(II) concentration in increments. One thing that needs to be emphasized is that DOC was measured before and after copper dose, and no change of DOC was found in both waters. Therefore, change in UV_{254} Abs can equivalently represent the change in $SUVA_{254}$, which is a good indicator of the humic fraction of DOC (Weishaar, et al., 2003).

The UV_{254} absorbance of either MRW DOC or HAW DOC increased linearly when increasing Cu(II) concentration in the bulk water. It shows that UV_{254} absorbance was increased by 70% when 840 µg/ L dissolved Cu(II) was dissolved in MRW. The $SUVA_{254}$ of MRW was correspondingly increased from 1.35 to 2.30 $L \cdot m^{-1} \cdot mg^{-1}$. In

HAW, only a 9% increase was calculated accordingly. The significant change in $SUVA_{254}$ of MRW DOC gives another point of evidence that dosed Cu(II) restructured the MRW DOC by bridging small molecules to form big ones via intermolecular dicarboxylate chelation, or converted some hydrophilic fractions to hydrophobic fractions through aggregation. The continuous removal of Cu-NOM_{uc} by $Fe(OH)_3$ flocs from MCW, which was previously discussed, also indicates that this aggregation could facilitate removal of the uncoagulable NOM (e.g. dominating NOM in MCW) by first converting them to coagulable NOM. On the other hand, the increase of UV_{254} absorbance caused by chelation between dissolved Cu(II) and small molecules in the HAW could be overshadowed by the originally high MW DOC with hydrophobic fractions mainly contained in the HAW, and hence made the percentage increase relatively insignificant.

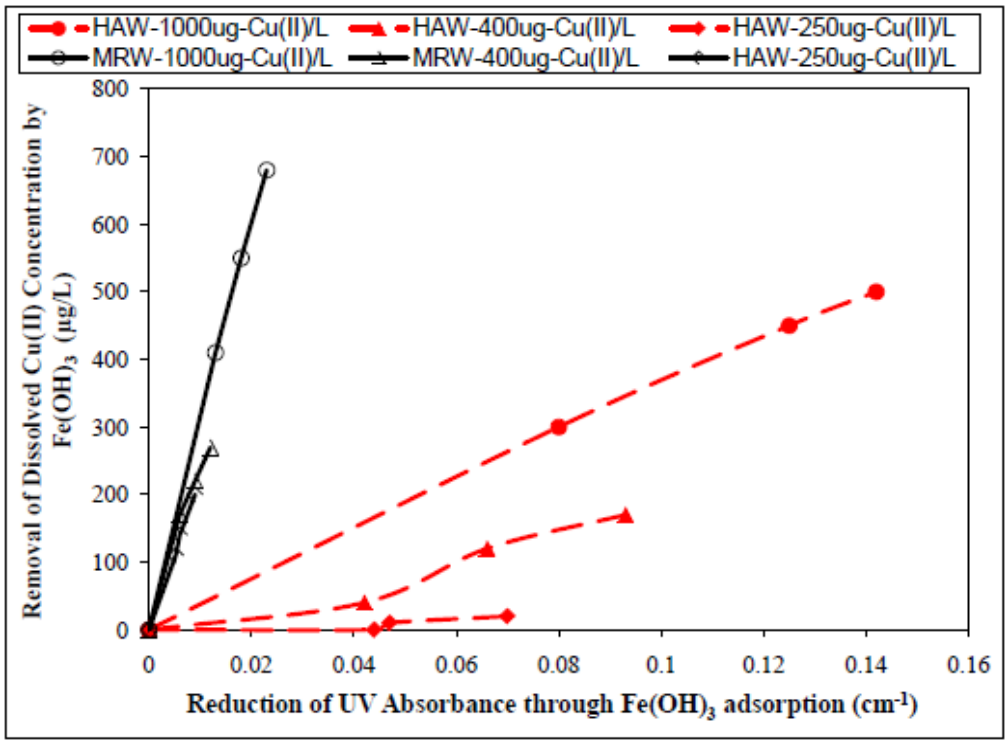

Figure 8.7 Reduction of UV_{254} absorbing DOC in MRW and HAW containing Cu(II) vs the removal of dissolved Cu(II) via $Fe(OH)_3$ adsorption (Legends: "HAW-

1000µg-Cu(II)/L": copper was dosed at 1000 µg-Cu(II)/L in humic acid sample. The others can be interpreted analogously.)

Figure 8.7 shows how the UV_{254} absorbing DOC was changing in dissolved Cu(II) containing MRW and HAW when $Fe(OH)_3$ flocs were added in increments to remove Cu(II). The reduction of UV_{254} absorbance after $Fe(OH)_3$ treatment (0.5, 1.0 and 2 mg-Fe/L) is plotted against removal of dissolved Cu(II) for different copper salt doses (250, 400 and 1000 µg-Cu(II)/L). Three solid lines connect experimental data points from MRW at three different copper doses (250, 400 and 1000 µg-Cu(II)/L). Counterparts from HAW are connected by dashed lines. The strikingly different slopes between solid lines and dashed lines, which represent the ratio of Cu(II) removal to the reduction of UV_{254} absorbance, reflect the degree to which dosed Cu(II) complexed with NOM and was subsequently removed via $Fe(OH)_3$ adsorption. Dissolved Cu(II) remained almost unremoved by the flocs in HAW for the 250 µg-Cu(II)/L copper dose case, though UV_{254} abs dropped by 0.07 after 2 mg-Fe(III)/L treatment. On the contrary, MRW showed a radical copper loss of 200 µg/L. This result supports the previous deduction that a relatively small amount of dosed copper (e.g 250 µg/L) may preferentially chelate with small hydrophilic molecules available in HAW. Increasing the copper dose made the binding sites on small molecules gradually saturated and then the dosed Cu(II) would have started complexing with large molecules in the hydrophobic fraction of HAW material, which was then readily removed upon $Fe(OH)_3$ addition.

8.4 Conclusion

The dosed copper used to inhibit nitrification in G&AWSS mainly existed in the forms of various Cu-NOM complexes. Acting as a bridging substance, the majority of dosed copper can aggregate small organic molecules by chelating on hydrophilic binding sites, which are dominant in the NOM of Mundaring water and the nitrified water. In bulk water containing large organic molecules with a hydrophobic fraction (e.g humic acid water), dosed copper salt still prefers to chelate with small molecules rather than large molecules until the saturation of this complexation is reached by increased copper dose. When ferric salts were added into bulk waters, they tended to coagulate or adsorb relatively large molecules first. Therefore, the presence of large MW organic matters might, to some degree, shield the dissolved Cu(II) bound with small molecules from removal.

CHAPTER 9

MODELLING THE LOSS OF DISSOLVED Cu(II) IN A CORRODED STEEL PIPELINE

9.1 Introduction

The previous chapters discuss the dominant species of dissolved Cu(II), quantify removal of the dissolved Cu(II) by trace ferrous/ferric salts based on the laboratory scale batch experiments and elucidate the mechanisms behind Cu-NOM complexation and the interactions between Cu-NOM and Fe(II)/Fe(III) salts. However, the previous experiments only investigated the Cu(II) loss after the reactions between dosed Cu(II) and Fe(II)/Fe(III) salts reached equilibrium status. In order to track the dissolved Cu(II) loss against elapsed time in the pipeline where the corrosion products are being continuously released, the dynamic process of copper removal by Fe(II)/Fe(III) salts must be studied.

Parameters of the model were initially derived from the results of removal of dissolved Cu(II) by $Fe(OH)_3$ flocs due to the following reasons:

- Compared with Fe^{2+} or Fe^{3+} ions, $Fe(OH)_3$ flocs are the long-lasting products adsorbing Cu(II) in bulk water (Fe^{2+}/Fe^{3+} ions can only exist for less than 5 minutes after being released into bulk water in terms of the observation during bulk water experiments).

- The well-established Freundlich isotherm can help find the equilibrium Cu(II) concentration, which is an important factor in the model when various copper and $Fe(OH)_3$ doses are studied.

To make up for the proportion of Cu(II) removal contributed by Fe^{2+} or Fe^{3+} ions, a coefficient is introduced to the model, based on the difference in capacity to remove Cu(II) between Fe^{2+}/Fe^{3+} ions and $Fe(OH)_3$ flocs, as discussed in Chapter 7.

Employing the C-K Extension main in G&AWSS as a prototype, where the field pilot experiment of copper dose has been undertaken, a simple pipeline model was established, with a series of predetermined parameters with respect to hydraulic conditions, copper doses and corrosion patterns. The parameters employed in the model with regard to the dynamic process of copper removal by ferric salts were derived from the experimental results. The model was programmed using Aquasim®.

9.2 The Dynamic Process of Dissolved Cu(II) Removal by Ferric Hydroxide Flocs in Mundaring Raw Water

9.2.1 Experimental Procedure

Chapter 6 discusses dissolved Cu(II) removal by $Fe(OH)_3$ flocs at various copper doses and $Fe(OH)_3$ additions. This experiment followed the same procedure as described in Chapter 6 (refer to Chapter 6, the Experimental Procedure and Method) with respect to copper salt dose, Fe(III) addition, dissolved Cu(II) measurement and bulk water jar test. The bulk water was sourced from Mundaring raw water (MRW). Doses of 250 µg-Cu/L

and 400 µg-Cu/L Cu(II) were used, with 1 mg-Fe/L addition. A 1000 µg-Cu/L Cu(II) dose was used with various $Fe(OH)_3$ additions of 0.5, 1 and 2 mg-Fe/L. However, instead of measuring equilibrium dissolved Cu(II) concentration remaining in the bulk water after $Fe(OH)_3$ treatment, aliquots were withdrawn from the bulk water at designated time intervals (5, 10, 20, 30, 60, 120 mins) during the jar test. By measuring the dissolved Cu(II) concentration in each aliquot, the decay of dissolved Cu(II) concentration was monitored in the course of ferric hydroxide treatment.

9.2.2 Results and Discussion

Figure 9.1 shows the decay of dissolved Cu(II) concentration after adding $Fe(OH)_3$ flocs. According to Figure 9.1, the rate of dissolved Cu(II) decay obeyed the Pseudo second order, regardless of different copper doses and ferric hydroxide floc additions.

$$\frac{dC\_Cu}{dt} = -\frac{k \times C\_Fe \times (C\_Cu - Ce\_Cu)^2}{(Cin\_Cu - Ce\_Cu)} \qquad \text{(E1)}$$

"k": Reaction rate constant

"C_Cu": Current dissolved Cu(II) concentration

"Ce_Cu": Equilibrium dissolved Cu(II) concentration

"C_Fe": $Fe(OH)_3$ flocs concentration in the bulk water

"Cin_Cu": Input dissolved Cu(II) concentration before ferric dose

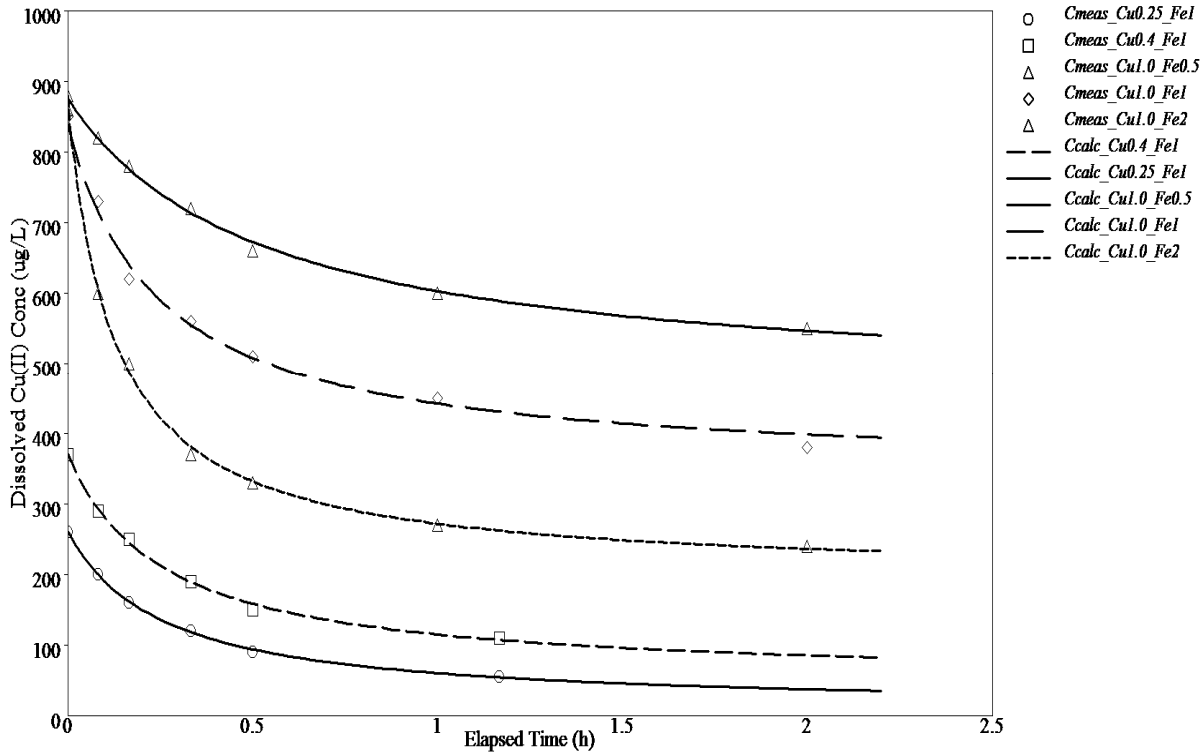

Figure 9.1: The dynamic process of dissolved Cu(II) removal by $Fe(OH)_3$ flocs

Note: The dots of various types represent the measured results of the experiment. The calculated modelling results from the pseudo second order equation are represented by different lines. The parameters of Pseudo second order equation were estimated with Aquasim®.

Legends' Interpretation

"Meas_Cu400_Fe1": Measured Cu concentration during the experiment. Cu dose was 400 µg/L; Fe dose was 1mg/L.

"Calc_Cu400_Fe1": Calculated Cu concentration obeying pseudo second order after Aquasim parameter estimation. Cu dose was 400 µg/L; $Fe(OH)_3$ addition was 1mg/L.

The rest of the legends can be interpreted analogously.

Table 9.1: The parameters of pseudo second order decay estimated by Aquasim®

Cu salt dose (µg-Cu/L)	Cin_Cu (µg/L)	C_Fe (µg/L)	k (L/h·µg)	Ce_Cu * (µg/L)
250	250	1000	0.00390	50
400	370	1000	0.00385	140
1000	880	500	0.00385	510
1000	850	1000	0.00401	350
1000	850	2000	0.00402	220

Ce_Cu*: The equilibrium dissolved Cu(II) concentrations were abstracted from Chapter 6 (Figure 6.2). "Ce_Cu" was input into equation (E 1) to help estimate the parameter "k".

Table 9.1 summarizes the Pseudo second order parameters input into the model that was estimated by Aquasim®. The equilibrium concentration of dissolved Cu(II) (Ce_C) depends on the Cu(II) dose (Cin_Cu) and $Fe(OH)_3$ concentration (C_Fe) present in the bulk water, which can be calculated using the Freundlich isotherm, as discussed in Chapter 6.

Another essential parameter that controls the reaction rate is "k", the pseudo second order rate constant. Although "k" varied slightly on Table 9.1 with different Cu(II) doses and $Fe(OH)_3$ additions, it is still reasonable to take the average value of "0.00392" as representative of the rate constant in E 1 to describe the dynamic decay of dissolved Cu(II) in Mundaring bulk water. This value has 2% relative standard deviation (RSD), indicating that it could be easily generalized.

Therefore, the rate of copper loss through $Fe(OH)_3$ adsorption is a function of Cu(II) dose (Cin_Cu) and $Fe(OH)_3$ concentration (C_Fe). To predict dissolved Cu(II) loss in a corroded pipe present with ferric salts, a simple model must be established with a series of predetermined parameters such as hydraulic conditions, Cu(II) dosing patterns and ferric addition patterns.

.

9.3 Modelling the Dissolved Cu(II) Loss in a Corroded Steel Pipe Releasing Ferric Salts

9.3.1 Introduction of the Pipe Model

The pilot Cu(II) salt dosing has been carried out in the CK Extension main. The Cu(II) salt dose was varied occasionally. Dissolved Cu(II) concentration had been monitored at CK12km and CK58km (See Appendix D). Figure 9.2 shows the pipe model based on the CK extension prototype. Cu(II) salt was dosed at the inlet of the pipe with discharge Qin.

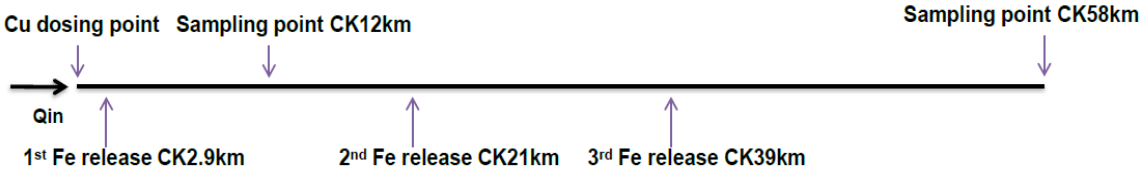

Figure 9.2: The sketch of CK Extension main

Pipe information:

The length of the pipe: 58km

The diameters of the pipe: ø450mm

The average discharge: Qin=5 ML/d

9.3.2 Cu(II) Salt Dosing and the Fe-time Release Pattern

Although the trial continued for a much longer time, data obtained in the initial period was used to validate the model. The dose of Cu(II) salt varied between 220 and 410

µg/L during the 104-day trial in 2006 between late April and early August (See Appendix D). One ideal way to simulate iron corrosion is to consider a uniform distribution of iron release points along the pipe. Due to lack of available data, it is very difficult to locate the actual corroded cavities in the field and quantify the iron release. However, iron release cavities could be reasonably assumed and three points shown in Figure 9.2 were found to be able to simulate the Cu(II) concentration which had been regularly monitored at two locations: CK12Km and CK58Km. Large amounts of copper sediments were also found and analysed at these two locations.

9.3.3 The methodology and the numerical solutions

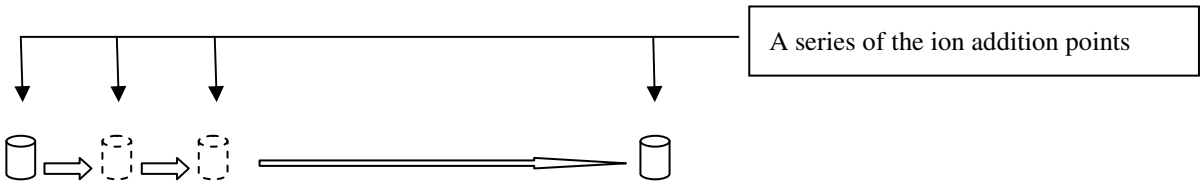

Figure 9.3: The concept of modelling bulk water travel through a pipeline containing a series of Fe release points

The La Grange method was employed to calculate dissolved Cu(II) loss in a bulk water travelling through a pipeline as shown in Figure 9.3. According to Figure 9.2, when a bulk water is travelling through a pipeline containing a series of Fe addition points, ferric concentration (C_Fe) in the bulk water changes as it passes by each Fe release point.

Ferric concentration accumulated in the bulk water: C_Fe = F (t, m)

"m": the number of Fe release cavities

The function of dynamic process of Cu(II) decay: C_Cu = Ψ (C_Fe, Cin_Cu, Ce_Cu, t). It is governed by pseudo second order:

$$\frac{dC\_Cu}{dt} = -\frac{k \times C\_Fe \times (C\_Cu - \alpha \times Ce\_Cu)^2}{(Cin\_Cu - \alpha \times Ce\_Cu)} \qquad \text{(E 2)}$$

E 2 is slightly different from E 1 with one coefficient "α". "α" is introduced to adjust equilibrium dissolved Cu(II) concentration when ferrous or ferric ions are initially released from corroded iron walls instead of $Fe(OH)_3$ flocs. In this model, the value of $\alpha = 0.5$ was chosen. (See Appendix E for the detailed discussion with regard to α value assessment).

The function of equilibrium status: Ce_Cu=f (Cin_Cu, C_Fe). It is obeying Freundlich adsorption isotherm.

$$\frac{Cin\_Cu - Ce\_Cu}{C\_Fe} = K_F \times Ce\_Cu^{1/n} \qquad \text{(E 3)}$$

According to Table 6.1 (Chapter 6), K_F= 0.003; n=1.16.

Hence, dissolved Cu(II) concentration at time t_1 after the bulk water has passed the first Fe release cavity can be calculated by integrating E 2:

$$\int_{Cin\_Cu}^{C\_Cu} \frac{dC\_Cu}{(C\_Cu - \alpha \times Ce\_Cu_1)^2} = \int_0^{t_1} -\frac{k \times C\_Fe_1 dt}{Cin\_Cu - \alpha \times Ce\_Cu_1} \quad t \in [0, t_1]$$

So,

$$\frac{1}{C\_Cu - \alpha \times Ce\_Cu_1} = \frac{1}{Cin\_Cu - \alpha \times Ce\_Cu_1} + \frac{k \times C\_Fe_1 \times t_1}{Cin\_Cu - \alpha \times Ce\_Cu_1}$$

When the bulk water passes by the second Fe release point at t_2:

$$\frac{1}{C\_Cu-\alpha\times Ce\_Cu_2}=\frac{1}{C\_Cu_{t=t_1}-\alpha\times Ce\_Cu_2}+\frac{k\times C\_Fe_2\times(t_2-t_1)}{Cin\_Cu-\alpha\times Ce\_Cu_2}$$

$t \in [t_1, t_2]$

……

Dissolved copper concentration after nth Fe release point can be expressed as:

$$\frac{1}{C\_Cu-\alpha\times Ce\_Cu_m}=\frac{1}{C\_Cu_{t=t_{m-1}}-\alpha\times Ce\_Cu_m}+\frac{k\times C\_Fe_m\times(t_m-t_{m-1})}{Cin\_Cu-\alpha\times Ce\_Cu_m}$$

$t \in [t_{m-1}, t_m]$

(E 4)

"Ce_Cu_m" is the result from E 3 after calculating C_Fe with a corresponding time interval.

9.3.3 Modelling Results and Discussion

The La Grange method discussed above was programmed into the modelling software Aquasim®. The data in Appendix D were input into Aquasim® to help assess the time patterns of iron release and simulate dissolved Cu(II) removal along the pipe.

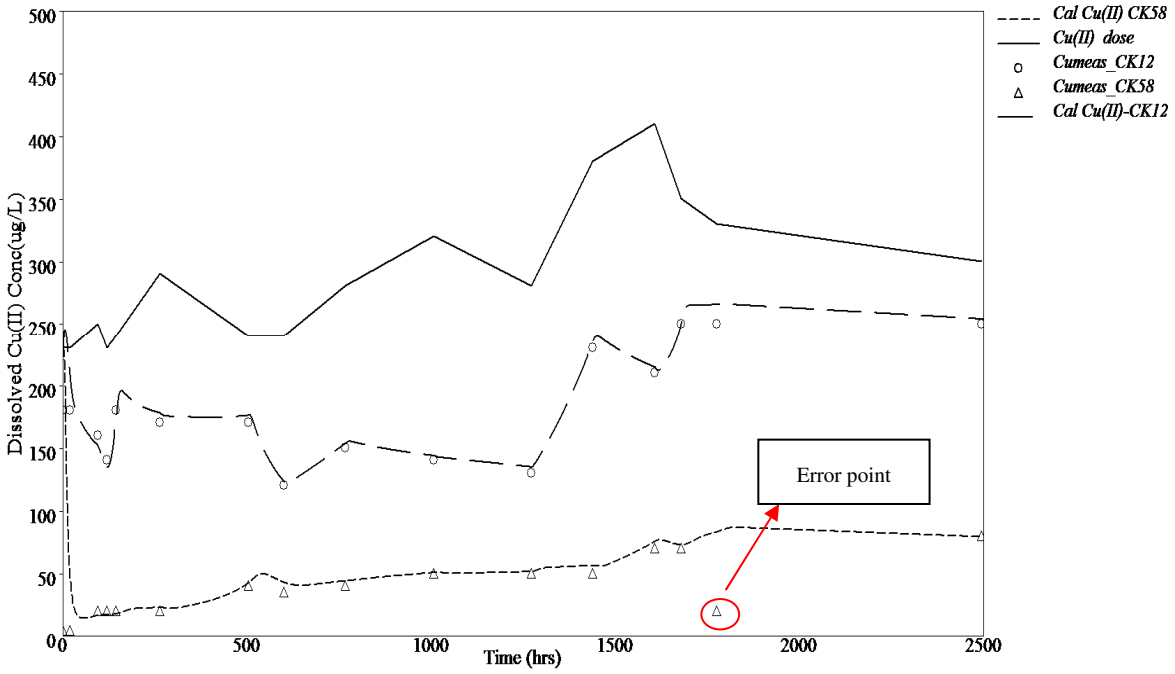

Figure 9.4 Comparison of dissolved Cu(II) concentration between the field data (CK12km and CK58km) and the modelling results

Legends: "Cu(II) dose"- Cu(II) salt dose at the inlet of CK Extension main; "Cumeas_CK12"-measured dissolved Cu(II) concentrations at CK12km in the field; "Cal Cu(II) CK12"-calculated dissolved Cu(II) concentrations at CK12km by the model. The data with regard to CK58km can be interpreted analogously.

Cu(II) input varied between 250 µg/L and 400 µg/L in the model to reflect the actual copper dose in the field. The Fe-time release pattern (Fe release vs elapsed time) was manipulated to achieve the best match between calculated Cu(II) concentration and the corresponding measured one. The equilibrium Cu(II) concentration (Ce_Cu) is governed by Cu(II) input and iron release. Two dashed lines were produced from the model representing the calculated dissolved Cu(II) concentration at CK12km and CK58km. They were compared with the measured dissolved Cu(II) concentrations in the field (the scattered circles and triangles in Figure 9.4). A good match was found between measured dissolved Cu(II) concentration and calculated one. The only point straying a little far away from the CK58km modelling curve happened at 1776 hours

(circled in Figure 9.4 as an error point). It showed that the measured Cu(II) concentration in the field was about 60 µg/L lower than what the model calculated. It might be due to the instrumental measuring error of ±20 µg/L and testing error in the field. Nonetheless, this point does not affect the general accuracy of the modelling results.

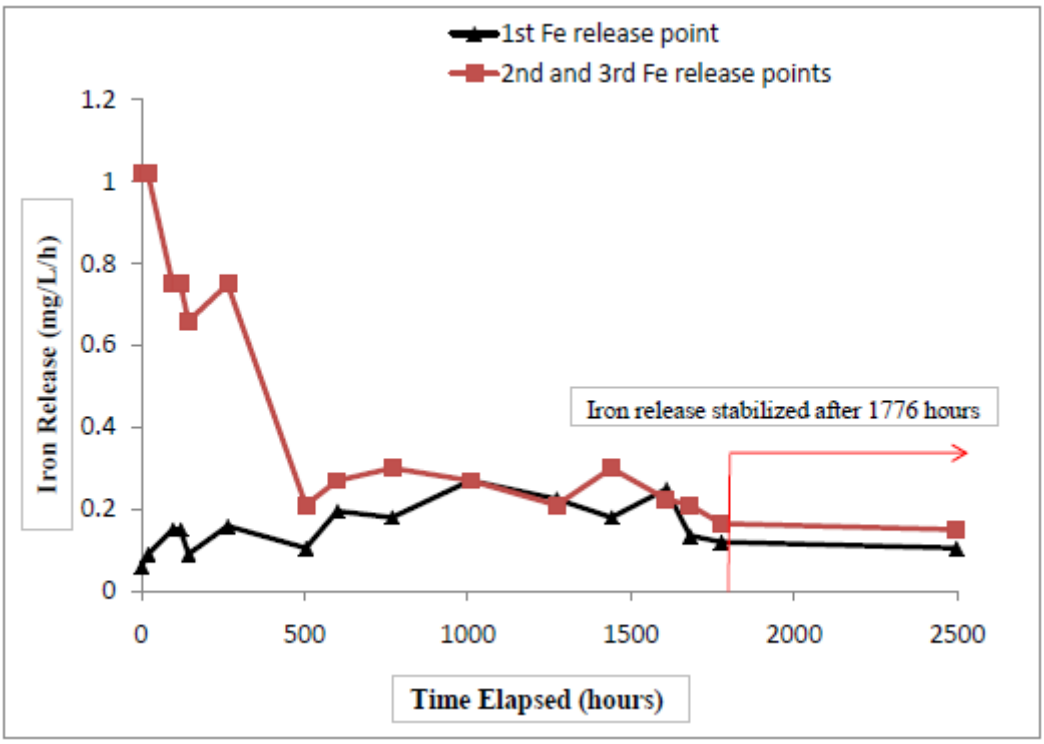

Figure 9.5 Fe-time release patterns at the three corroded cavities in the 104-day field trial

Figure 9.5 shows the Fe-time release pattern adopted for the modelling during the simulation. In the real system, corroded cavities upstream of the pipeline are saturated first and followed with downstream ones. This explains the striking discrepancy of iron release in the initial 500 hours (Figure 9.5) between the first corroded point and the second and third points, indicating how the corroded cavities along the pipeline were being saturated. In addition, other factors can cause copper loss other than corrosion alone. For example, biofilms can sequester copper. The demand in fact coming from the

biofilm could be the reason leading to the high calculated iron release rate at the early stage in the model that only considered corrosion process. The effect from biofilms would diminish and become saturated as equilibriums were achieved, leaving corrosion to be the dominant mechanism. Therefore, what was observed after 1776 hours in the model was considered to reflect the actual iron release. The average iron release of 80 g/d/km was hence calculated by integrating the area (after 1776 hours) below the corresponding curve and multiplying it by the water discharge.

Generally, this model prediction, irrespective of the fact that pre-existing iron or biofilm sequestration was not assumed to exist, has shown interesting and useful insight into the processes happening in the pipeline. Modelling copper sequestration by the biofilm is out of scope for this study. However, proper incorporation will lead to a better prediction in the future.

9.4 Conclusion

The dynamic process of adsorption of dissolved Cu(II) by $Fe(OH)_3$ flocs can be described as Pseudo second order adsorption. It can combine with Freundlich isotherms, which were used to find equilibrium dissolved Cu(II) concentrations when different copper doses and $Fe(OH)_3$ additions were experimented, to model dissolved Cu(II) loss in the pipeline. A coefficient “” can be added in the Pseudo second order equation if Cu(II) loss in corrosion Stage I (Cu(II) removal by ferrous and ferric ions) is considered. The iron pipe corrosion model established based on the dynamic process of adsorption is capable of simulating the trend of Cu(II) loss by reasonably assuming iron corrosion scenarios in the CK Extension pipeline. However, the modelling result

indicated that the other mechanisms (e.g. pre-existing iron sediments and biofim) might have also contributed to the copper loss. The fate of dissolved copper in the distribution system can be better predicted by properly incorporating copper removal by pre-existing iron sediments and biofilm.

CHAPTER 10

SUMMARY, DISCUSSION AND RECOMMENDATIONS

10.1 Summary and Discussion

10.1.1 Cu(II) Solubility and Speciation in Bulk Waters

Both Cu(II) solubility and speciation in bulk water depend on aqueous conditions, including pH, carbonate alkalinity, DOC concentration and NOM character. In this research, Cu(II) species are categorized into four basic forms: free cupric ions, inorganic Cu(II) compounds, Cu-NOM complexes and Cu(II)-containing particles. Dominant Cu(II) species under various aqueous conditions and their proportions in different bulk water samples were quantified. Results are summarized as follows:

The concentration of free cupric ions (Cu^{2+}) is negligible (< 10 µg/L) at pH > 7.5, which is the usual pH maintained in the water distribution system.

In open and closed (depending on partial pressure of CO_2) systems, Cu(II) solubility is controlled by the equilibrium with tenorite ($CuO_{(s)}$) and copper hydroxide ($Cu(OH)_{2(s)}$) respectively. Increasing aqueous carbonate concentration (CO_3^{2-}, HCO_3^-) can slightly increase dissolved Cu(II) concentration through formation of inorganic Cu(II) compounds ($CuOH^-$, $CuCO_3^o$), around 10% of dosed copper salt was found to be dissolved Cu(II) when 50 mg/L $CaCO_3$ was added in the Milli-Q water.

Cu(II) solubility is dramatically increased in the source water (MRW) of G&AWSS, the water containing nitrifying bacteria (NW) and humic acid water (HAW) due to NOM contained in these bulk waters. Cu-NOM complexes were found to be the dominant dissolved Cu(II) forms in these bulk water samples which had a DOC concentration of around 2.5 mg-C/L, though Cu(II) solubility slightly differed in these bulk waters due to different NOM character.

10.1.2 Cu(II)-NOM Chelation in the Bulk Waters

In Mundaring water, dosed Cu(II) is able to chelate with both coagulable and uncoagulable NOM. The deprivation of coagulable NOM (Mundaring water after coagulation) can considerably decrease Cu(II) solubility: only 350 µg/L dissolved Cu(II) was found when a high copper salt dose was added (1000 µg/L) in MCW, much lower than that (840 µg/L) in MRW in the corresponding situation, indicating that coagulable NOM can also bind with Cu(II).

Acting as a bridging substance, the majority of dosed copper can aggregate small organic molecules via intermolecular dicarboxylate chelation which is thought to be a dominating chelation between Cu(II) and organic compounds in MRW, MCW and NW. In the bulk water containing large organic molecules with a hydrophobic fraction (e.g HAW), salicylate chelation may be prevalent due to availability of more salicylate type binding sites. Moreover, the dosed Cu(II) is believed to preferentially chelate with small molecular weight (MW) organic compounds rather than large MW ones until the saturation of this complexation reaches by increased Cu(II) dose. Once they are

saturated even higher molecular weight NOM were found to be chelating with dissolved Cu(II), as it was concluded from the behaviour of chelation in MRW and MCW.

10.1.3 Dissolved Cu(II) Removal by Low-level Iron Corrosion Products via Two-stage Corrosion process and the Impact of Bulk Water NOM Character on the Removal

Iron pipe corrosion has been identified as one of the main causes leading to dissolved Cu(II) loss in the distribution system. Considerable dissolved Cu(II) removal by corrosion products (Fe^{2+}, Fe^{3+} and $Fe(OH)_3$) at low concentration (< 2 mg/L) was observed in the laboratory scale experiments. The data obtained by the metal analysis of sediments collected from the field also show a high proportion of both Cu(II) and Fe contents.

The removal of dissolved Cu(II) occurs via a two-stage process sequentially during corrosion: Stage I-coagulation and aggregation by released ferrous/ferric ions; Stage II-adsorption imposed by iron hydroxide flocs formed afterwards. MRW and NW showed nearly equal contribution from each stage to dissolved Cu(II) removal, except the case of 0.1 mg-Fe/L ferric ions addition in which the total dissolved Cu(II) removal had nearly finished in Stage I. The degree to which dissolved Cu(II) was removed can be affected by NOM composition in bulk waters. The effect of coagulation on Cu(II) removal in Stage I was attenuated in HAW due to the presence of large organic molecules. Therefore, less dissolved Cu(II) removal was observed in HAW.

Both ferrous/ferric ions and iron hydroxide flocs demonstrated considerable capacity to remove dissolved Cu(II) in bulk water. Ferrous and ferric ions show considerable and similar capacity to remove dissolved Cu(II) in the Mundaring water (MRW) and the

water containing nitrifying bacteria (NW). Cu-NOM in humic acid water demonstrated relatively high resistance to removal by the ions. However, 2 mg/L ferric ions were still able to remove the majority of dissolved Cu(II) in HAW.

$Fe(OH)_3$ flocs show fair capacity to remove dissolved Cu(II) from MRW and NW. The interaction between dissolved Cu(II) and $Fe(OH)_3$ flocs in the Mundaring water and NW can be explained as multi-layer adsorption obeying the Freundlich isotherm. Cu(II) containing particles (e.g. $CuO_{(s)}$, $Cu(OH)_2$) remaining in bulk water can reduce the flocs' capacity to remove dissolved Cu(II), depending on the proportion of the particles. It may be due to preferential adsorption of the large copper-based precipitates on the $Fe(OH)_3$ flocs. $Fe(OH)_3$ flocs show much weaker capacity to remove dissolved Cu(II) from HAW.

The characteristics of NOM contained in bulk waters have effects on both Cu-NOM complexation and dissolved Cu(II) removal. Dosed Cu(II) is thought to be preferentially complexed with small organic molecules. The similar Freundlich isotherm parameters found in the Mundaring water and coagulated Mundaring water, when 250 and 400 µg-Cu(II)/L copper salt doses were added, indicate dosed Cu(II) may preferentially chelate with uncoagulable NOM in the Mundaring water. Slightly high Cu(II) solubility and less dissolved Cu(II) removal observed in NW indicate a proportion of small soluble organic substances produced to chelate with Cu(II) during nitrification. In humic acid water (HAW), Cu(II) bound with small MW organic matter is shielded by a relatively high proportion of large MW organic matter, as coagulation preferentially removes larger molecular compounds. It explains why the much lower removal of dissolved Cu(II) was observed in HAW.

10.1.4 Modelling Cu(II) loss in a Corroded Iron Pipeline

The dynamic process of dissolved Cu(II) removal by $Fe(OH)_3$ flocs can be described as Pseudo second order decay. It can be combined with Freundlich isotherms, which were used to find equilibrium dissolved Cu(II) concentrations when different copper doses and $Fe(OH)_3$ additions were used, to model dissolved Cu(II) loss in the pipeline. From the comparison of dissolved Cu(II) loss between the modelling results and the field data in the CK Extension, it demonstrated that the loss of dissolved Cu(II) can be explained by removal caused by iron corrosion and modelled by reasonably presuming an Fe corrosion situation in the CK Extension pipeline.

10.2 Recommendations for Cu(II)-based Inhibition and Chloramination Strategies

Single-point cupric sulphate dose has been continuously carried out at the CK main of G&AWSS. Iron pipe corrosion is inevitable for this historic pipeline project, considering pipe aging, extensive temperature fluctuation, chlorination and nitrification. The laboratory scale experiments in this study, the sediment data collected from the field and the comparison between the Cu(II) loss modelling results with the ones occurring in the field all point to a serious threat from corrosion to maintaining an expected soluble Cu(II) concentration in pipelines. Although corrosion is believed to be a key factor causing dissolved Cu(II) loss, other factors such as Cu(II)-sulphide precipitation and Cu(II) accumulation on a biofilm cannot be ruled out, as they were not fully investigated. Consequently, maintaining the expected soluble Cu(II) concentration (0.25~0.40 mg/L) has become a key challenge in the field.

By dosing cupric sulphate the nitrifying activity is successfully inhibited based on bench scale work as long as the required soluble Cu(II) concentration is maintained (Koska, 2008). Similar results were found in the field. Free cupric ions are believed to be the most toxic Cu(II) species (Allen and Hansen, 1996). This study shows that the majority of dosed Cu(II) exist in the forms of Cu(II)-NOM complexes. In this sense, Cu-NOM is the one that inhibited nitrification in the bench scale work. Further work needs to be done on effectiveness of various Cu(II) species.

Our recent study found that dosed Cu(II) only marginally reduced chloramine decay, by controlling nitrification, possibly due to a soluble microbial product produced under severe nitrification conditions (Sarker and Sathasivan, 2010). This finding renders another challenge of controlling the chloramine residual in the distribution system.

To summarize, the recommendations for further research are made as follows:

- To further investigate impacts and contributions from the factors other than corrosion (e.g. Cu(II)-sulphide precipitation, Cu(II) accumulation on biofilm) on dissolved Cu(II) loss in the distribution system.

- To identify the effectiveness of Cu(II)-NOM on inhibiting nitrifying bacteria and continue the study on alternative Cu(II) species (e.g. a suitable Cu(II) complexing agent) for inhibition since cupric ions rarely exist in the distribution system.

- To consider alternative copper salt dosing strategies in the field: instead of one-point dose, re-dose of copper salt or dosing copper into reservoirs may be investigated.

- To investigate the synergistic effect of copper and chloramine and understand exactly where copper could be dosed.

REFERENCES

Allen**,** H. E. and Hansen, D. J. The importance of trace metal speciation to water quality criteria. *Water Environ Res* **1996,** 68**,** 42**–**54.

Allpike, B.P., Heitz, A., Joll, C.A., Kagi, R., Brinkman, T., Abbt-Braun, G., Frimmel, F., Her, N. and Amy, G. Size exclusion chromatography to evaluate DOC removal in drinking water treatment processes. *Environ. Sci. Technol*. **2005**, 39**,** 2334-2342.

AWWARF. 1996. Internal corrosion of water distribution systems. AWWARF-DVGW-TZW cooperative research report, Denver, CO, 586.

Benjamin, M. M.; Sontheimer, H.; Leroy, P. 1996. Corrosion of iron and steel. In: Internal corrosion of water distribution systems. Denver, CO: AWWA Research Foundation. 29–70.

Benjamin, M. M.; Sletten, R. S.; Bailey, R. P.; Bennett, T. Sorption and filtration of metals using iron-oxide-coated sand. *Water Research.* **1996**, 30 (11), 2609-20.

Breault, R. F.; Colman, J. A.; Aiken, G. R. and McKnight, D. Copper speciation and binding by organic matter in copper contaminated streamwater. *Environ. Sci. Technol.* **1996***,* 30, 3477–3486.

Broo, A. E.; Berghult, B.; Hedberg, T. Drinking water distribution-the effect of natural organic matter (NOM) on the corrosion of iron and copper. *Water Science and Technology*. **1999**, 9 (40), 17-24.

Bruland, K. W.; Donat, J. R. and Hutchins, D. A. Interactive influences of bioactive trace metals on biological production in oceanic waters. *Limnol. Oceanogr*. **1991**, 36, 1555- 1577.

Cantor, A. F.; Bushman, J. B.; Glodoski, M. S.; Kiefer, E.; Bersch, R. and Wallenkamp, H. Copper pipe failure by microbiologically influenced corrosion. *Materials Performance*. **2006**, 45 (6), 38.

Chadik, P.A. and Amy, G.L. Molecular weight effects on THM control by coagulation and adsorption. J. *Environ. Eng.* **1987**, 113 (6), 1234.

Chapelle, F. H. and lovely, D. R. Competitive exclusion of sulphate reduction by Fe(III)-reducing bacteria: A mechanism for producing discrete zones of high-iron ground water. *Groundwater*. **1992**, 30(29).

Davies, G.; Ghabbour, E. A. and Khairy, K. A. Humic substances-structures, properties and uses. The Royal Society of Chemistry. UK, 1998.

Dodrill, D. M.; Hidmi, L. and Edwards, M. Proceedings of the Toronto AWWA National Conference, American Water Works Association, Denver, CO, 1996, p. 719.

Douglas, I.; Guthman, J.; Muylwyk, Q. and Snoeyink, V. 2004. Corrosion control in the city of Ottawa- Caparison of alternatives and case study for lead reduction in drinking water. Proc. 11th Canadian National Conference and 2nd Policy Forum on Drinking Water, Calgary, Alta, Can.

Dryer, D. J.; Korshin, G. V.; Heitz, A.; Joll. C. 2008. Characterization of proton and copper binding properties of natural organic matters from an Australian drinking water source by differential absorbance spectroscopy. *Water Science and Technology: Water Supply*. 8 (6), 611-614.

Edwards, M. and Nicolle, S. Organic matter and copper corrosion by-product release: a mechanistic study. *Corrosion Science*. **2001**, 43, 1-18.

Edwards, M. and Triantafyllidou, S. Chloride-to-suphate mass ratio and lead leaching to water. *Jour. AWWA*. **2007**, 99(7), 96.

Elder, J. F. and Horne, A. J. Copper cycles and $CuSO_4$ algicidal capacity in two California lakes. *Environ. Manag.* 1978, 2, 17–30.

Emde, K. M. E.; Smith, D. W. and Facey, R. Initial investigation of microbially influenced corrosion in a low temperature water distribution system. *Water Research*. **1992**, 26(2), 169.

Gamble, D. S.; Underdown, A. W.; Langford, C. H. Cu(II) titration of fulvic acid ligand sites with theoretical, potentiometric, and spectrophotometric analysis. *Anal. Chem.* **1980**, 52, 1901-1908.

Gamble, D. S.; Langford, C. H.; Underdown, A. W. Light scattering measurements of Cu(II)-fulvic acid complexing: The interdependence of apparent complexing capacity and aggregation. *Org Geochem*. **1985**, 1 (8), 35-39.

Gedge, G. Corrosion of cast iron in potable water service. Corrosion and Related Aspects of Materials for Potable Water Supplies. Proc. Inst. **1992**, *Materials Conf.* London

Kirmeyer P.E, G.; Martel P.E, K.; Thompson, G.; Radder, L.; Klement, W.; Lechevallier, M.; Baribeau, H. and Flores, A. 2004. Optimizing Chloramine Treatment, Second Edition; AWWARF & AWWA: U.S.A.

Hankins, N. P.; Lu, N. and Hilal, N. Enhanced removal of heavy metal ions bound to humic acid by polyelectrolyte flocculation. *Separation and Purification Technology*. **2006**, 51, 48-56.

Haughey, M. A.; Anderson, M. A.; Whitney, R. D.; Taylor, W. D. and Losee, R. F. Forms and fate of Cu in a source drinking water reservoir following $CuSO_4$ treatment. *Water Res.* **2000**, 34, 3440–3452.

Hoffmann, M. R.; Yost, E. C.; Eisenreich, S. J.; Maier, W. J. Characterization of soluble and colloidal-phase metal complexes in river water by ultrafiltration-A mass balance approach. *Environ. Sci. Technol.* **1981**, 15, 655–661.

Holden, B,; Greetham, M.; Croll, B. T. and Scutt, J. The effect of changing inter process and final disinfection reagents on corrosion and biofilm growth in distribution pipes. *Water Science and Technology*. **1995**, 32(8), 213-220.

Hullebusch, Eric Van.; Chatenet, P.; Deluchat, V. Copper accumulation in a reservoir ecosystem following copper sulphate treatment (ST.GERMAIN LES BELLES, FRANCE). *Water, Air and Soil Pollution*. **2003**, 150, 3-22.

Kastl, G.; Sathasivan, A.; Fisher, I.; Van Leeuwen, J. Modeling DOC removal by enhanced coagulation. *J. Am. Water Works Assoc*. **2004**, 92(2), 79-89

Koska, L. 2008. Treatment of Chloraminated Water. U.S. Patent 7465401, December 16.

Krishna, KC and Sathasivan, A. (2010) Accelerated decay observed in severely nitrifying bulkwaters: Possible role of soluble microbial products. *Water Research (Accepted)*

Lai, C. H. and Chen, C. Y. Removal of metal ions and humic acid from water by iron-coated filter media. *Chemosphere*. **2001**, 44, 1177-1184.

Lehman, R. M.; Mills, A. L. Field evidence for copper mobilization by dissolved organic matter. *Water Res*. **1994**, 28, 2487-2497.

Lipponen, M. T.; Suutari, M. H.; Martikainen, P. J. (2002) Occurence of nitrifying bacteria and nitrification of finnish drinking water distribution systems. 36, 4319-4329.

Louis, Y.; Garnier, C.; Lenoble, V.; Mounier, S.; Cukrov, N.; Omanović, D and Pižeta, I. Kinetic and equilibrium studies of copper-dissolved organic matter complexation

in water column of the stratified Krka River estuary (Croatia). *Marine Chemistry*. **2009**, 114 (3-4), 110-119.

McNeill, L. S. and Edward, M. Iron pipe corrosion in distribution systems. *Journal AWWA*. **2001**, 93 (7), 88-100.

Moffett, J. W. and Brand, L. E. Production of strong, extracellular Cu chelators by marine cyanobacteria in response to Cu stress. *Limnol. Oceanogr*. **1996**, 41 (3), 388-395.

Murphy, B.; O'Connor, J. T. and O'Connor, T. L. 1997a. Willmar, Minnesota, Battle copper corrosion-Part 2: Nitrification, bacteria and copper corrosion in household plumbing. *Public Works*. 128(12), 44.

Nemati, M. and Webb, C. A kinetic model for biological oxidation of ferrous iron by thiobacillus ferrooxidans. *Biotechnol. & Bioengrg*. **1997**, 53(5), 478.

Olsson, S.; van Schaik, J. W. J.; Gustafsson, J. P.; Kleja, D. B.; van Hees, P. A. W. Copper(II) binding to dissolved organic matter fractions in municipal solid waste incinerators bottom ash lechate. *Environ. Sci. Technol*. **2007**, 41, 4286-4291.

Perdue, E. M.; Lytle, C. R. A distribution model for binding of protons and metal ions by humic substances. *Environ. Sci. Technol*. **1983**, 17 (11), 654-660.

Powell, R. Implementation of chlorination by a Florida utility: The Good, The Bad, The Ugly. Proc, 2004, *AWWA WQTC*, San Antonio, Texas.

Rajec, P.; Gerhart, P.; Macášek, F.; Shaban, I. S. and Bartoš, P. Size exclusion (radio) chromatography of aqueous humic acid solutions with cesium and strontium. *Journal of Radioanalytical and Nuclear Chemistry***. 1999**, 241 (1), 37-43.

Ridge, A. C.; Sedlak, D. L. Effect of ferric chloride addition on the removal of Cu and Zn complexes with EDTA during municipal wastewater treatment. *Water Research*. **2004,** 38 (4), 921-932.

Sarathy, V and Allen, H. E. Copper complexation by dissolved organic matter from surface water and wastewater effluent. Ecotoxicology and Environmental Safety. **2005**, 61, 337-344.

Sarin, P.; Snoeyink, V. L.; Bebeeb, J.; Jim, K. K.; Beckett, M. A.; Krivena, W. M.; Clements, J. A. Iron release from corroded iron pipes in drinking water distribution systems: effect of dissolved oxygen. *Wat Research*. **2004**, 38 (5), 1259–1269.

Sathasivan, A.; Fisher, I.; Kastle G. Simple method for quantifying microbiologically assisted chloramine decay in drinking Water. *Environ. Sci. Technol.* **2005**, 39, 5407-5413.

Sathasivan, A.; Ohgaki, S. Application of new bacterial regrowth potential method for water distribution system-a clear evidence of phosphorous limitation. *Water Research*. **1999**, 33 (1) 137-144.

Sathasivan, A.; Fisher, I.; Tam, T. Onset of severe nitrification in mildly nitrifying chloraminated bulk waters and its relation to biostability. *Water Research*. **2008**, 42(14), 3623-3632.

Sillen, L. G.; Martell, A. E. (1971) Stability constants of metal ion complexes. Special Publication NO. 25. *The Chemistry Society*, London.

Skopp, J. Derivation of the Freundlich isotherm from kinetics. *J. Chem. Educ*. **2009**, 86(11), 1341-1343.

Smith, D. S. and Kramer, J. R. Multisite metal binding to fulvic acid determined using multiresponse fluorescence. *Analytica Chemica Acta* . 2000, 416, 211-220.

Snoeyink, Vernon L.; Jenkins, David. *Water Chemistry*; John Wiley & Sons, Inc: New York, 1980; pp 220-221.

Streat, M.; Hellgardt, K. and Newton, N. L. R. Hydrous ferric oxide as an adsorbent in water treatment-part 1 preparation and physical characterization. *Process Safety and Environmental Protection*. **2008**, 86, 1-9.

Sun, Z. X.; Skold, R.O. A multi-parameter titration method for the determination of formation pH for metal hydroxide. *Minerals Engieering*. **2001**, 14, 1429-1443.

Sunda, W. G. Trace metal/phytoplankton interactions in the sea. In G. Bidoglio and W. Stumm [eds.], Chemistry of aquatic systems: Local and global perspectives. **1994**, Kluwer.

Takacs, M.; Alberts, J.J.; Egeberg, P. (1999) Characterization of NOM from Eight Norwegian Surface Waters: Proton and Copper Binding. *Environmental International,* 25, 315-323.

Tang, Z.; Hong, S.; Xiao, W.; Taylor, J. Characteristics of iron corrosion scales established under blending of ground, surface, and saline waters and their impacts on iron release in the pipe distribution system. *Corrosion Science*. **2006**, 48, 322-342.

Teng, F.; Guan, Y. T.; Zhu, W. P. Effect of biofilm on cast iron pipe corrosion in drinking water distribution system: Corrosion scales characterization and microbial community structure investigation. *Corrosion Science*. **2008**, 50, 2816-2823

Tessier, A. and Turner, D. R. Metal Speciation and Bioavailability in Aquatic Systems. **1995**, John Wiley & Sons, New York, NY, U.S.A., 661 pp.

Twardowska, I and Kyziol, J. Sorption of metals onto natural organic matter as a function of complexation and adsorbent–adsorbate contact mode. *Environmental International*. **2003**, 28, 783-791.

Van Hullebusch, E.; Chatellete P.; Deluchat, V.; Chazal, P.; Froissard, D.; Botineau, M.; Ghestem, A.; Baudu, M. (2003) Copper accumulation in a reservoir ecosystem

following copper sulphate treatment (St.Germain Les Belles, France). *Water, Air and Soil Pollution,* 150, 3-22.

Vikesland, P.; Ozekin, K.; Valentine, R. Monochloramine decay in model and distribution system water. *Water. Research.* **2001**, 35, 1766-1776.

Volk, C.; Bell, K.; Ibrahim, E.; Verges, D.; Amy, G.; Lechevallier M. Impact of enhanced and optimized coagulation on removal of organic matter and its biodegradable fraction in drinking water. *Water Research*. **2000**, 34 (12), 3247-3257.

Wagemann, R.; Barica, J. Speciation and rate of loss of copper from lake water with implications to toxicity. *Water Res*. **1978**, 13, 515-523.

Wang, Y.; Zhang, X.J.; Niu, Z. B.; Chen, C.; Lu, P. P.; Tang, F. Effect of chloramine residual on iron release in drinking water distribution systems. *Water Science & Technology: Water Supply-WSTWS.* **2009**, 9 (4), 349-355.

Warton, B., Heitz, A., Zappia, L., Masters, D., Alessandrino, M., Franzmann, P., Joll, C., Allpike, B., O'Leary, B. and Kagi, R. Magnetic Ion Exchange (MIEX) Drinking Water Treatment in a Large Scale Facility. *Journal of the American Waterworks Association*. **2007**, 99, 89-101.

Weishaar, J.; Aiken, G.; Bergamaschi, B.; Fram, M.; Fujii, R.; Mopper, K. Evaluation of specific ultraviolet absorbance as an indicator of the chemical composition and reactivity of dissolved organic carbon. *Environ. Sci. Technol*. **2003**, 37, 4702-4708.

Whitaker, J.; Barica, J.; Kling, H. and Buckley, M. Efficacy of copper sulphate in the suppression of Aphanizomenon flos-aquae blooms in prairie lakes. *Environ. Pollut.* **1978**, 15, 185–194.

World Health Organization. Guidelines for Drinking-water Quality; Geneva, 2008; incorporating 1st and 2nd addenda, Vol.1, Recommendations.-3rd ed.

Zhan, W. 2007. The Fate of Dosed Copper to Inhibit Nitrification in Chloraminated Water Distribution System. Master Thesis, Curtin University of Technology, Perth, WA.

Zhan, W.; Sathasivan, A.; Nolan, P.; Koska, L.; Heitz, A.; Joll, C. Effectiveness of ferric salts in removing low levels of dosed copper from NOM-containing natural water. *Journal of Water Supply: Research and Technology-AQUA*. **2009**, 58 (7), 443-449.

Zhan, W.; Sathasivan, A.; Heitz, A.; Kristiana, I. 2010. Impact of released trace ions from iron corrosion on dosed copper against nitrification in bulk waters. *OZWater'10 Conference*, Brisbane. (Refereed)

Zhang, Y. 2009. Nitrification in premise plumbing and its effect on corrosion and water quality degradation. Civil and Environmental Engineering, Virginia Tech, Blacksburg, VA.

Zhang, Y and Edwards, M. Anticipating effects of water quality changes on iron corrosion and red water. *Jour. Water. Supply. Res. & Technol-AQUA*. **2007**, 56 (1), 55.

Appendix A

Results of Total Chloramine Decay

Chemical Decay vs Microbiologically Assisted Decay

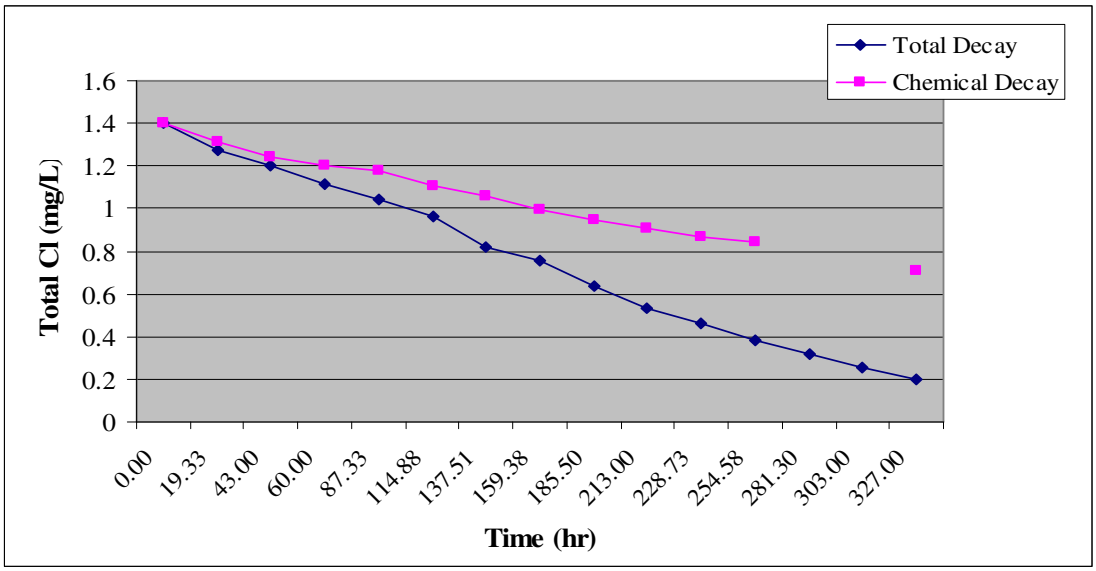

Figure A1 Comparison between an Inhibited and an Unprocessed Sample (sample 1) (total decay: concentration due to total decay; chemical decay: concentration due to chemical decay)

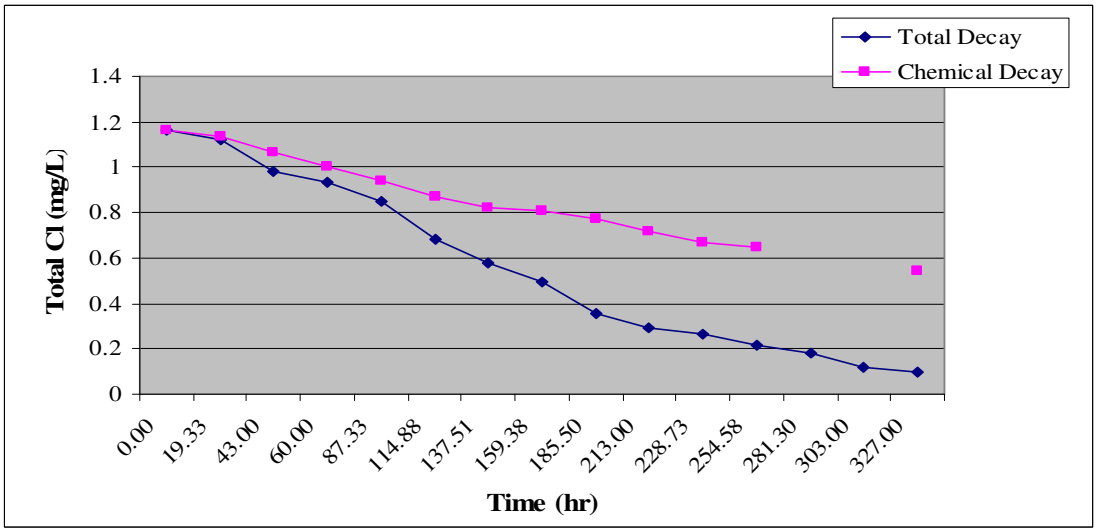

Figure A2 Comparison between an Inhibited and an Unprocessed Sample (sample 2) (total decay: concentration due to total decay; chemical decay: concentration due to chemical decay)

Note: Sample 1 and Sample 2 were collected from two places within the C-K reticulation system, where nitrification was detected. Silver nitrate was used as an inhibitor.

Sample 1: Kc = 0.0021 hr^{-1} Km = 0.0039 hr^{-1} Fm = 1.86 (Fm = Km/Kc)

Sample 2: Kc = 0.0032 hr^{-1} Km = 0.0045 hr^{-1} Fm = 1.41 (Fm = Km/Kc)

Appendix B

Particle Size Distribution of Ferric Hydroxide Flocs used in Dissolved Cu(II) Removal Experiments

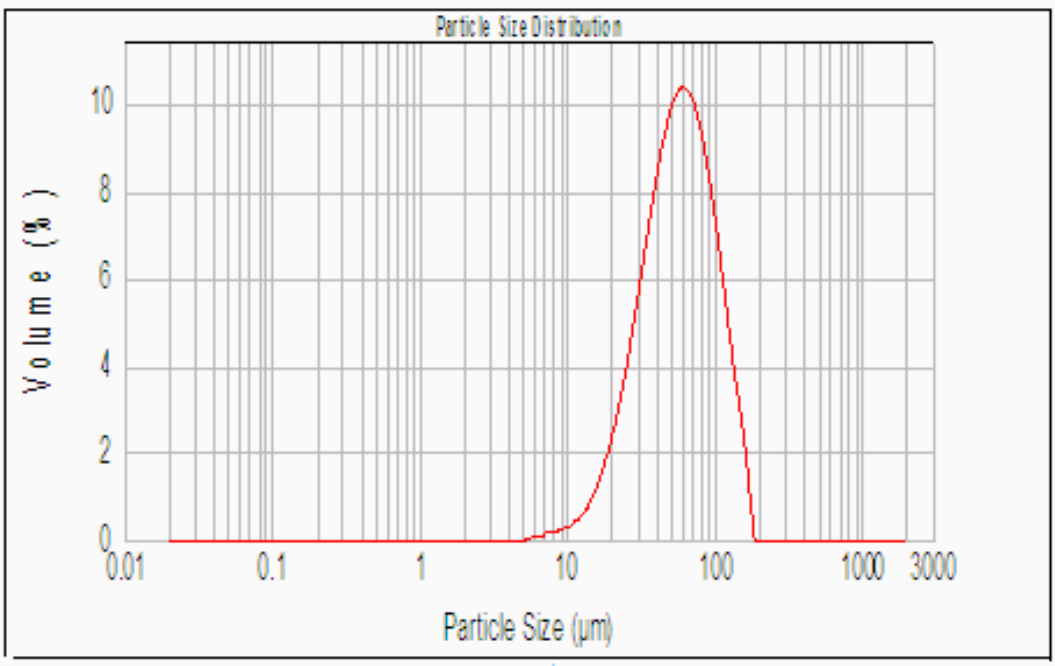

Figure B: Particle size distribution of $Fe(OH)_3$ flocs used in the dissolved Cu(II) removal experiments

Appendix C

Dissolved Cu(II) Concentration in Mundaring Bulk Water after Cu Salt Dose

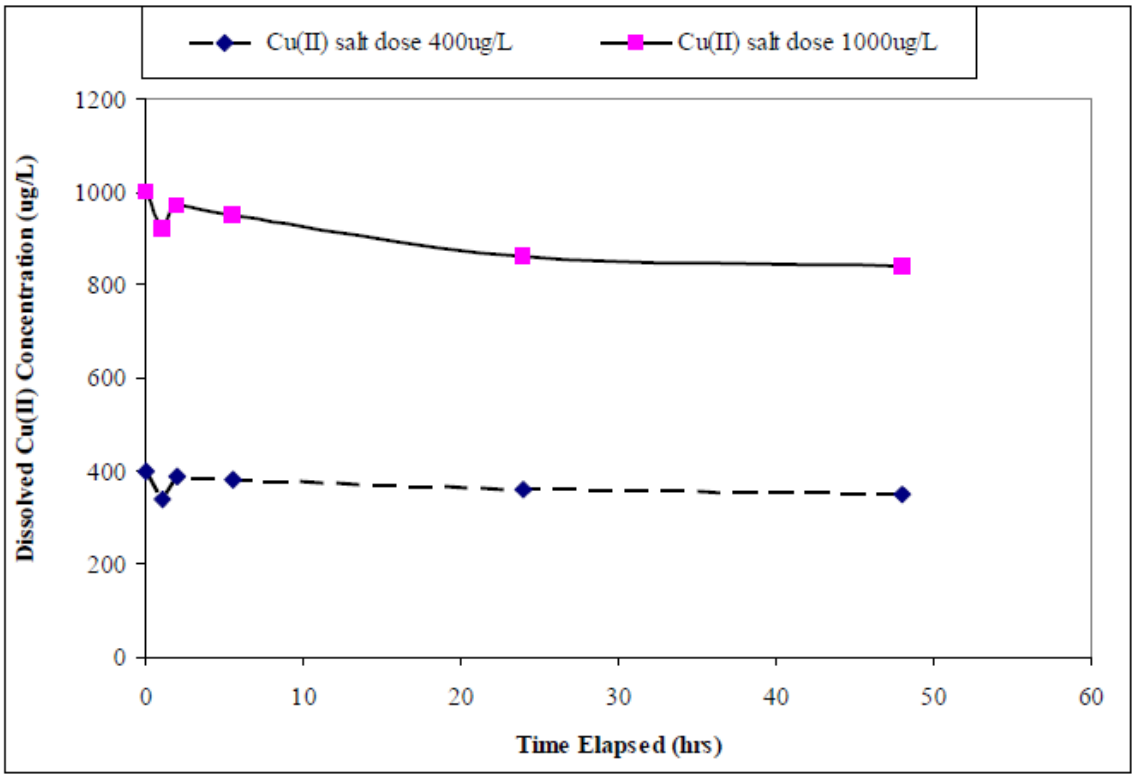

Figure C: Dissolved Cu(II) concentration vs elapsed time after Cu salt dose in Mundaring raw water

Figure C demonstrates that 24 hours after Cu salt dosing is a sufficient time to stabilize dissolved Cu(II) concentration in Mundaring raw water.

Appendix D

Field Data: Cu Salt Dose and Dissolved Cu(II) Concentration Monitored at CK12km and CK58km in the Main of the CK Extension

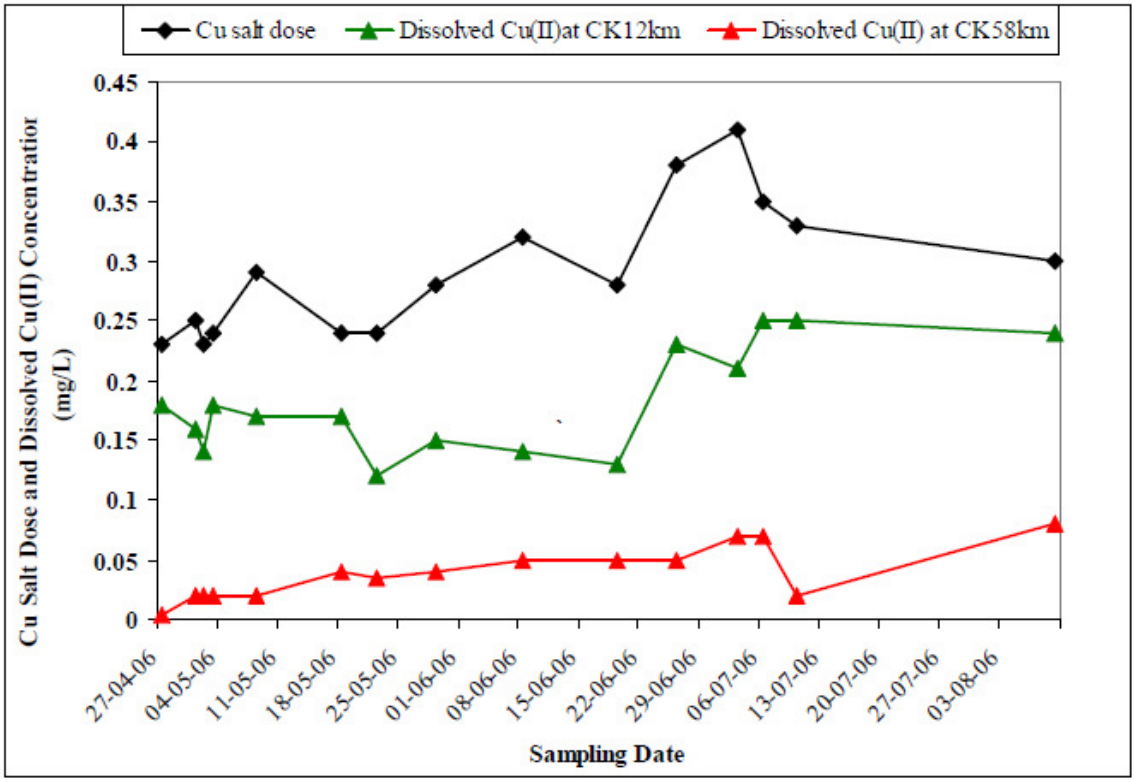

Figure D: Cu salt dose and dissolved Cu(II) concentrations measured in the field (CK12km and CK58km) during the 104-day pilot copper dose experiment in the CK Extension Pipeline in 2006

The Cu salt dose as a function of time was programmed into the model in Chapter 9 to help calculate the dissolved Cu(II) concentrations at CK12km and CK58km when a certain corrosion pattern was presumed.

Appendix E

Comparison of Dissolved Cu(II) Removal in Mundaring Raw Water by Ferric Hydroxide Flocs and Ferric Ions

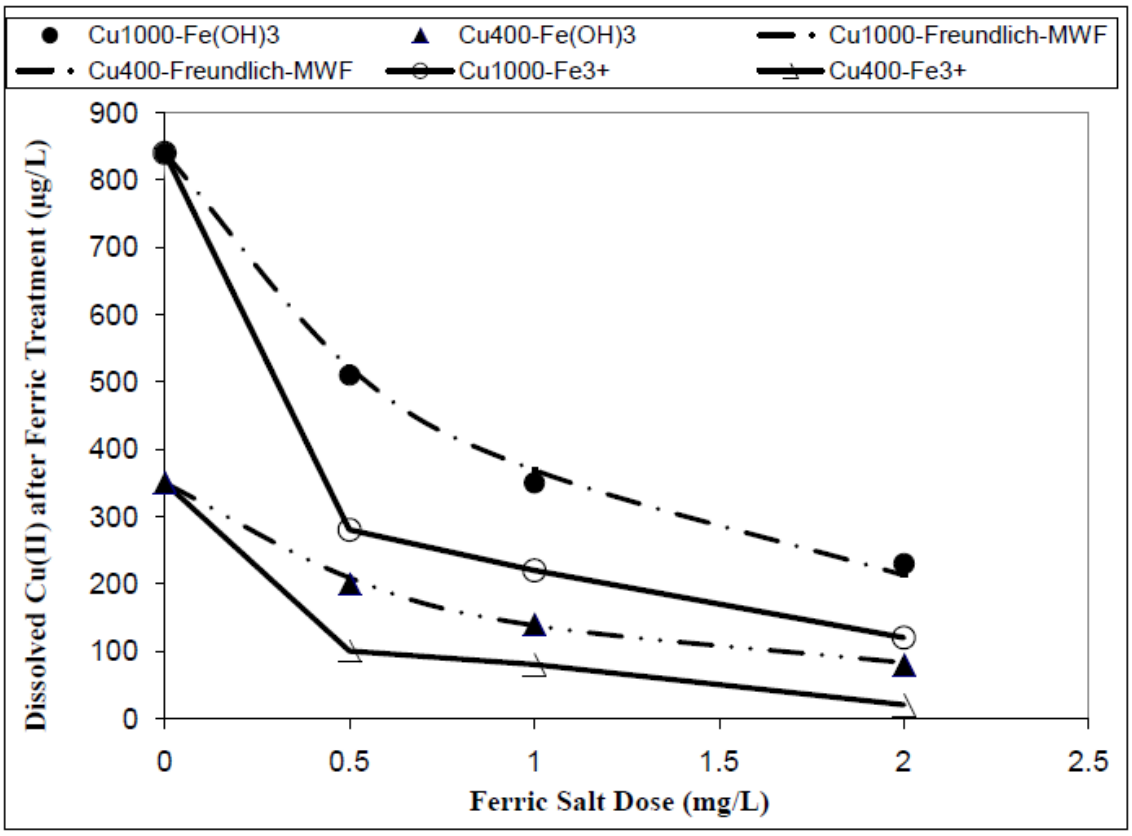

Figure E: Comparison of dissolved Cu(II) removal in Mundaring raw water by ferric hydroxide flocs and ferric ions

Legends:

"Cu1000-Fe$(OH)_3$": Cu salt dose was 1000µg/L; Fe$(OH)_3$ flocs were added to remove dissolved Cu(II). "Cu1000-Freundlich-MWF": The Freundlich isotherm curve connecting the measured results from "Cu1000-Fe$(OH)_3$". "Cu1000-Fe^{3+}": Cu salt dose was 1000µg/L; ferric ions were added to remove dissolved Cu(II).

The other legends can be interpreted analogously.

Figure E shows that the equilibrium dissolved Cu(II) concentration (Ce_Cu: refer to Chapter 9) after ferric ion treatment at each Fe dose (0.5, 1.0 and 2.0 mg-Fe/L) was half of that when Fe$(OH)_3$ flocs were used. Therefore, an "α" value of 0.5 was adopted in E2 (Chapter 9).

Appendix F

Field Data on Contents of Sediments Collected from the CK Extension

Table F: Composition of Cu, Fe and Ca in Sediments along C-K Extension (by courtesy of Water Corporation, WA)

C-K 58km					C-K 12km				
Date	**Fe (mg/kg)**	**Cu (mg/kg)**	**Ca (mg/kg)**	**Cu/Fe ratio (%)**	**Date**	**Fe (mg/kg)**	**Cu (mg/kg)**	**Ca (mg/kg)**	**Cu/Fe ratio (%)**
8/06/2006	45630	1168	132043	2.56	8/06/2006	39283	338	3571	0.86
21/06/2006	127167	4818	6061	3.79	21/06/2006	77405	958	7742	1.24
1/08/2006	219747	5914	6593	2.69	1/08/2006	57057	7696	7143	13.49
28/08/2006	72359	5848	4655	8.08	28/08/2006	32405	6378	5405	19.68
28/09/2006	174975	10404	8750	5.95	28/09/2006	99575	19225	10000	19.31
25/10/2006	85686	9261	11429	10.81	25/10/2006	33208	13917	33333	41.91
24/11/2006	86251	10969	5490	12.72	24/11/2006	87466	14972	2500	17.12
25/01/2007	57741	3690	5926	6.39	23/02/2007	118625	9894	6250	8.34
23/02/2007	118188	15375	18750	13.01	20/04/2007	126455	20091	18182	15.89
20/04/2007	249896	14302	8333	5.72	25/05/2007	32228	24735	7353	76.75
25/05/2007	214727	12955	3030	6.03	27/07/2007	34392	7468	2400	21.71
27/07/2007	157686	13817	4615	8.76					
Average	**134171**	**9043**	**8056**	6.74		**67100**	**11424**	9444	17.03

Note:
Along the main pipeline from the copper dosing point to the service water tank, sediments have been drawn and analysed at two places. One is 12 km away from the dosing point (C-K12km), the other is 58 km away (C-K58km). To collect sediments, target pipe sections were flushed using the associated hydrant.

Appendix G

AQUASIM Model Output of Cu(II) Loss along CK Extension

****

AQUASIM Version 2.1f (win/mfc) - List File

****

Name of plot: Cuw

Type:	Argument	Value	Argument	Value	Argument	Value	Argument	Value	Argument	Value
Variable:	t	C_Cuw	t	Cin_Cu	t	Cumeas_CK12km	t	Cumeas_CK58km	t	C_Cuw
Parameter:										
CalcNum:		0		0		0		0		0
Compart.:		bw_20		bw_1		bw_6		bw_20		bw_4
Zone:	Bulk Volume		Bulk Volume		Bulk Volume		Bulk Volume		Bulk Volume	
Time/Space:		0		0		0		0		0
Unit:	h	ug/l	h	ug/L	h	ug/L	h	ug/L	h	ug/l
Legend:		Cal Cu(II) CK58				Cu(II) dose				Cumeas_CK12
		Cumeas_CK58		Cal Cu(II)-CK12						
	0	230	0	230	0	180	0	4	0	230
	10	164.6	20	230	20	180	20	4	10	202.4
	20	48.51	96	250	96	160	96	20	20	178.6
	30	20.61	120	230	120	140	120	20	30	175.8
	40	13.3	144	240	144	180	144	20	40	167.8
	50	11.42	264	290	264	170	264	20	50	160.7
	60	11.27	504	240	504	170	504	40	60	155.1
	70	11.68	600	240	600	120	600	35	70	150.6
	80	12.26	768	280	768	150	768	40	80	146.7
	90	12.92	1008	320	1008	140	1008	50	90	143.5
	100	13.58	1272	280	1272	130	1272	50	100	139.4
	110	13.81	1440	380	1440	230	1440	50	110	133
	120	13.78	1608	410	1608	210	1608	70	120	128.2
	130	13.91	1680	350	1680	250	1680	70	130	131.8
	140	14.29	1776	330	1776	250	1776	20	140	145.7

150	14.85	2496	300	2496	250	2496	80	150	165.8
160	15.66							160	172.7
170	16.52							170	171.6
180	17.21							180	170.2
190	17.67							190	169
200	17.92							200	168.1
210	18.07							210	167.3
220	18.18							220	166.8
230	18.27							230	166.3
240	18.36							240	165.9
250	18.45							250	165.7
260	18.53							260	165.5
270	18.54							270	164.2
280	18.3							280	163
290	18.11							290	162.8
300	18.16							300	162.6
310	18.4							310	162.4
320	18.76							320	162.3
330	19.19							330	162.2
340	19.66							340	162
350	20.16							350	161.9
360	20.7							360	161.8
370	21.27							370	161.8
380	21.88							380	161.7
390	22.53							390	161.6
400	23.23							400	161.6
410	23.99							410	161.6
420	24.8							420	161.6
430	25.69							430	161.6
440	26.64							440	161.6
450	27.68							450	161.7
460	28.82							460	161.8
470	30.07							470	161.9
480	31.44							480	162.1
490	32.96							490	162.3
500	34.64							500	162.5
510	36.59							510	162.8
520	38.89							520	158.2
530	40.78							530	152

540	41.62	540	146.6
550	41.44	550	141.8
560	40.68	560	137.5
570	39.69	570	133.7
580	38.67	580	130.1
590	37.68	590	126.9
600	36.72	600	123.8
610	35.98	610	122.8
620	35.48	620	124.2
630	35.16	630	126
640	35	640	127.8
650	35.02	650	129.6
660	35.17	660	131.4
670	35.39	670	133.3
680	35.64	680	135.2
690	35.89	690	137.1
700	36.14	700	139
710	36.39	710	140.9
720	36.64	720	142.9
730	36.88	730	144.9
740	37.13	740	146.9
750	37.37	750	148.9
760	37.62	760	151
770	37.86	770	153
780	38.05	780	154
790	38.23	790	154
800	38.48	800	153.8
810	38.81	810	153.7
820	39.15	820	153.6
830	39.48	830	153.5
840	39.79	840	153.4
850	40.09	850	153.3
860	40.39	860	153.2
870	40.7	870	153.2
880	41	880	153.1
890	41.3	890	153.1
900	41.61	900	153
910	41.92	910	153
920	42.22	920	152.9

930	42.53	930	152.9
940	42.84	940	152.9
950	43.15	950	152.8
960	43.46	960	152.8
970	43.77	970	152.8
980	44.08	980	152.8
990	44.4	990	152.8
1000	44.71	1000	152.8
1010	45.01	1010	152.7
1020	45.05	1020	151.7
1030	44.92	1030	151.1
1040	44.79	1040	150.6
1050	44.71	1050	150.1
1060	44.68	1060	149.6
1070	44.7	1070	149.1
1080	44.73	1080	148.6
1090	44.77	1090	148.1
1100	44.82	1100	147.6
1110	44.87	1110	147.1
1120	44.91	1120	146.6
1130	44.96	1130	146.1
1140	45.01	1140	145.6
1150	45.06	1150	145
1160	45.11	1160	144.5
1170	45.16	1170	144
1180	45.21	1180	143.5
1190	45.26	1190	143
1200	45.31	1200	142.5
1210	45.36	1210	142
1220	45.42	1220	141.4
1230	45.47	1230	140.9
1240	45.53	1240	140.4
1250	45.58	1250	139.9
1260	45.64	1260	139.4
1270	45.69	1270	138.8
1280	46.11	1280	140.7
1290	47.2	1290	144.7
1300	48.26	1300	149
1310	49.03	1310	153.3

1320	49.57	1320	157.8
1330	50.03	1330	162.3
1340	50.48	1340	166.9
1350	50.93	1350	171.7
1360	51.36	1360	176.5
1370	51.79	1370	181.4
1380	52.21	1380	186.4
1390	52.63	1390	191.6
1400	53.03	1400	196.8
1410	53.43	1410	202.2
1420	53.82	1420	207.8
1430	54.2	1430	213.5
1440	54.58	1440	219.3
1450	54.69	1450	222.3
1460	54.63	1460	222.2
1470	54.96	1470	221.6
1480	55.81	1480	221.1
1490	56.97	1490	220.5
1500	58.24	1500	220
1510	59.53	1510	219.5
1520	60.84	1520	219.1
1530	62.2	1530	218.6
1540	63.59	1540	218.2
1550	65.04	1550	217.8
1560	66.53	1560	217.4
1570	68.07	1570	217
1580	69.66	1580	216.7
1590	71.3	1590	216.3
1600	73.01	1600	216
1610	74.73	1610	215.3
1620	75.38	1620	212.9
1630	75.19	1630	214
1640	74.68	1640	216
1650	74.06	1650	218.4
1660	73.58	1660	221.4
1670	73.35	1670	225.2
1680	73.28	1680	230.2
1690	73.92	1690	236.9
1700	75.16	1700	237.4

1710	76.27	1710	236.5
1720	76.98	1720	235.6
1730	77.22	1730	234.6
1740	77.07	1740	233.7
1750	76.7	1750	232.7
1760	76.25	1760	231.8
1770	75.78	1770	230.9
1780	75.33	1780	230.1
1790	75.14	1790	230.1
1800	75.15	1800	230
1810	75.34	1810	229.9
1820	75.68	1820	229.8
1830	76.1	1830	229.6
1840	76.54	1840	229.5
1850	76.99	1850	229.4
1860	77.45	1860	229.3
1870	77.92	1870	229.2
1880	78.39	1880	229
1890	78.87	1890	228.9
1900	79.36	1900	228.8
1910	79.85	1910	228.7
1920	80.35	1920	228.6
1930	80.85	1930	228.5
1940	81.36	1940	228.3
1950	81.88	1950	228.2
1960	82.41	1960	228.1
1970	82.94	1970	228
1980	83.49	1980	227.9
1990	84.04	1990	227.8
2000	84.6	2000	227.6
2010	85.16	2010	227.5
2020	85.74	2020	227.4
2030	86.32	2030	227.3
2040	86.91	2040	227.2
2050	87.51	2050	227.1
2060	88.12	2060	226.9
2070	88.74	2070	226.8
2080	89.37	2080	226.7
2090	90.01	2090	226.6

2100	90.66	2100	226.5
2110	91.32	2110	226.4
2120	91.99	2120	226.2
2130	92.67	2130	226.1
2140	93.36	2140	226
2150	94.06	2150	225.9
2160	94.78	2160	225.8
2170	95.51	2170	225.7
2180	96.25	2180	225.6
2190	97	2190	225.5
2200	97.76	2200	225.3
2210	98.54	2210	225.2
2220	99.33	2220	225.1
2230	100.1	2230	225
2240	101	2240	224.9
2250	101.8	2250	224.8
2260	102.6	2260	224.7
2270	103.5	2270	224.6
2280	104.4	2280	224.4
2290	105.3	2290	224.3
2300	106.2	2300	224.2
2310	107.1	2310	224.1
2320	108.1	2320	224
2330	109	2330	223.9
2340	110	2340	223.8
2350	111	2350	223.7
2360	112.1	2360	223.6
2370	113.1	2370	223.4
2380	114.2	2380	223.3
2390	115.3	2390	223.2
2400	116.4	2400	223.1
2410	117.6	2410	223
2420	118.7	2420	222.9
2430	119.9	2430	222.8
2440	121.2	2440	222.7
2450	122.4	2450	222.6
2460	123.7	2460	222.5
2470	125	2470	222.4
2480	126.4	2480	222.3

2490	127.8	2490	222.1
2500	129.2	2500	222.1